WT-1449

AEC Category: HEALTH AND SAFETY
Military Category: 32

OPERATION PLUMBBOB

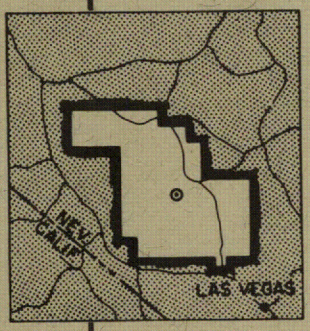

NEVADA TEST SITE
MAY-OCTOBER 1957

Project 30.2

RESPONSE OF DUAL-PURPOSE REINFORCED-CONCRETE MASS SHELTER

Issuance Date: September 15, 1962

CIVIL EFFECTS TEST GROUP

NOTICE

This report is published in the interest of providing information which may prove of value to the reader in his study of effects data derived principally from nuclear weapons tests.

This document is based on information available at the time of preparation which may have subsequently been expanded and re-evaluated. Also, in preparing this report for publication, some classified material may have been removed. Users are cautioned to avoid interpretations and conclusions based on unknown or incomplete data.

PRINTED IN USA
Price $2.50. Available from the Office of
Technical Services, Department of Commerce,
Washington 25, D. C.

USAEC Division of Technical Information Extension, Oak Ridge, Tennessee

Report to the Test Director

RESPONSE OF DUAL-PURPOSE REINFORCED-CONCRETE MASS SHELTER

By

E. Cohen
E. Laing
A. Bottenhofer

Approved by: H. J. JENNINGS
Director
Program 30

Approved by: R. L. CORSBIE
Director
Civil Effects Test Group

Ammann & Whitney
New York, New York
April 1961

ABSTRACT

Project 30.2 was conducted to test a reinforced-concrete dual-purpose underground parking garage and personnel shelter designed for a long-duration incident pressure of 40 psi. The shelter was exposed to shot Priscilla, an approximately 37-kt 700-ft balloon burst (June 24, 1957), at a ground range of 1600 ft (predicted 35-psi peak incident-pressure level). The recorded peak incident pressure at the shelter was approximately 39 psi.

Postshot soil borings were made to obtain undisturbed samples for determining soil characteristics.

Preshot and postshot field surveys were made to determine the total lateral and vertical displacement of the structure.

Blast instrumentation consisted of Wiancko pressure gauges, Carlson earth-pressure gauges, dynamic-pressure gauges, and a self-recording pressure gauge. Structural response was recorded by Ballistic Research Laboratories deflection gauges.

Radiation measurements were taken using film dosimeters, gamma-radiation chemical dosimeters, and one gamma-rate telemetering unit.

ACKNOWLEDGMENTS

The authors wish to express sincere appreciation to the following individuals for their cooperation in behalf of this project:

U. S. Atomic Energy Commission

R. L. Corsbie, Director, Civil Effects Test Group

Office of Civil and Defense Mobilization

E. R. Saunders, Assistant to the Director, Civil Effects Test Group
B. C. Taylor, Director, Engineering Office
H. J. Jennings, Director, Program 30
L. N. FitzSimons, Engineering Representative

Ballistic Research Laboratories

J. J. Meszaros, Project Officer, Project 30.5

Ammann & Whitney, Consulting Engineers

N. Dobbs, structural engineer
G. Pecone, structural engineer

CONTENTS

CONTENTS (Continued)

ILLUSTRATIONS

CHAPTER 1 INTRODUCTION

ILLUSTRATIONS (Continued)

ILLUSTRATIONS (Continued)

TABLES

Chapter 1

INTRODUCTION

1.1 OBJECTIVES

The primary objective of Project 30.2 was to evaluate the protection afforded by a reinforced-concrete dual-purpose underground parking garage and personnel shelter against effects of a nuclear detonation. Secondary objectives were to obtain additional information regarding blast load transmitted to underground structures, to obtain information regarding reflected and dynamic pressures in the ramp and on the entranceway door, to obtain data on nuclear-radiation attenuation characteristics of the structure, and to check assumptions used in design procedures.

Structure 30.2, a typical full-scale section of the prototype and the largest shelter tested in Operation Plumbbob, was located at the predicted 35-psi peak overpressure level.

1.2 BACKGROUND

In the summer of 1956, the Office of Civil and Defense Mobilization (formerly Federal Civil Defense Administration) contracted with Ammann & Whitney, Consulting Engineers, to prepare a preliminary layout for a dual-purpose reinforced-concrete underground parking garage and shelter and to design a structurally representative portion of such a structure to be exposed to nuclear blast for test purposes.

Studies were made of prototype architectural layouts and various types of roof framing, which included (1) flat-slab system with drop panels, (2) two-way slab systems with girders of various depths, and (3) hipped-plate construction. After consulting with OCDM, the structure was designed using a flat-slab roof system. Figure 1.1 shows the prototype layout of the flat-slab type construction.

The structure design is based on a peak incident blast pressure of 40 psi and a megaton range weapon. During the test the structure was subjected to a peak incident pressure of 39 psi.

1.3 DESCRIPTION OF TEST STRUCTURE

The test section (shown in Fig. 1.2) was a below-grade flat-slab structure with an interior floor area of 7569 sq ft (87 by 87 ft) and nine interior columns 29 ft on center (Fig. 1.3). Entrance into the shelter was by a 14-ft-wide vehicular ramp along one side of the structure (Figs. 1.4 and 1.5). The roof slab was 3 ft below grade. The walls of the structure, except for the exposed wall along the ramp (which was 4 ft 6 in. thick for radiation protection), were

12 in. thick. The floor slab was 9 in. thick and the roof slab was 30 in. thick with 14-in. drop panels 14 ft square. The vertical load was carried to the foundation by circular reinforced-concrete columns 33 and 36 in. in diameter. The footings were two-way slabs 15 ft to 16 ft 9 in. square. However, the footing near the entranceway was a two-column continuous member. Maximum thickness of the square footings varied from 3 ft 11 in. to 4 ft 3 in. The entranceway to the structure (Figs. 1.6 to 1.8) was protected by a 29-ft long by 10-ft high by 4-ft 6-in. thick reinforced-concrete rolling door; there was a 3-in.-wide inflatable rubber gasket seal around the perimeter.

Operating equipment for the door was not included in this test, and space for maintenance around the door was kept to a minimum. Although the operation of the test door required more effort than was anticipated in the design, this could have been greatly reduced by minor field adjustments to improve the as-built tolerances, alignment, smoothness, and lubrication of the door and frame.

A personnel escape exit had originally been included in the design but was deleted because personnel exits either were included in other projects or had been previously tested.

The structure was located with the center line of the ramp radial to Ground Zero (GZ). Figure 1.9 indicates the orientation of the structure, main blast line, and goal post and stake line with respect to GZ.

The design drawings for the test structure are included in Appendix A, and the construction report is included in Appendix B.

1.4 THEORY

The shelter was designed for dynamic behavior using ultimate strength theory and theoretical loadings consistent with a peak incident shock of 40 psi for a megaton-range weapon.[1–5]

The roof slab, columns, footings, and earth-covered walls of the shelter were designed to utilize additional strain energy available in the elastoplastic and plastic ranges. The exposed shelter wall and rolling door at the ramp were increased in thickness to provide the radiation protection specified by OCDM. This additional thickness provided sufficient strength so that only minimum reinforcement was required to produce elastic behavior.

The roof slab was designed for a 40-psi long-duration load as a flat slab using yield-line theory.[3] The earth-covered walls of the shelter were designed for a 15-psi long-duration load as one-way panels spanning vertically with the reinforcement continuous with that of the roof slab. The wall loading for this test was not expected to be greater than 20 per cent of the incident shock. The floor slab was designed for conventional loading plus blast-load reaction of the walls. The foundations were designed to use an allowable bearing equal to an ultimate strength of 10 tsf. OCDM recommended the ultimate strength value because the soil-boring data were not available at that time.

The test structure was intended to be a typical section of an actual garage-shelter structure, and the design assumed it could be oriented in any direction with respect to GZ. An actual garage-shelter could also have at least two vehicular ramps oriented in opposite directions, as shown in Fig. 1.1, plus at least two emergency personnel exits.

Because of the alternate means of entrance and exit and the many possible orientations, it was decided to design the retaining walls for a nominal loading equal to one-third the incident pressure acting normal to the wall in either direction. The structure was tested with the center line of the ramp oriented on a radial line with GZ because this was the most unfavorable orientation for the end wall and rolling door at the garage entrance.

The end wall, and to a lesser extent the side walls within the region of high reflected and stagnation pressure, was expected to undergo large plastic deformations and fully utilize the restraint afforded by passive resistance of the backfill.

The material strengths used for design of the structure were as follows:

Concrete	4,000 psi (ultimate)
Reinforcing steel (intermediate grade)	47,500 psi (yield)
Structural steel	38,000 psi (yield)

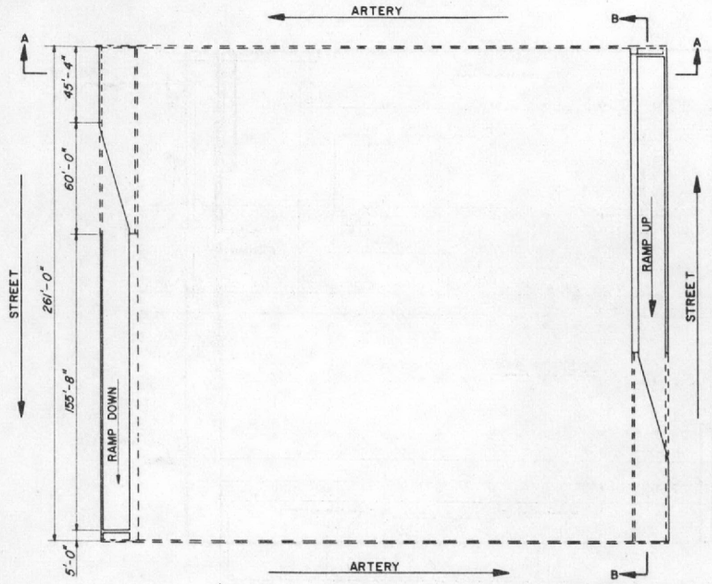

ROOF PLAN

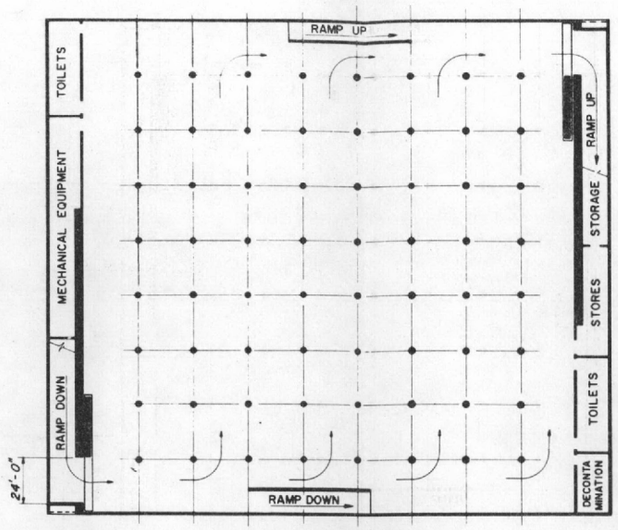

FLOOR PLAN

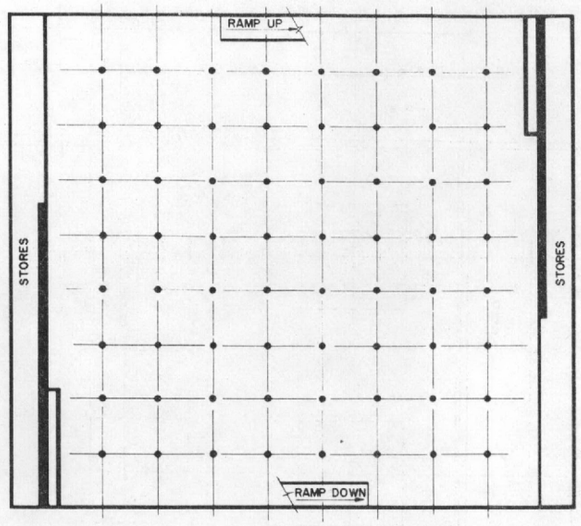

BASEMENT PLAN

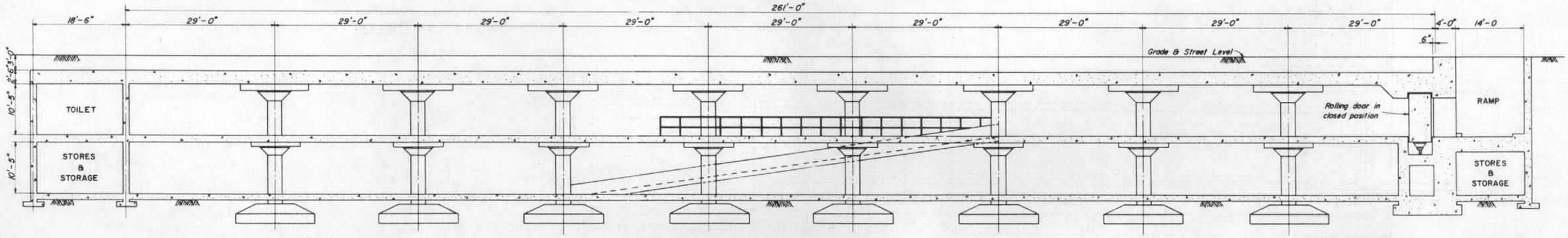

SECTION A-A

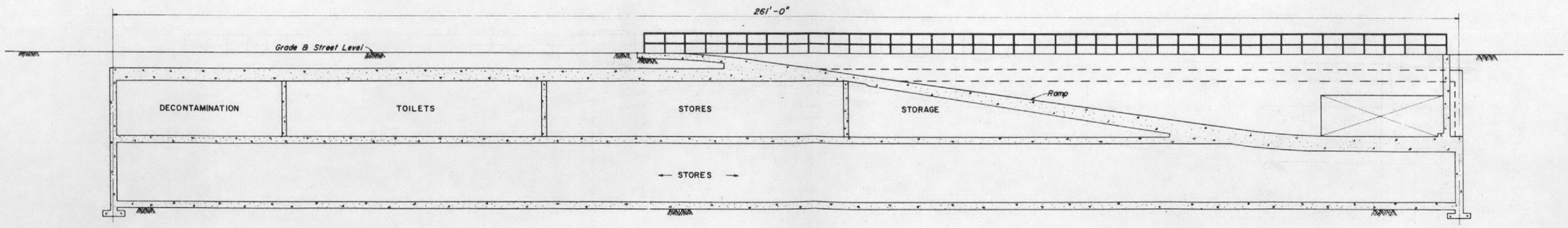

SECTION B-B

Fig. 1.1—Preliminary layout of prototype flat-slab structure.

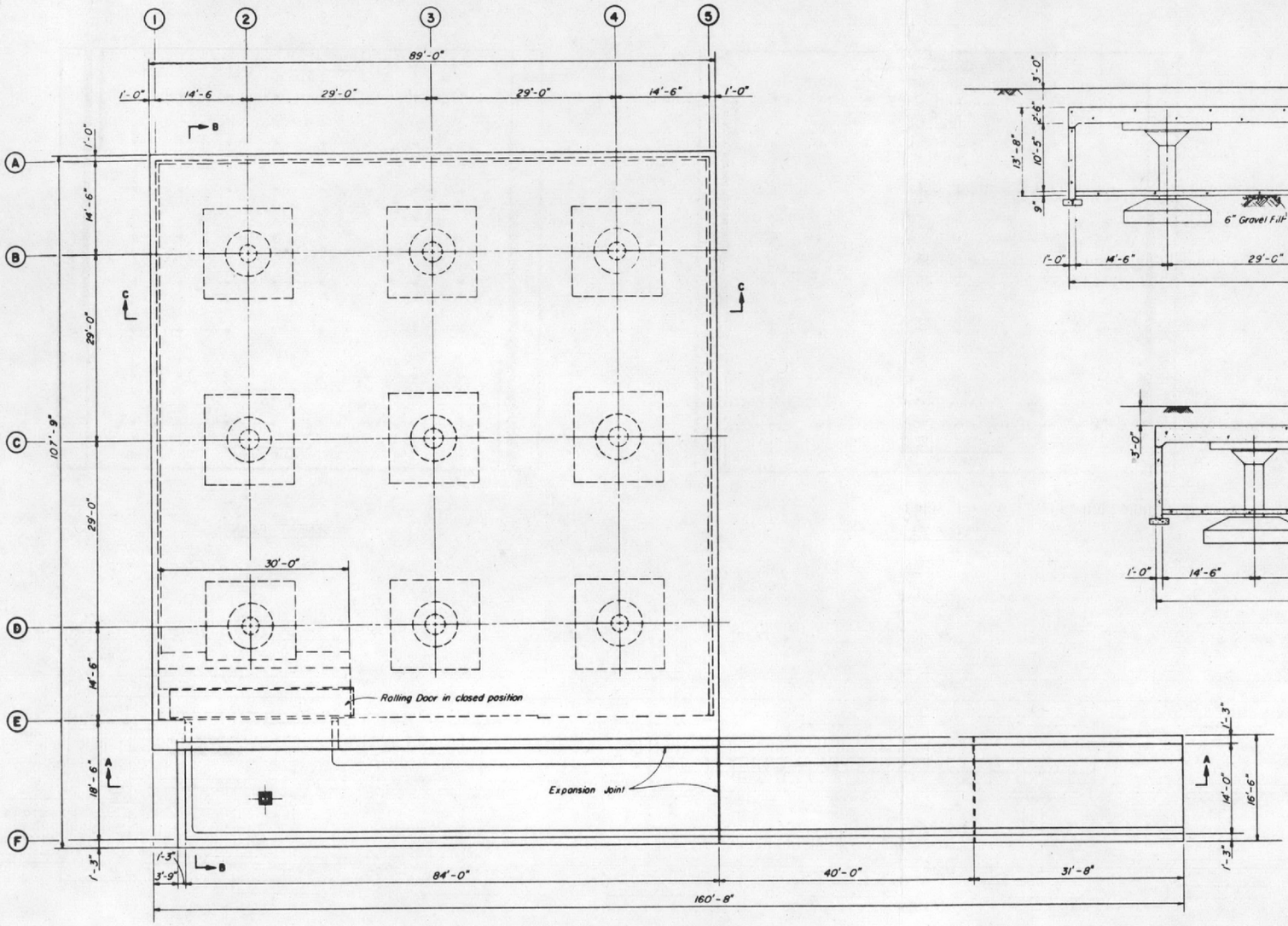

ROOF PLAN

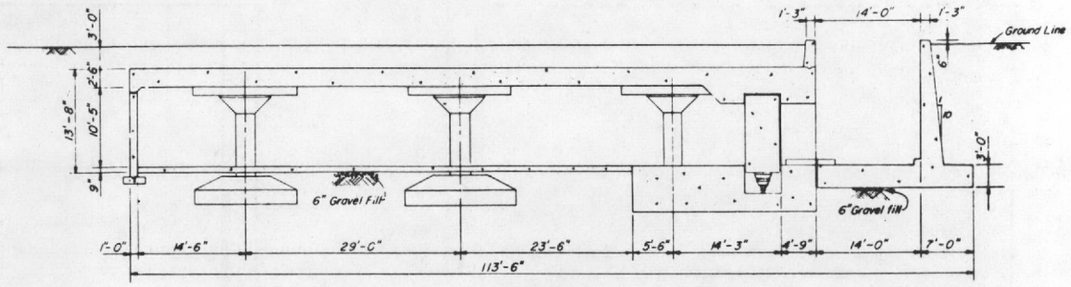

SECTION B-B

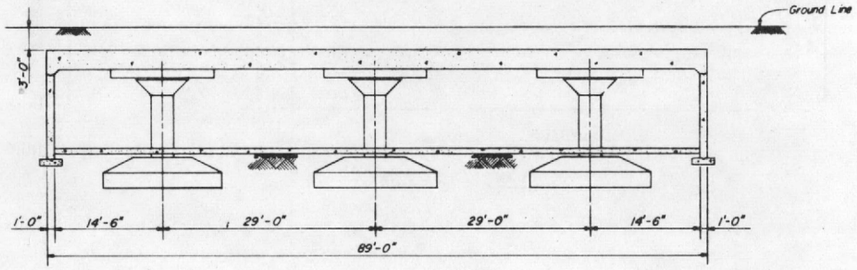

SECTION C-C

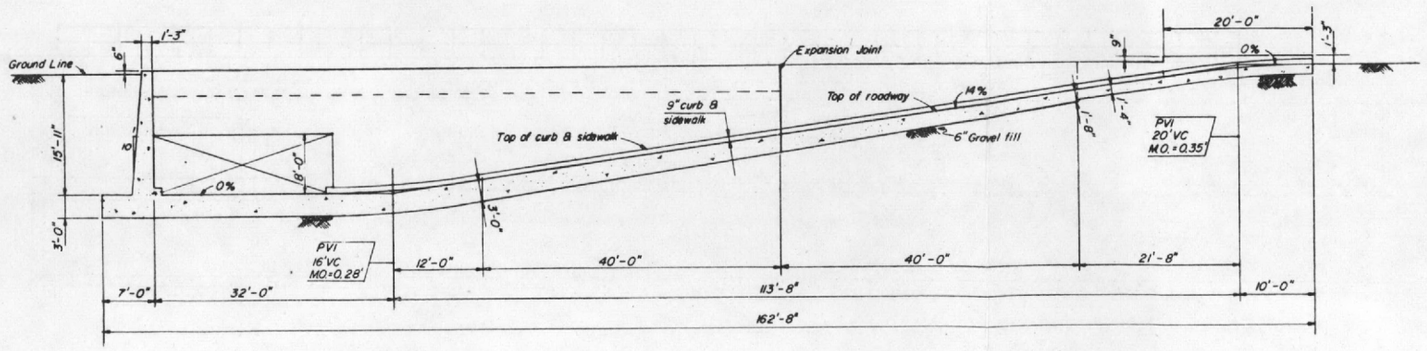

SECTION A-A

Fig. 1.2—Parking garage-shelter underground test section.

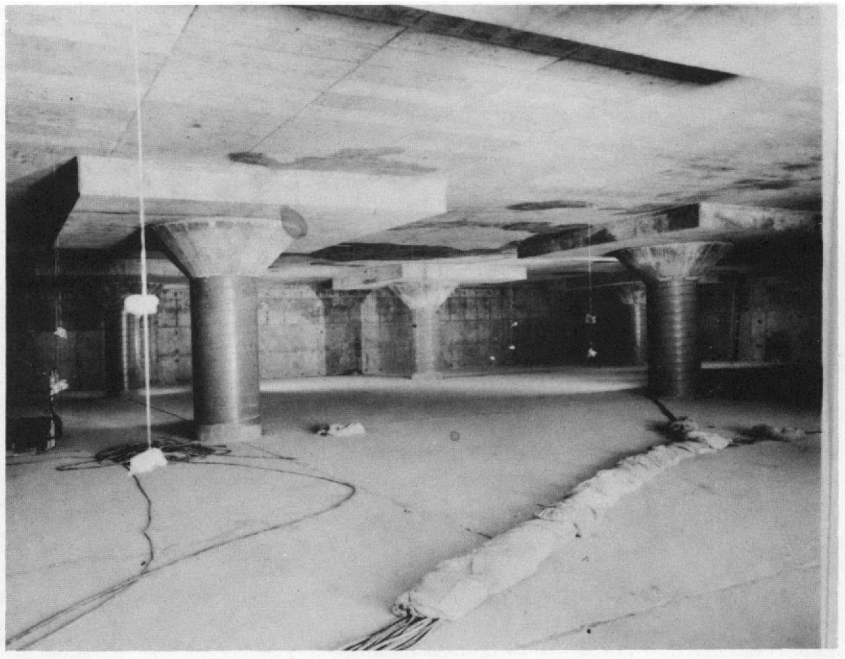

Fig. 1.3 — Interior view showing columns.

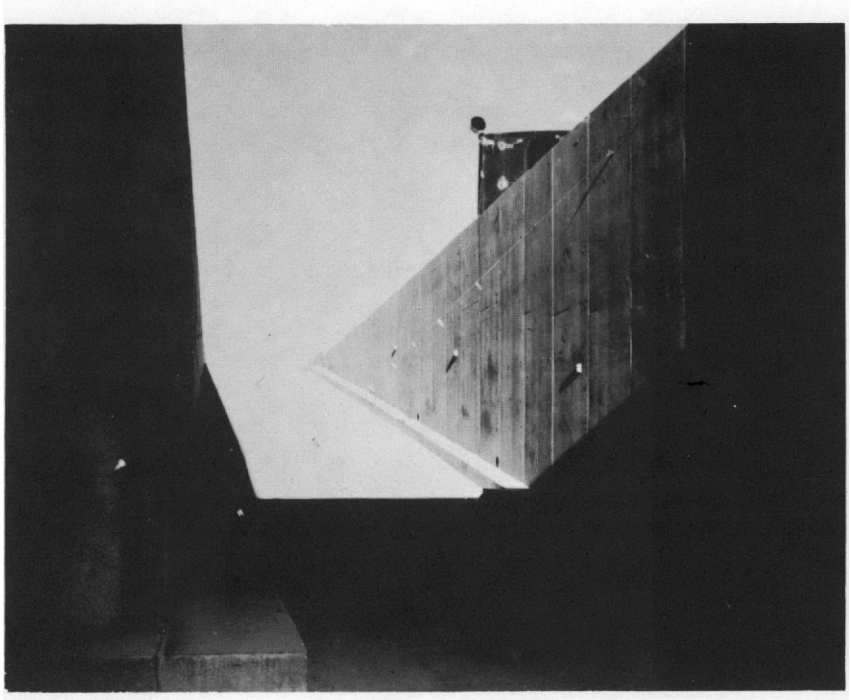

Fig. 1.4 — View of ramp looking up from end wall.

Fig. 1.5—View of ramp looking down toward end wall.

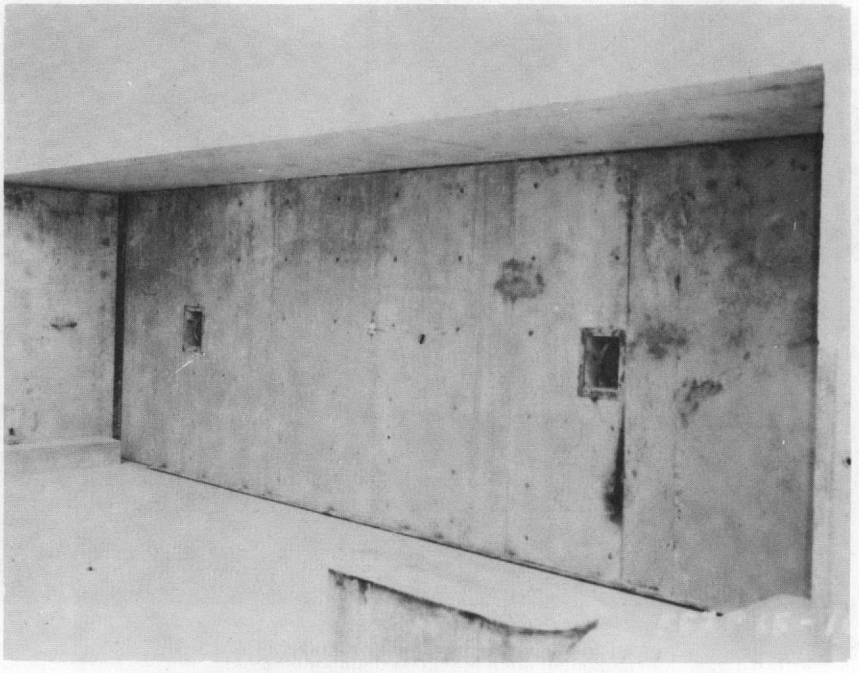

Fig. 1.6—Exterior view of door in closed position.

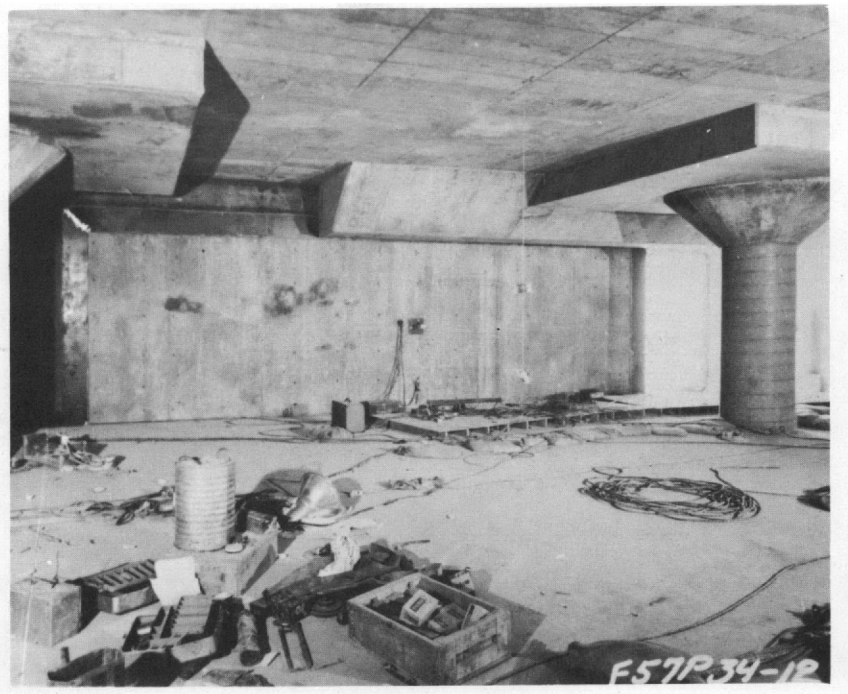

Fig. 1.7—Interior view of door partly open during installation of instruments.

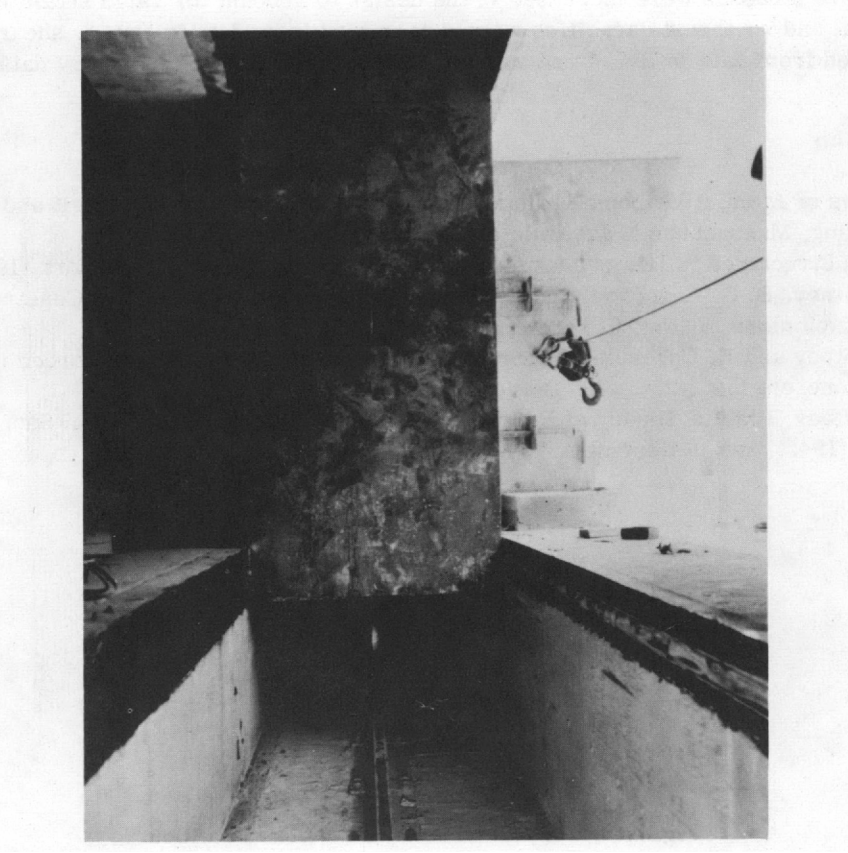

Fig. 1.8—End view of door from door pit.

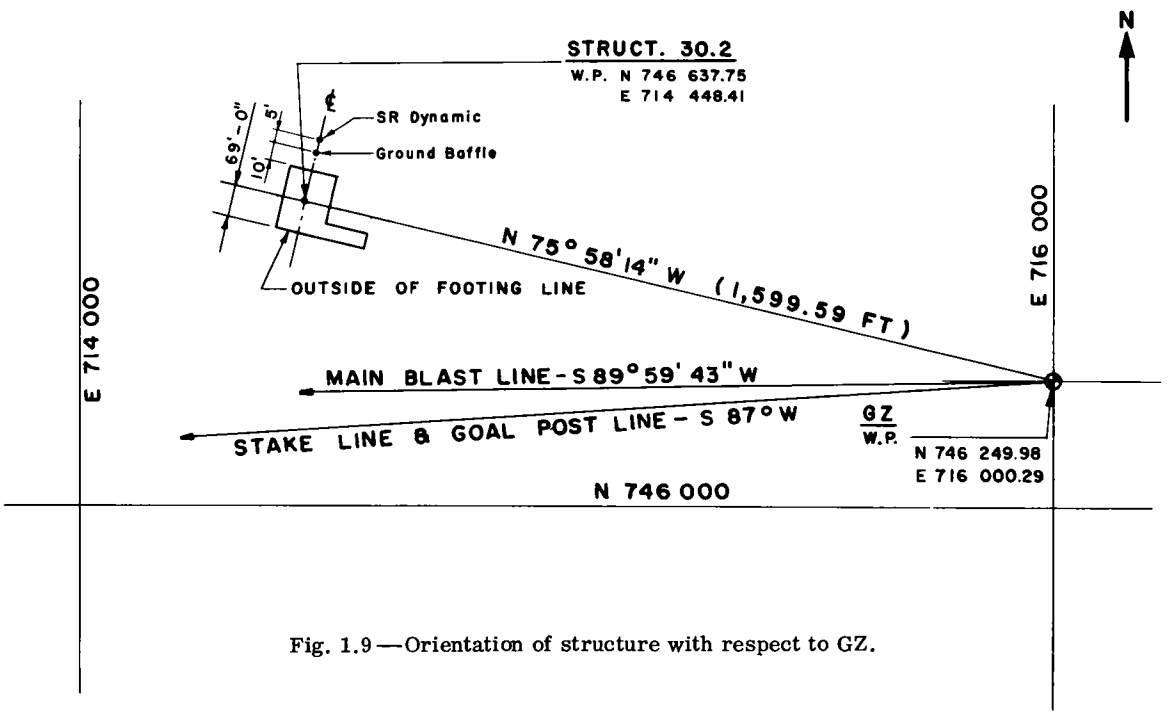

Fig. 1.9 —Orientation of structure with respect to GZ.

The above stresses were increased in the design to account for rapid strain rates.[1,3]

Flexural and/or thrust capacities were determined from data in Ref. 3; shear capacity was computed from data in Ref. 1 and was checked using available laboratory data.

REFERENCES

1. Principles of Atomic Weapons Resistant Construction, Department of Civil and Sanitary Engineering, Massachusetts Institute of Technology, 1954.
2. Design of Structures to Resist Atomic Blast, Ammann & Whitney, New York, 1954.
3. C. S. Whitney, B. G. Anderson, and E. Cohen, Design of Blast Resistant Construction for Atomic Explosions, J. Am. Concrete Inst., 20(7): 589 (March 1955).
4. C. S. Whitney and E. Cohen, Guide for Ultimate Strength Design of Reinforced Concrete, J. Am. Concrete Inst., 28(5) 455 (November 1956).
5. C. S. Whitney, Plastic Theory of Reinforced Concrete Design, Trans. Am. Soc. Civil Engrs., 107: 251 (1942), and in December 1940 proceedings.

Chapter 2

PROCEDURE

2.1 SOIL INVESTIGATIONS

Soil investigations were made by International Testing Corporation,[1] under the direction of Holmes and Narver, at the request of Ammann & Whitney. Three 16-in.-diameter borings 40 ft deep and one 48-in.-diameter shaft 40 ft deep were drilled at the site of the underground parking garage (Fig. 2.1). One 48-in.-diameter shaft and one 16-in.-diameter boring[2] were drilled at the site of the nearby test vault, Project 30.4. The large-diameter shafts were used to obtain undisturbed samples at various depths.

The following tests were made on the samples from the 48-in. holes:

1. Field density
2. Liquid and plastic limit
3. Sieve analysis
4. Unconfined compression tests
5. Consolidation tests to determine the natural vertical state of stress
6. Triaxial tests

The soil encountered was unusual in character and possessed remarkable properties.

The soil consisted of many thinly stratified layers cemented together. The soil was very fine grained (more than 95 per cent passing No. 200 sieve), and was nonplastic or slightly plastic in character ($0 \leq$ plasticity index ≤ 10). There was little variation in soil material, but variations in density occurred from layer to layer, or in small pockets. Pronounced horizontal planes of weakness existed. The cementing agent was thought to be calcium carbonate, which existed in some beds in pieces $\frac{1}{8}$ in. in diameter.

Analysis of the consolidation- and triaxial-test data from undisturbed samples of soil removed from the 48-in.-diameter shafts at the garage structure and the nearby test vault indicated that, within the significant depth region, the soil possessed a natural prestress of about 10 tsf. Table 2.1 contains selected values from the test results. The high triaxial stresses and small strains at failure are especially noted as peculiar characteristics of this soil in its natural state.

A complete description of the sampling methods, testing procedures, and test results is contained in Appendix C. Additional information[3] is available as a result of the soil-testing program of the Waterways Experiment Station, Vicksburg, Miss., and is reported in the Project 3.8 Report, WT-1427.

2.2 SURVEYS

Preshot and postshot high-order field surveys of the horizontal and vertical coordinates of the structure were requested to determine the absolute and relative lateral and vertical displacement of the structure during the blast. The survey points are shown in Fig. 2.2.

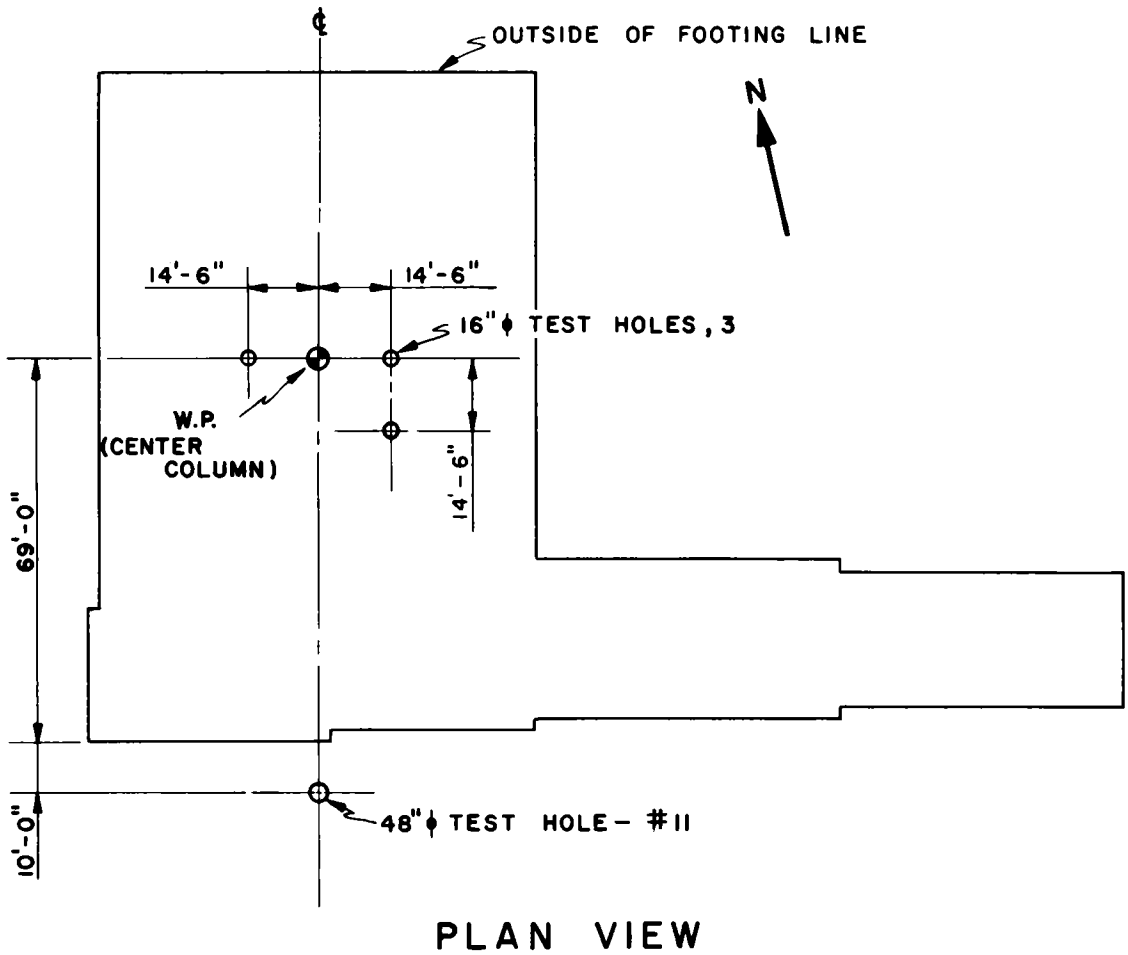

Fig. 2.1— Test holes for structure 30.2.

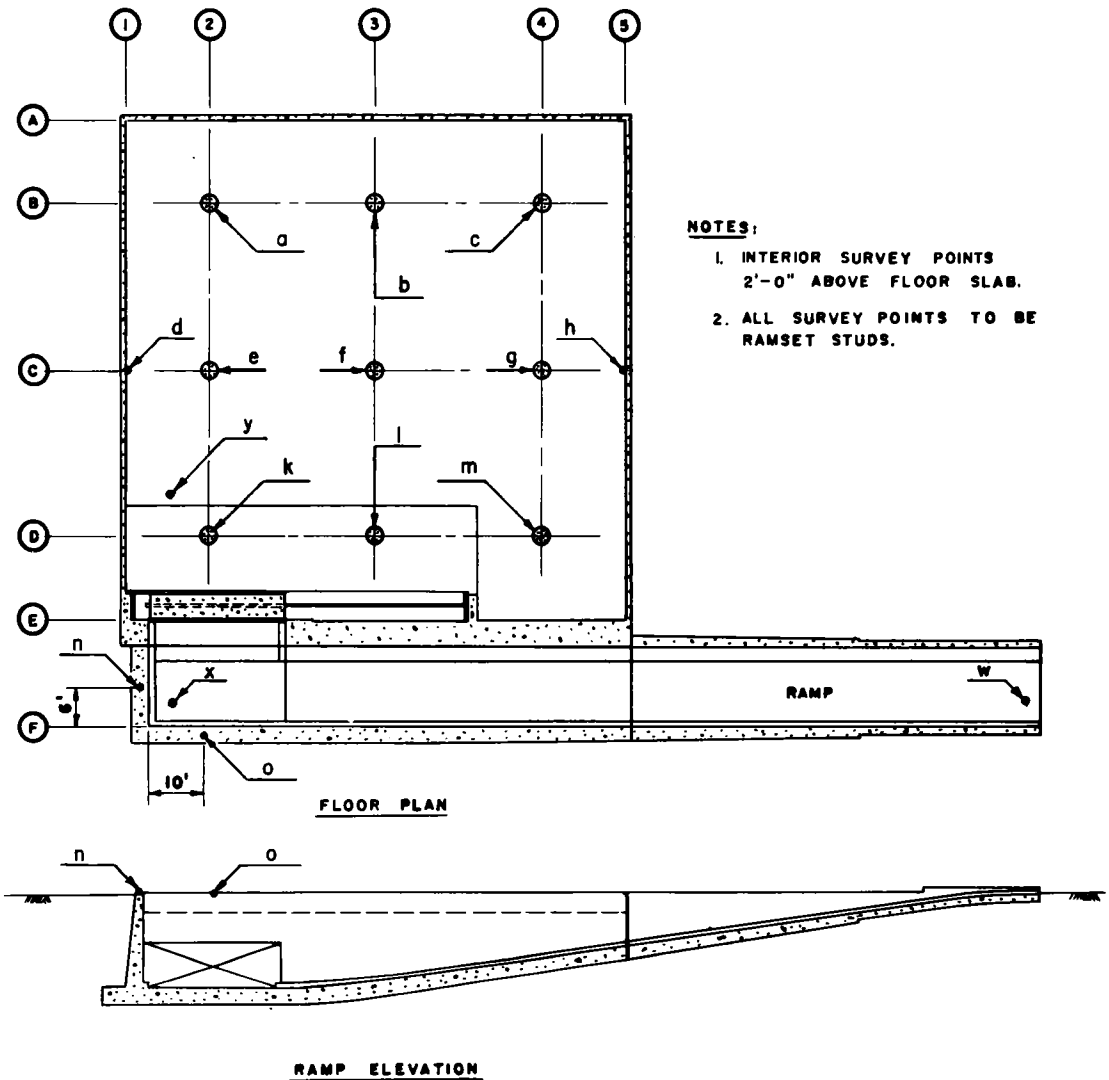

Fig. 2.2—Survey points for structure 30.2.

TABLE 2.1—STRESS-STRAIN RELATIONS, FAILURE-STRESS CONDITIONS, AND SHEARING STRENGTH OF SOILS BY TRIAXIAL TESTS AT A DEPTH OF 17 FT IN 48-IN. BORING[2] OF PROJECT 30.2

Lateral stress (p_3)		Triaxial failure stress		Strain at failure	Max. shearing strength, Tsf
Psi	Tsf	Psi	Tsf	in./in.	
20	1.44	154		0.06	
		140/147	10.6	0.04	5.3
40	2.88	217		0.02	
		238/228	16.4	0.06	8.2
50	3.6	276	19.8	0.07	9.9
61	4.1	197	14.2	0.08	7.1
80	5.8	303*	21.6	0.08	10.8

*No failure.

2.3 INSTRUMENTATION

2.3.1 Pressure and Structural Response

Blast instrumentation,[4] provided by OCDM, was installed by Ballistic Research Laboratories (BRL) and is described in detail in the Project 30.5 Report, WT-1452. Blast instrumentation of the structure proper (Fig. A.10) consisted of Wiancko pressure gauges, a self-recording peak-pressure gauge, Carlson earth-pressure gauges, and a dynamic-pressure gauge near the bottom of the access ramp.

Free-field incident overpressure data were supplied by a BRL self-recording pressure–time gauge located in a ground baffle 10 ft north of the north wall of the structure at about the same radial distance as the structure (Fig. 1.9). A single self-recording dynamic-pressure gauge was also located on a 3-ft-high tower 15 ft north of the north wall (Fig. 1.9).

In addition to the free-field pressure instrumentation supplied for Project 30.5, blast-line instrumentation[5] between 350 and 6000 ft from GZ was supplied by BRL as a part of Project 1.1. A total of 37 self-recording gauges was installed at 16 stations along the main blast line to obtain the desired data for shot Priscilla. Table 2.2 indicates the station numbers, distances, and the numbers and types of gauges used. The gauges referred to as P_t are BRL self-recording pressure–time gauges and q refers to the self-recording dynamic-pressure–time gauges.

Structural response was recorded by BRL deflection gauges. Over-all vertical motion of the central column was referenced to a 29.5-ft-long 4-in.-diameter steel pipe, in an oversized (16 in.) casing, anchored in a concrete block 26 ft below the floor slab (Fig. B.41).

2.3.2 Radiation Instrumentation

Film dosimeters, gamma-radiation differential chemical dosimeters, and one gamma-rate telemetering unit were used to measure radiation. These were supplied by Projects 39.1 (Ref. 6), 39.1a (Ref. 7), and 39.9 (Ref. 8) and were located as shown in Fig. 2.3 and described below.

1. Points a through y have two film dosimeters at each point located 3 and 5 ft above the floor.
2. Points l and u, in addition to the two film dosimeters, have one chemical dosimeter located 2 ft above the floor.
3. Point z is the telemetering unit.
4. Points 1 through 16 have one film dosimeter at each point located as follows:
   a. Points 1 and 2 are on top of the concrete door bumper.
   b. Point 3 is on the inside face of the door 4 ft 6 in. above the top of the floor slab.
   c. Points 4 and 5 are on the bottom of the door pit on each side of the steel rail.

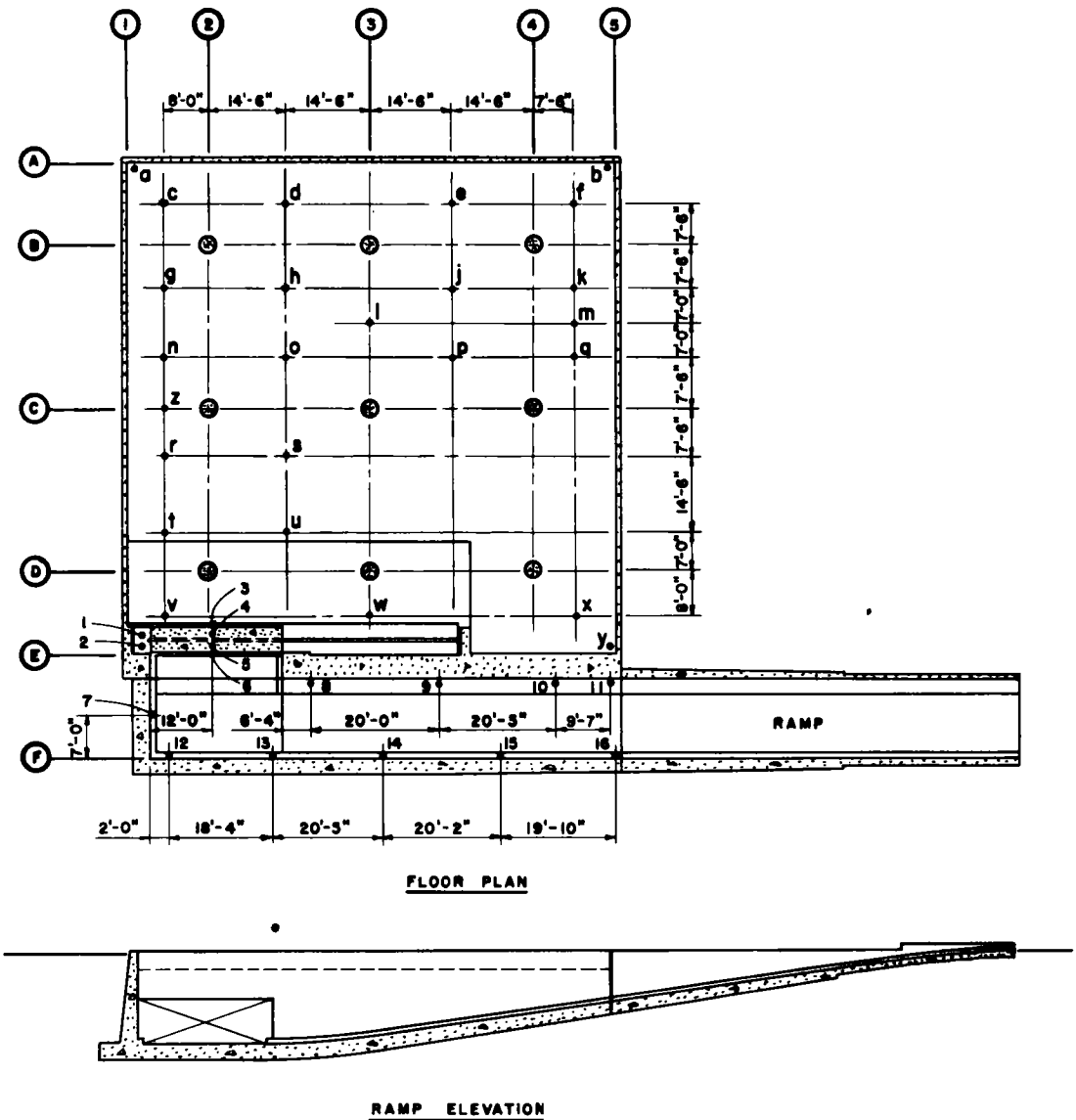

Fig. 2.3—Locations of radiation detectors for structure 30.2.

TABLE 2.2—SUMMARY OF MAIN BLAST-LINE GAUGE INSTALLATION

Station No.	Ground range, ft	No. of gauges P-t	q*
F1.1-9039.01	350	2	
F1.1-9039.02	450	2	
F1.1-9039.03	650	2	
F1.1-9040.01	850	2	1
F1.1-9040.02	1050	2	1
F1.1-9041.00	1350	2	2
F1.1-9042.01	1650	1	1
F1.1-9042.02	2000	1	1
F1.1-9042.05	2250	1	1
F1.1-9042.06	2500	1	2
F1.1-9042.07	3000	1	2
F1.1-9042.03	3500	1	1
F1.1-9042.08	4000	1	2
F1.1-9042.04	4500	1	1
F1.1-9043.01	5000	1	1
F1.1-9043.02	6000	1	

* Where two q gauges are listed for one station, the second q gauge was a new design undergoing proof testing.

d. Point 6 is on the outside face of the door 4 ft 6 in. above the top of the ramp slab.
e. Points 7 through 16 are on the garage and ramp walls 5 ft above the top of the curb and sidewalk.

The date of placement of the various detectors located at the points indicated on Fig. 2.3 are as shown in Table 2.3.

Film dosimeters and gamma-radiation differential chemical dosimeters were used to measure radiation along the stake and goal-post lines. These were supplied and installed by Projects 39.1a and 39.1, respectively. Exact date of placement of the free-field dosimetry is not known, but it is presumed to be within D−3 before the shot.

TABLE 2.3—DATE OF PLACEMENT OF RADIATION-DETECTION EQUIPMENT

Point	Detector type	Date placed
a through y	Film dosimeter	6-18-57
l and u	Chemical dosimeter	
z	Telemetering unit	6-21-57
1 through 6	Film dosimeter	6-22-57
7 through 16	Film dosimeter	6-20-57

REFERENCES

1. Soil Test Data, Frenchman Flat, Nevada Test Site, Mercury, Nevada, prepared by Nevada Testing Laboratories, Ltd., Las Vegas, Nevada, and International Testing Corporation, Long Beach, California.
2. E. Cohen, E. Laing, and A. Bottenhofer, Response of Protective Vaults to Blast Loading, Operation Plumbbob Report, WT-1451, Ammann & Whitney, April 1961.

3. T. B. Goode et al., Soil Survey and Backfill Control in Frenchman Flat, Operation Plumbbob Report, WT-1427, Oct. 23, 1959.
4. J. J. Meszaros et al., Instrumentation of Structures for Air-Blast and Ground-Shock Effects, Operation Plumbbob Report, WT-1452, January 1960.
5. E. J. Bryant, J. H. Keefer, and J. G. Schmidt, Basic Air-Blast Phenomena, Part I, Operation Plumbbob Report, ITR-1401, Oct. 25, 1957. (Classified)
6. S. Sigoloff et al., Gamma Measurements Utilizing the USAF Chemical Dosimeters, Operation Plumbbob Report, WT-1500, November 1958. (Classified)
7. Edgerton, Germeshausen & Grier, Inc., Gamma Dosimetry by Film-badge Techniques, Operation Plumbbob Report, WT-1466, July 1959. (Classified)
8. H. M. Borella and S. C. Sigoloff, Remote Radiological Monitoring, Operation Plumbbob Report, WT-1509, November 1958.

Chapter 3

BLAST RESULTS

3.1 STRUCTURAL

The exposed wall of the garage withstood the blast with no damage. The ramp wall at column line F had several large cracks between the end wall and a point about 30 ft up the ramp (Fig. 3.1). The top of the ramp side wall opposite the door entrance was pushed into the earth about 1 ft at the end. The top edge of the ramp wall farther up the ramp showed little

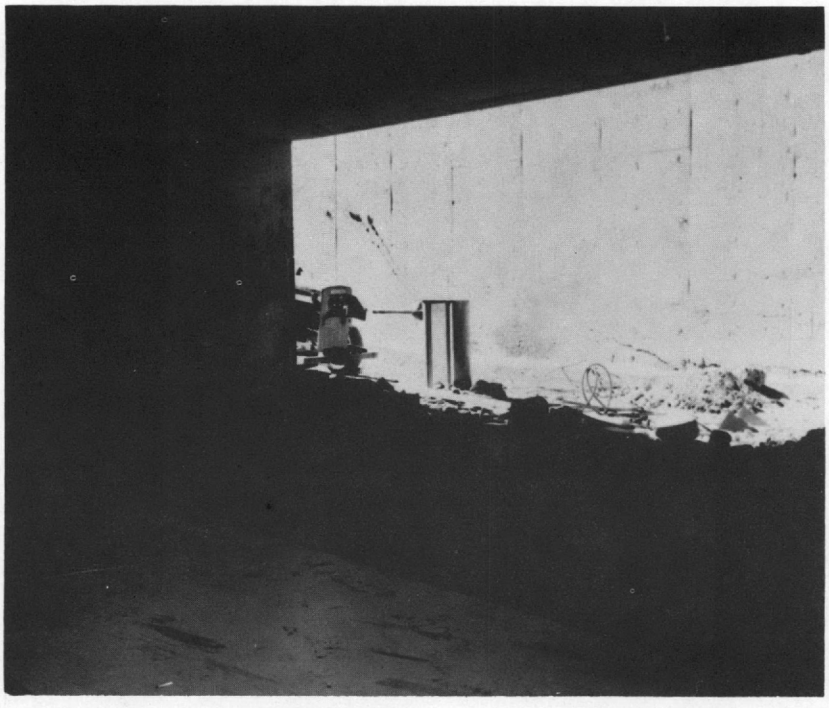

Fig. 3.1 — Cracks in ramp side wall opposite door. View from interior of garage through door opening (postshot).

apparent displacement. Although there was no visible damage to the ramp slab, the slab was separated up to ½ in. from the main garage structure at the expansion joint (Fig. 3.2), and the ½-in. joint filler was blown down or out. Gravel backfill was sucked through the weepers onto the ramp (Fig. 3.3). More gravel was found opposite the weepers at the mid-length and toward the top of the ramp than opposite the weepers at the lower end.

Fig. 3.2—Open joint between ramp slab and wall of main garage structure (postshot).

Fig. 3.3—Gravel backfill at weepers (postshot).

The end wall of the ramp was the only area badly damaged (Figs. 3.4 and 3.5). The top 8 ft of the end wall was broken off as a single unit on a nearly horizontal plane at the top of the splice of the vertical steel. It tipped into the backfill and slipped over the lower section until it wedged tightly between the garage wall and the longitudinal wall of the ramp. It was torn

Fig. 3.4—View of ramp looking toward damaged end wall (postshot).

loose on a diagonal through the corner at its junction with the longitudinal retaining wall. In its final position the top was displaced approximately 5 ft 6 in. into the earth backfill, which was pushed up and mounded. It was estimated that it may have been displaced approximately 8 ft before sliding back. The concrete cover had split off most of the lower section, and the bars had separated at the splice, apparently without having developed their yield strength. Near the middle of the panel where the concrete had not split, three bars had fractured after necking down at the top of the splice (Fig. 3.6).

The bars in the lower section were bent away from the displaced concrete; the cover was deposited at the base (Fig. 3.7). The remaining concrete behind the bars was reduced to rubble, which varied in size from 6 in. to 3 ft in diameter. Fractures, including the one at the bottom of the top section of the damaged end wall, revealed no breaks through the aggregate. The concrete had also separated on the plane of the rear-face reinforcement.

The end corner of the 1-ft 3-in. parapet wall at the lower end of the ramp was cracked as shown in Fig. 3.5.

The door withstood the blast without any evidence of shifting or disalignment. Locking bolts in the door were intact and retracted freely (Fig. 3.8). The ¼-in. cover-plate angle at the exposed top edge of the door frame was separated from the concrete at several locations. The 12-in. steel guide plate on the 4.5-ft wall was not made continuous as intended and was torn back by the door during the postshot opening (Fig. 3.9). The door wheels were not damaged, and the track was not displaced (Fig. 3.10). The door and end pilaster were partially blackened by thermal radiation.

The pneumatic gasket around the door frame was blown in and torn apart by the blast pressure (Fig. 3.11). The gasket had a slow leak prior to the shot, and a compressed-air cylinder was installed outside in the doorway recess to maintain the air pressure. The cylinder and air hose were sandbagged and were not damaged by the blast. No information is available regarding the condition of the gasket at shot time.

No damage to the garage interior was observed. Lateral movement of the isolated columns was indicated by a small amount of concrete spalling and cracking of the floor slab around the perimeter of the column. The cracking occurred at the blast side of the columns, and the spalling occurred at the leeward side.

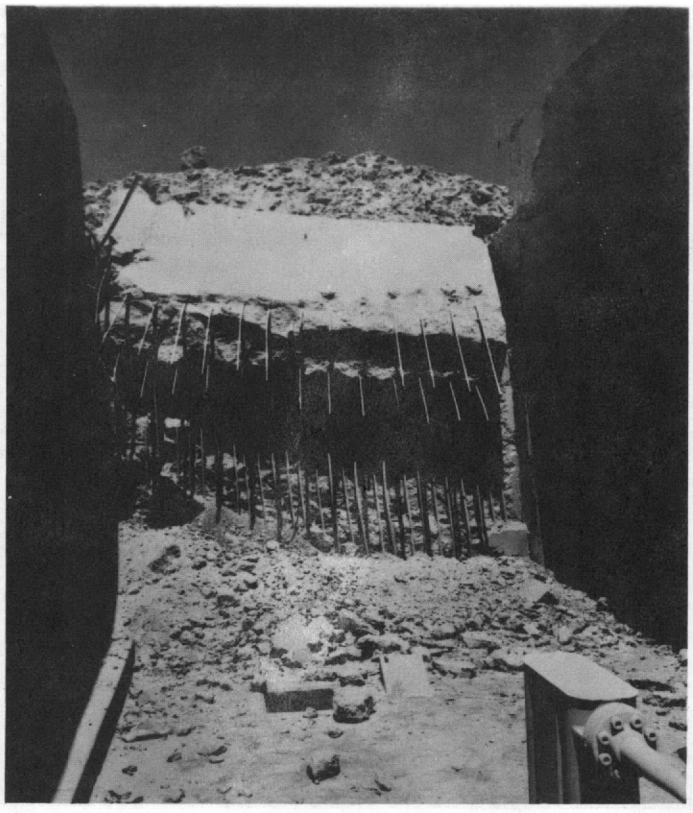

Fig. 3.5 — Close-up of damaged end wall (postshot).

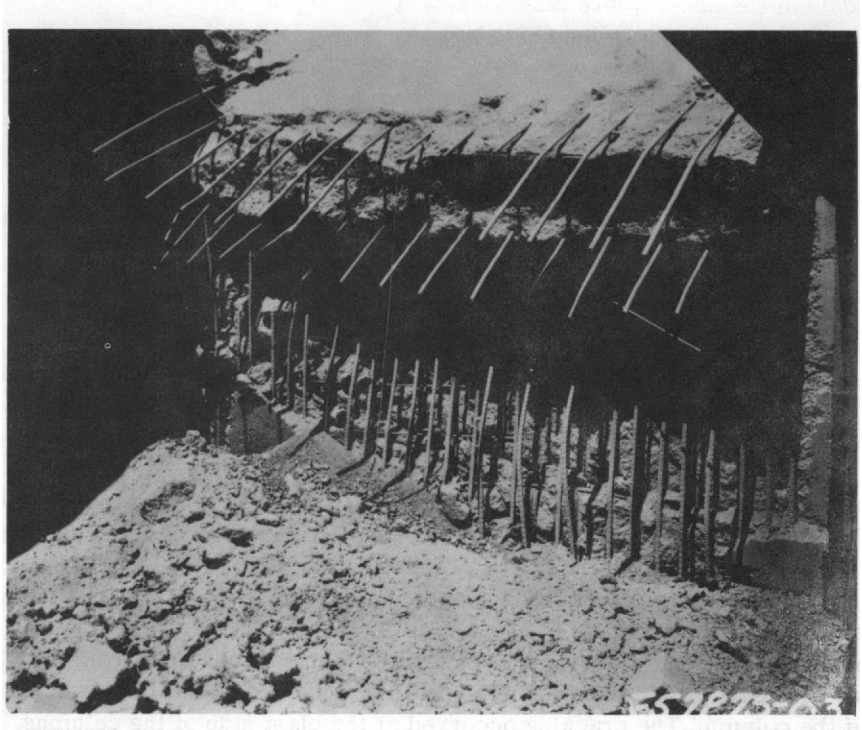

Fig. 3.6 — Detail of failure showing fractured bars (postshot).

Fig. 3.7— Detail of lower portion of wall (postshot).

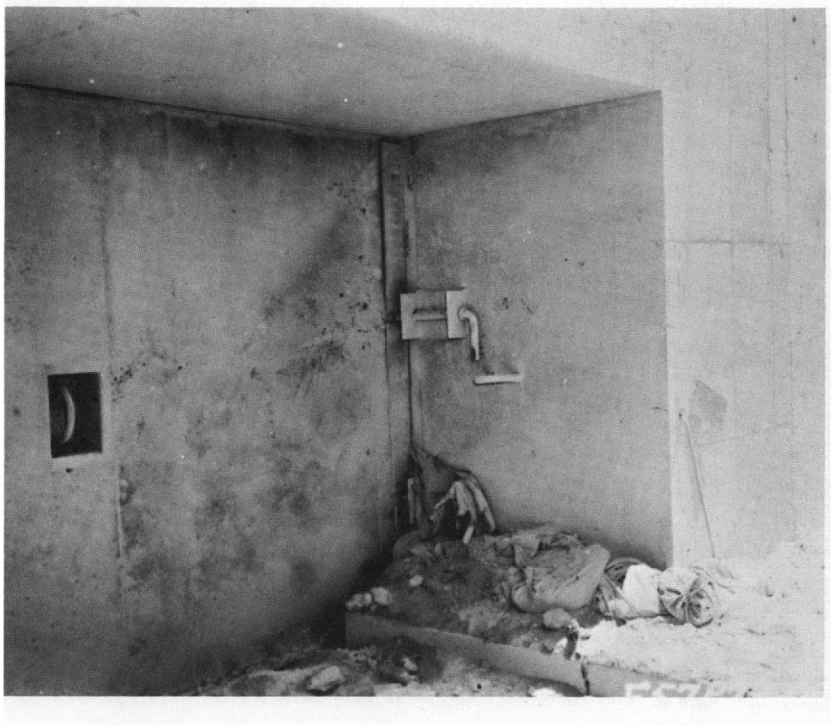

Fig. 3.8— View of door showing locking bolts (postshot).

Fig. 3.9 — Torn guide plate before removal to allow opening of door (postshot).

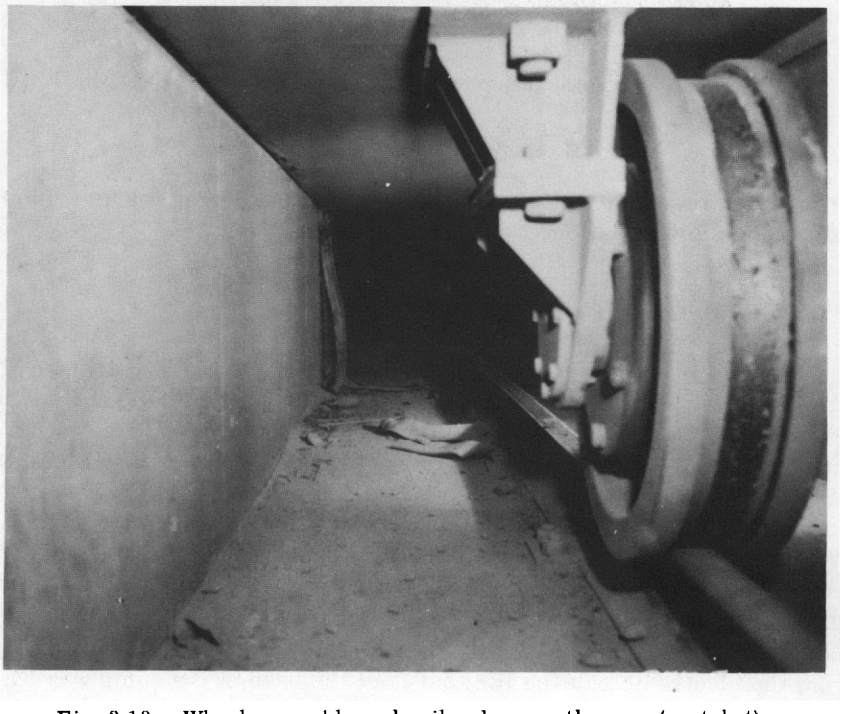

Fig. 3.10 — Wheel assembly and rails, door partly open (postshot).

There was no obvious soil settlement in the vicinity of the garage. However, surface soil cracks up to $2\frac{1}{2}$ in. wide were opened around the projected perimeter of the roof slab of the structure. Another surface crack was opened parallel to the ramp wall at column line E (Fig. 1.2) about 6 ft from the outside face of the parapet wall, extending from a position about 30 ft from the top of the ramp to the crack along column line 5. A similar crack was observed

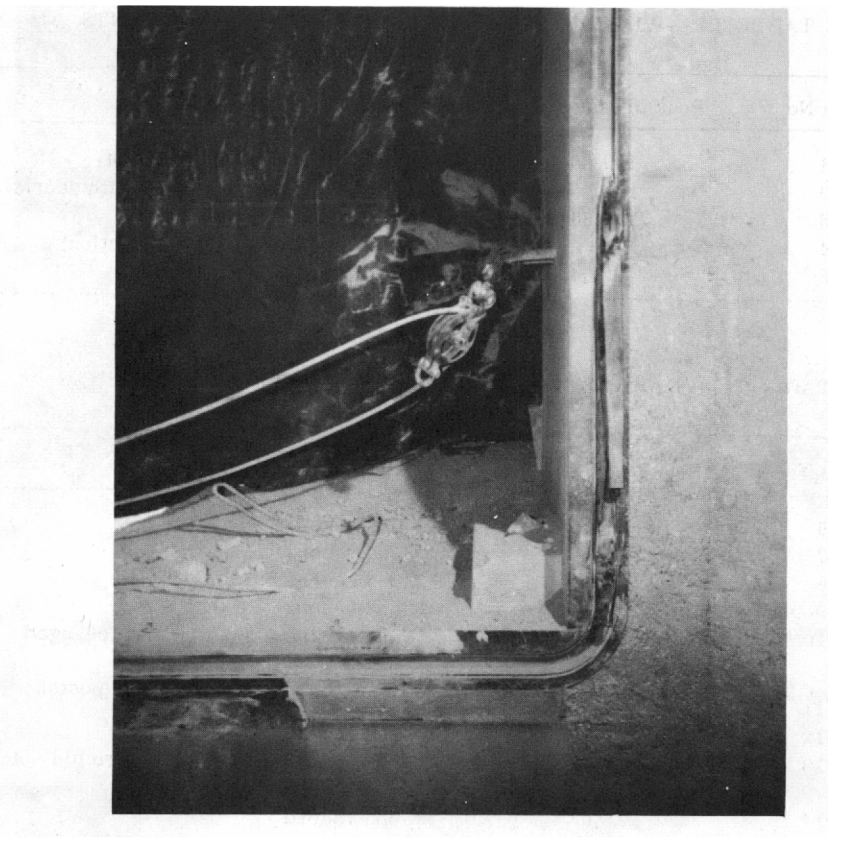

Fig. 3.11 — Damaged gasket at lower corner of door opening (postshot).

about 6 ft away from the ramp wall at column line F, extending as far as column line 3 along the approximate line of excavation.

3.2 PRESSURE AND STRUCTURAL RESPONSE

The peak results from records obtained from the Project 30.5 instrumentation program[1] are summarized in Tables 3.1 to 3.3. Table 3.1 lists the peak values for the Wiancko pressure gauges which were located on the rolling door and the ramp end and side walls. Results of the Carlson earth-pressure gauges in the shelter roof slab, rolling door, and walls, and in the ramp end and side walls are given in Table 3.2. Table 3.3 contains the peak values obtained from the deflection gauges placed inside the structure and on the ramp.

The BRL self-recording peak-pressure gauge placed within the structure was equipped with a 5-psi capsule. This gauge functioned as required, and a peak interior overpressure of approximately 1.0 psi was recorded. The electronic dynamic-pressure (QD) gauge placed at the base of the ramp was packed with debris, and no record was obtained. The peak pressure obtained from the electronic side-on (QS) gauge at the base of the ramp was 54.36 psi.

The self-recording pressure-time gauge in the free-field ground baffle (Fig. 1.9) recorded a peak pressure of 38.95 psi, and the peak dynamic pressure at the same radial distance was recorded by a self-recording dynamic-pressure gauge. The peak dynamic and peak side-on pressures for this gauge were 112 psi (corrected) and 40 psi, respectively.

The pressure–time and deflection–time records for the gauges on the structure (Fig. A.9) are shown in Figs. 3.12 to 3.16.

Tabulated results[2] of the maximum values obtained from the blast-line instrumentation provided by Project 1.1 are given in Tables 3.4 and 3.5. Table 3.4 contains the values for the

TABLE 3.1—WIANCKO AIR-PRESSURE-GAUGE MEASUREMENTS
(PEAK VALUE)

Gauge No.	Peak pressure, psi	Remarks
P1	109.65	Good record (shift during shot)
P2	266.46	Good record (gauge packed with debris)
P3	104.86	Good record
P4		Record no good (faulty connection)
P5	22.04	Good record

TABLE 3.2—CARLSON EARTH-PRESSURE-GAUGE MEASUREMENTS
(PEAK VALUE)

Gauge No.	Peak pressure, psi	Remarks
$\bar{P}6$	21.27	Good record
$\bar{P}7$	32.11	Good record
$\bar{P}8$	31.05	Good record
$\bar{P}9$	28.17	Good record
$\bar{P}10$		Unreadable (system balance changed before shot)
$\bar{P}11$	41.51	Good record
$\bar{P}12$	3.55	Good record
$\bar{P}13$	2.81	Good record (ground pressure did not return to original zero)
$\bar{P}14$	5.05	Good record
$\bar{P}15$		No record (gauge cable broken)
$\bar{P}16$		Record no good (faulty connection)

maximum overpressure, arrival time, positive duration, and total positive-phase impulse for the self-recording pressure-time (P_t) gauges. The maximum values of the total pressure, static overpressure, pressure difference, dynamic pressure, and Mach number for the self-recording dynamic-pressure (q) gauges are given in Table 3.5. The curves of maximum overpressure vs. ground distance for the P_t gauges are given in Fig. 3.17. Figure 3.18 is the curve of corrected dynamic pressure vs. ground range for the q gauge maximum values.

A complete description of the results obtained from the instrumentation program can be found in the Project 30.5 Report, WT-1452 (Ref. 1), and the Project 1.1 Report, ITR-1401 (Ref. 2).

A comparison of the free-field pressure data recorded at the blast-line 1600-ft range (interpolated from Tables 3.4 and 3.5) with the data recorded by the gauges (Fig. 1.9) adjacent to the garage (gauges approximately 445 ft from the blast line and 1600 ft from GZ) is given in Table 3.6.

3.3 RADIATION INSTRUMENTATION

All radiation-detection equipment was located as indicated in Fig. 2.3.

Owing to the high exterior residual-radiation level, it was not possible to open the structure until D + 6. Consequently the recovery of all interior radiation-detection equipment was delayed until this time.

The results of the gamma-radiation film dosimeters placed at points a through y at the 3- and 5-ft heights and the single film dosimeters at points 1 and 2 are indicated in Table 3.7. There are no records available for the film dosimeters placed on the inside face of the door or in the door pit, locations 3, 4, and 5.

TABLE 3.3—DEFLECTION-GAUGE MEASUREMENTS (PEAK VALUE)

Gauge No.	Peak wire movement, in.	Peak deflection, in.	Remarks
D1	0.1196	0.25	Good record (center column)
D2	0.2851	0.48	Bad record (column strip)
D3	0.1900	0.32	Good record (column strip)
D4	0.2913	0.49	Good record (column strip)
D5	0.2274	0.38	Good record (column strip)
D6	0.1889	0.31	Good record (column strip)
D7	0.1182	0.20	Good record (column strip)
D8	0.1133	0.19	Good record (column strip)
D9	0.1761	0.29	Good record (column strip)
D10	0.2154	0.46	Good record (center of panel)
D11	0.2723	0.58	Good record (center of panel)
D12	0.2411	0.52	Good record (center of panel)
D13	0.1964	0.42	Good record (center of panel)
D14	−0.0572, +0.0434	−0.16, +0.12	Good record (wall at line 5)
D15			Unreadable (system balance changed before shot)
D16			Gauge destroyed at blast arrival
D17			Gauge destroyed at blast arrival
D18			Unreadable (system balance changed before shot)

All film dosimeters in the ramp that were fastened with a single wire and two ramset bolts were dislodged. One of the two exterior film dosimeters fastened with two 1-in. light-gauge steel straps and four expansion bolts was damaged and remained on the outside face of the door (location 6). However, no evaluation of this dosimeter was obtained.

In the interior of the structure, at points l and u, a gamma-radiation chemical dosimeter was located 2 ft above the floor slab. The doses, however, were too low to be read with the chemical dosimeters.

At point z, a gamma-radiation telemetering instrument[3] was placed as a part of Project 39.9. The decay pattern for the radiation intensity (mr/hr) vs. time (min), as obtained from this remote radiological monitoring instrument, is indicated in Fig. 3.19. There is no record from time of detonation until time of first challenge (H + 5 min); therefore the integrated dose cannot be obtained from this record.

(Text continues on page 50)

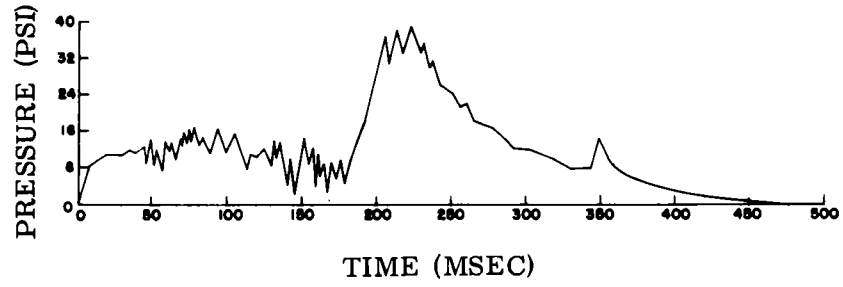

Fig. 3.12—Free-field ground baffle, pressure-time record.

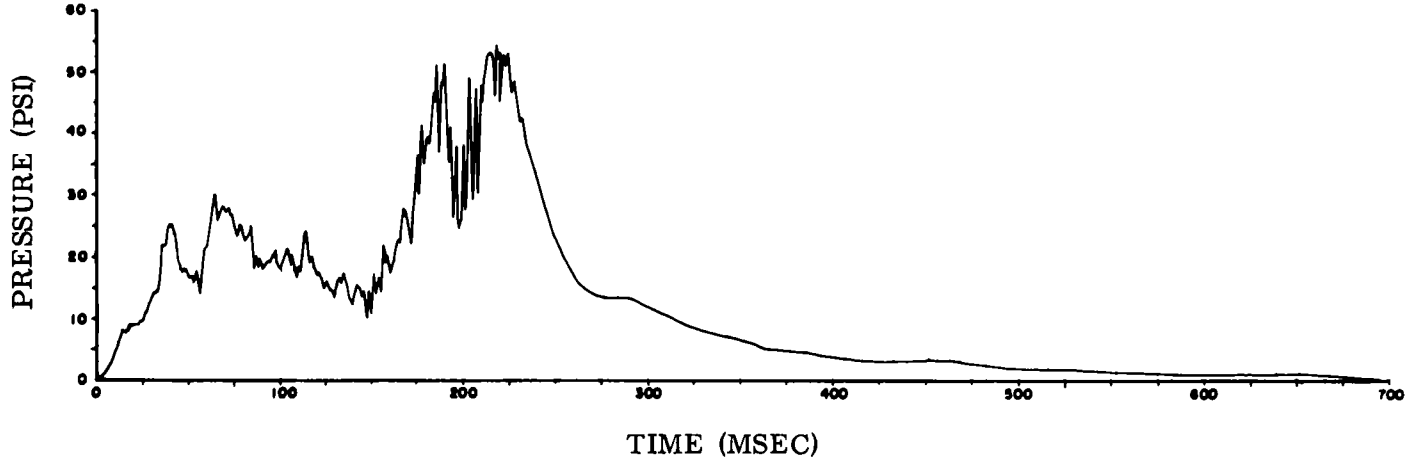

Fig. 3.13—Base of ramp, side-on pressure-time record.

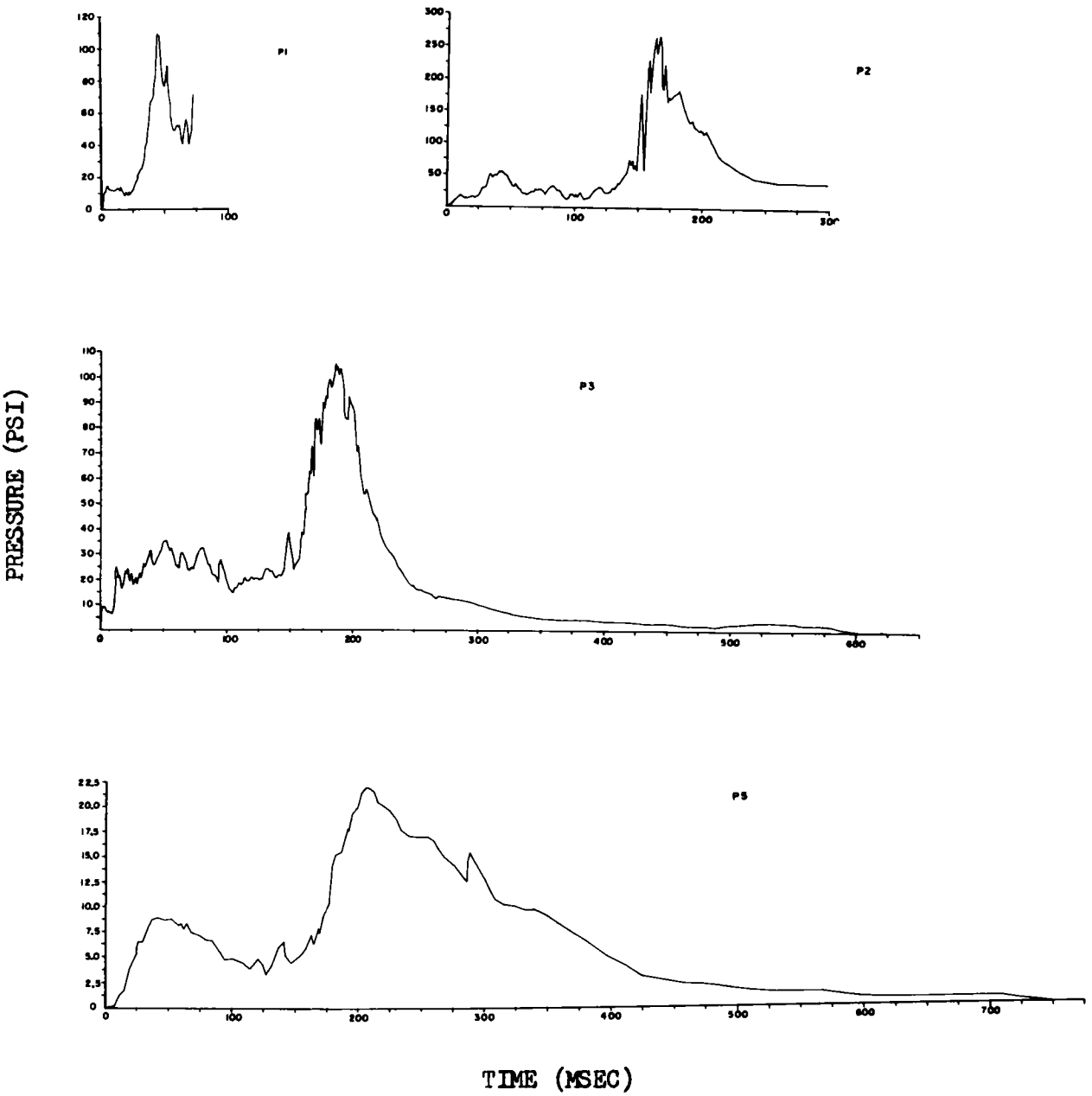

Fig. 3.14—Wiancko air-pressure-gauge records.

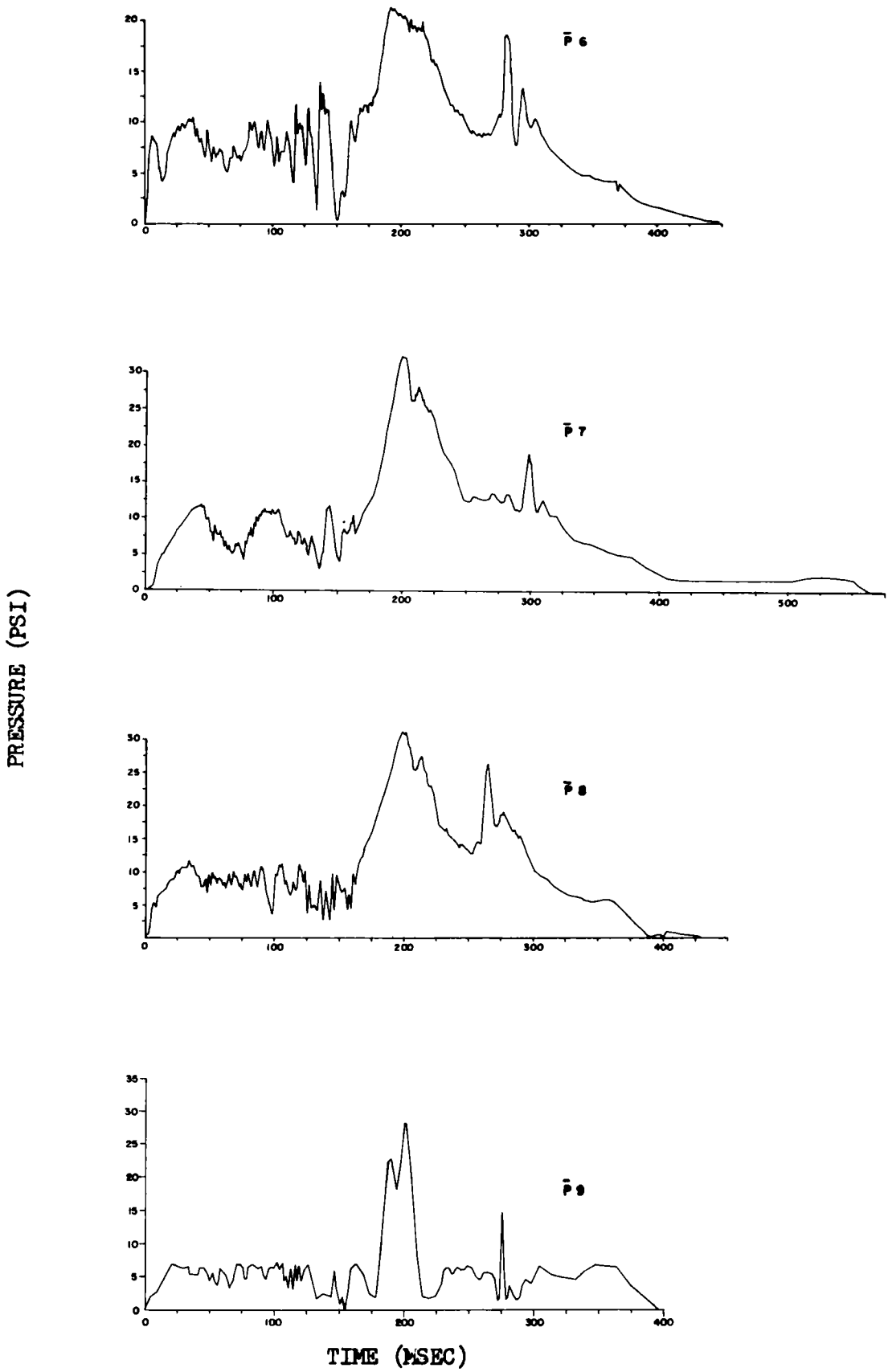

Fig. 3.15—Carlson earth-pressure-gauge records.

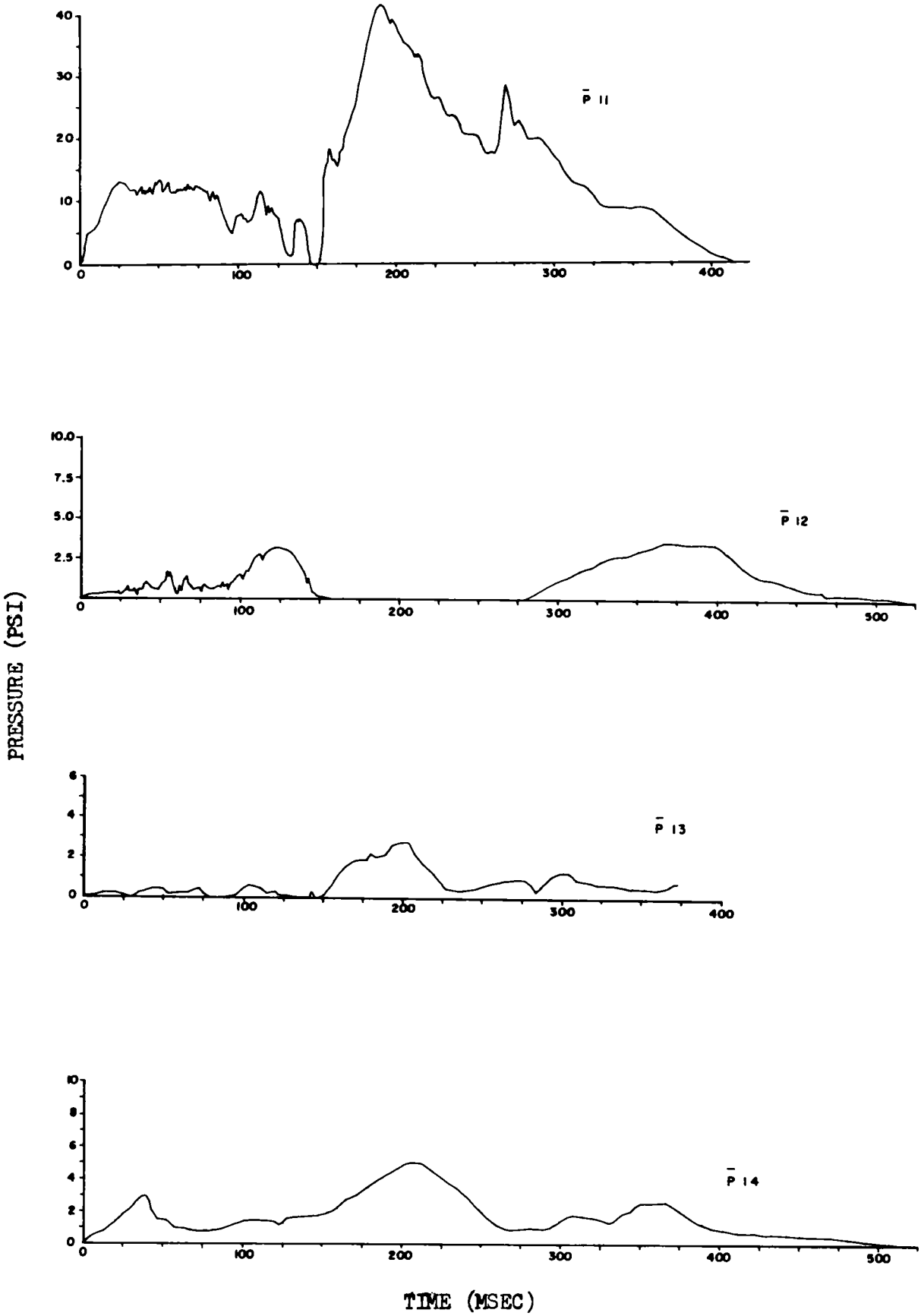

Fig. 3.15—(Continued)

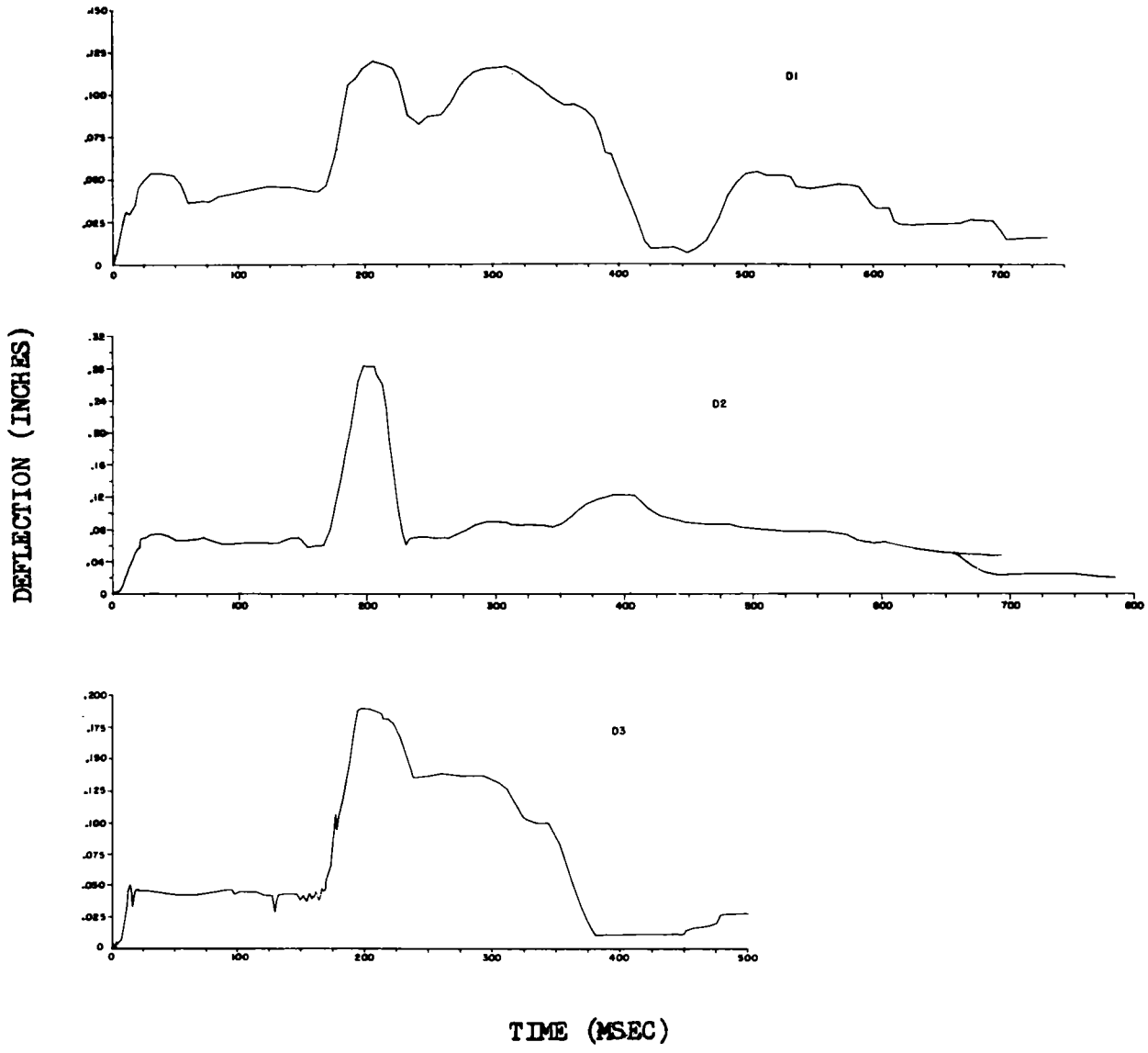

Fig. 3.16—Deflection-gauge records.

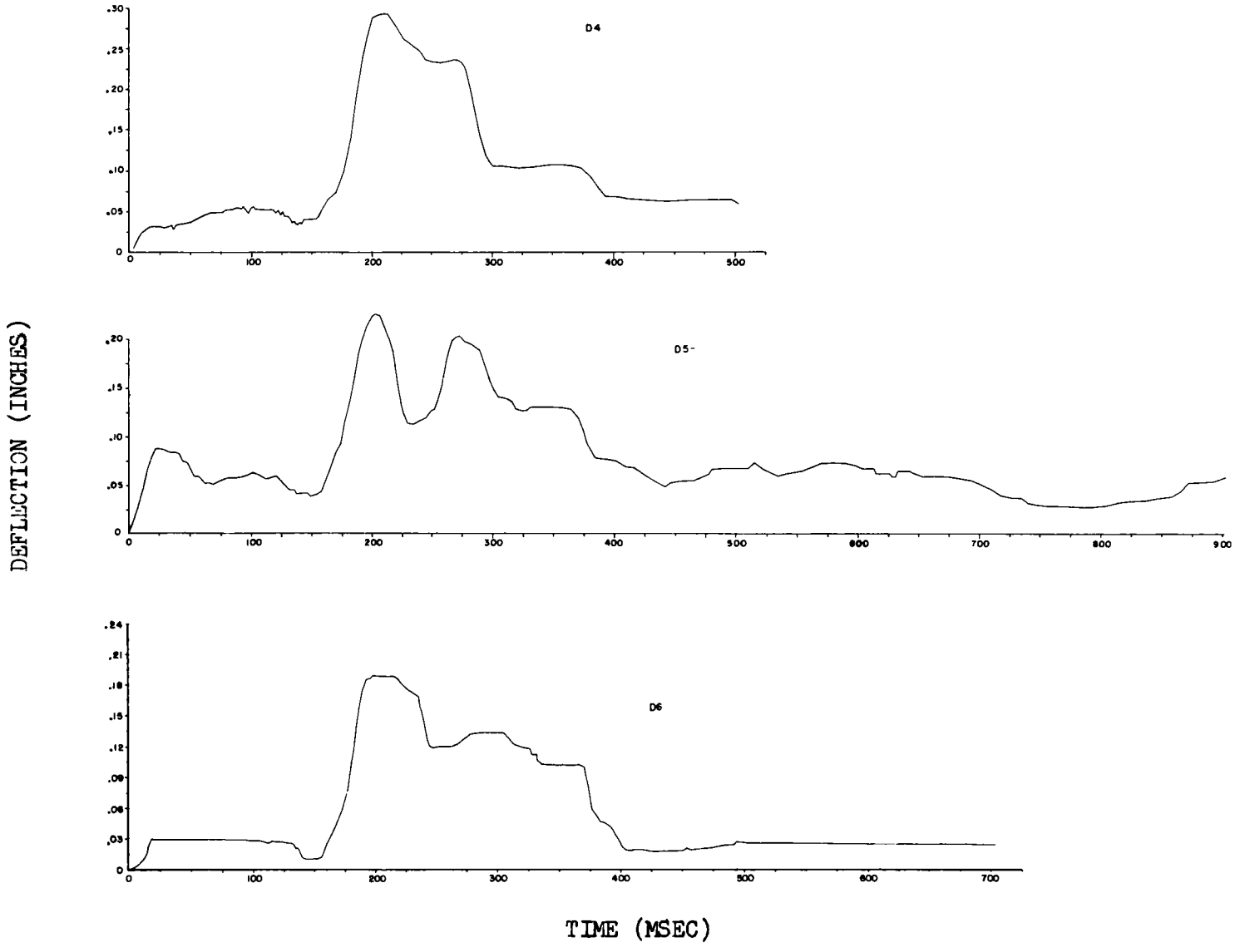

Fig. 3.16—(Continued)

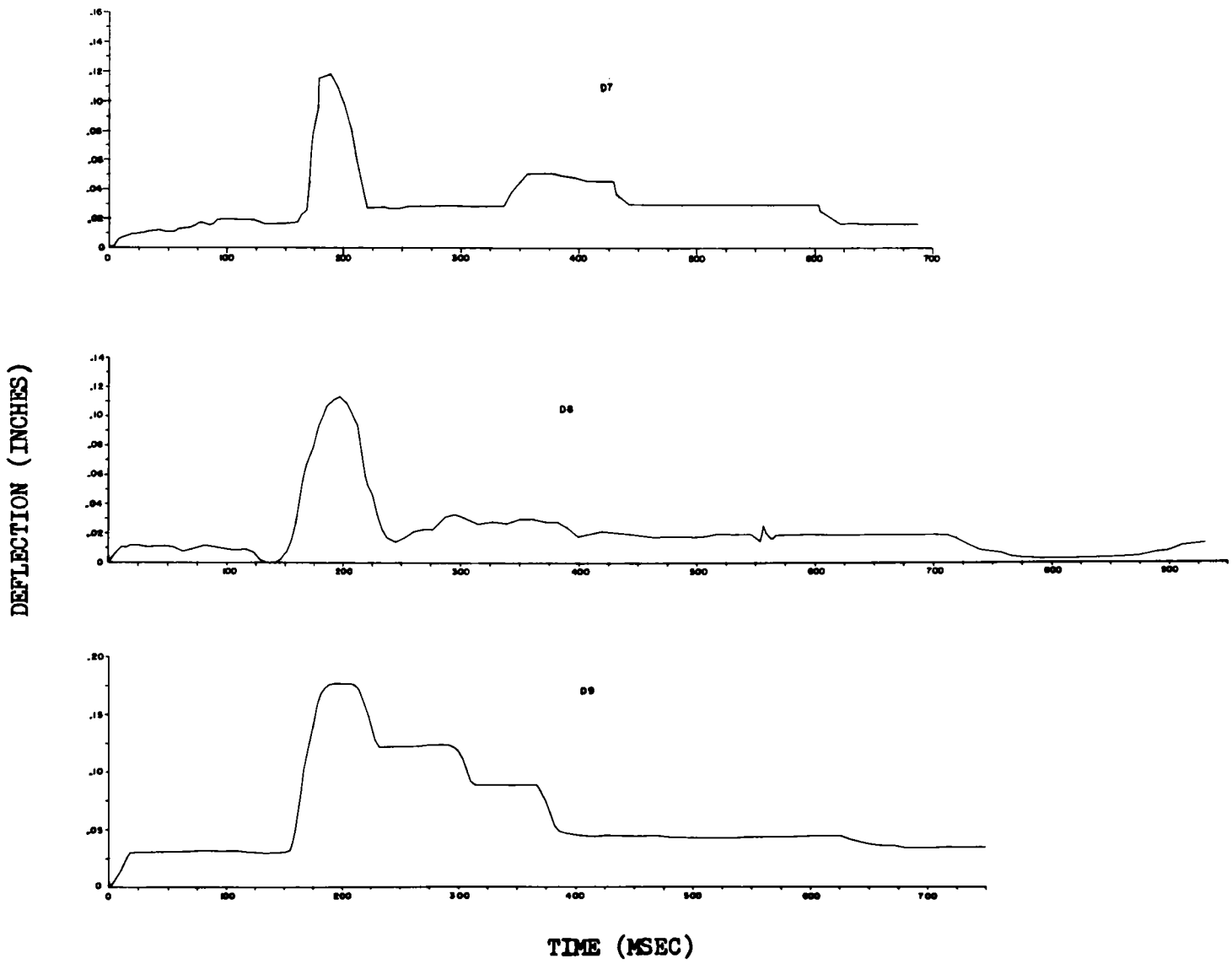

Fig. 3.16—(Continued)

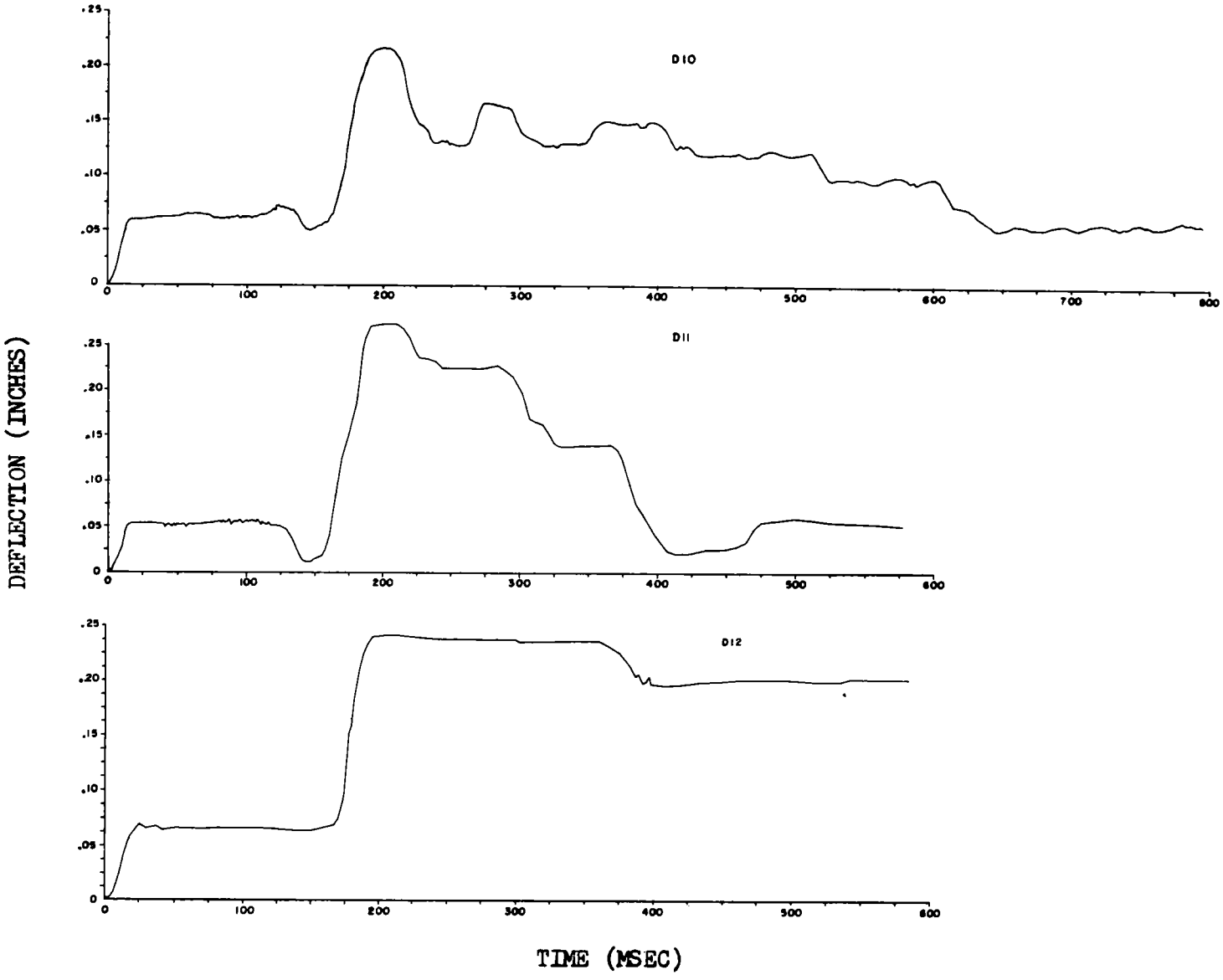

Fig. 3.16—(Continued)

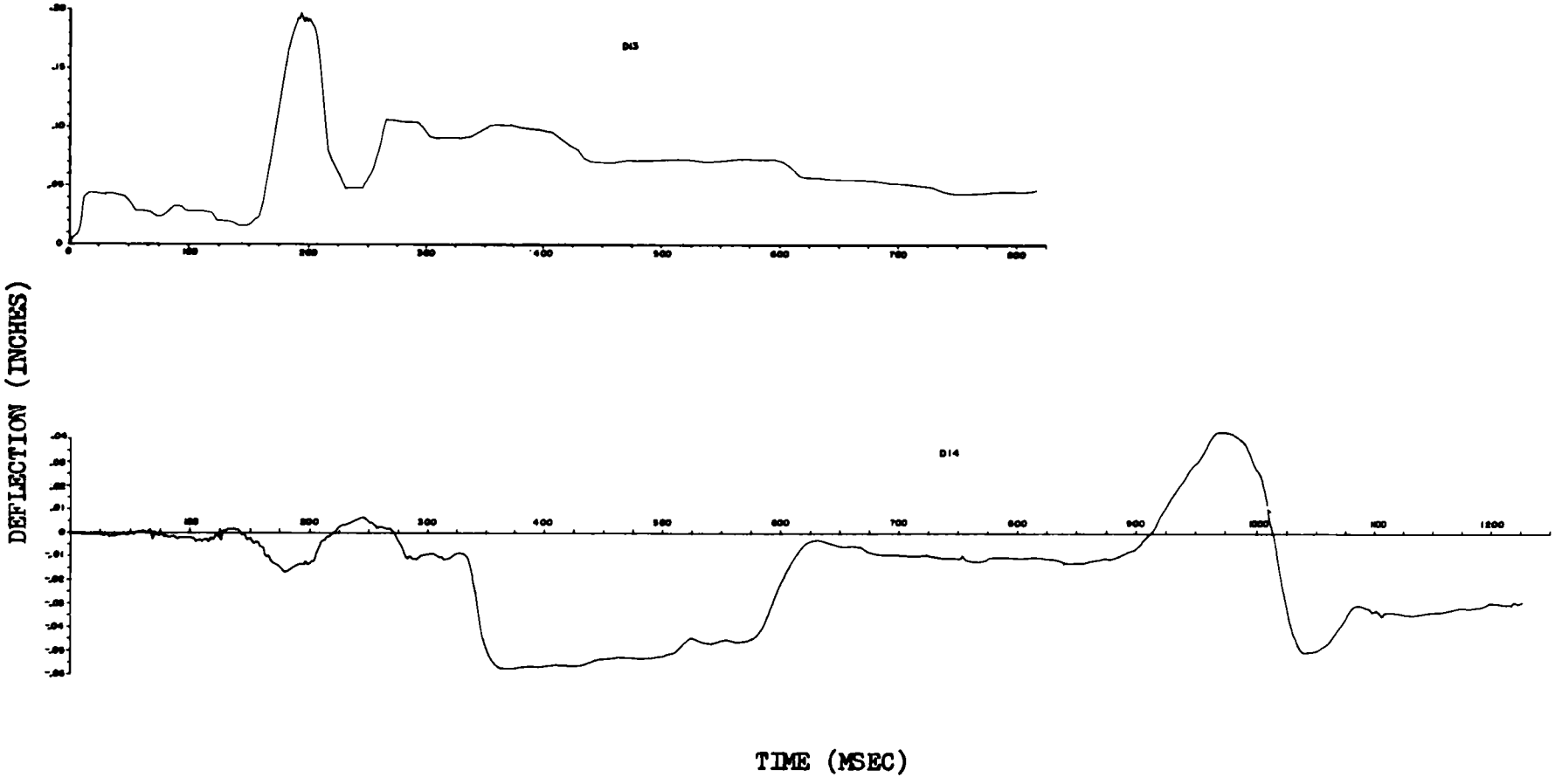

Fig. 3.16—(Continued)

TABLE 3.4 — P-t GAUGE RESULTS, MAIN BLAST LINE

Station	Ground range, ft	Maximum overpressure, psi	Arrival time, sec	Positive duration, sec	Positive-phase impulse, psi-sec
F1.1-9039.01A	350	No record			
F1.1-9039.01B	350	1030			
F1.1-9039.02A	450	760			
F1.1-9039.02B	450	750		0.175	
F1.1-9039.03A	650	480	0.364	0.095	10.562
F1.1-9039.03B	650	400	0.676	0.162	8.896
F1.1-9040.01A	850	225		0.236	11.957
F1.1-9040.01B	850	206			
F1.1-9040.02A	1050	125		0.233	6.156
F1.1-9040.02B	1050	138		0.195	5.613
F1.1-9041.00A	1350	60.0		0.343	4.503
F1.1-9041.00B	1350	62.0	0.512	0.280	4.501
F1.1-9042.01	1650	31.0		0.467	3.973
F1.1-9042.02	2000	16.3			
F1.1-9042.05	2250	12.4	0.570	0.687	4.039
F1.1-9042.06	2500	9.2	0.523	0.852	4.179
F1.1-9042.07	3000	9.1		0.727	2.849
F1.1-9042.03	3500	9.9			
F1.1-9042.08	4000	8.8	1.729	0.818	2.595
F1.1-9042.04	4500	7.4			
F1.1-9043.01	5000	5.9		0.916	
F1.1-9043.02	6000	No record			

TABLE 3.5 — q GAUGE RESULTS, MAIN BLAST LINE*

Station*	Ground range, ft	Total pressure, psi	Static overpressure, psi	Pressure difference $[(P_p - P_0)^{*\prime}]$, psi	Dynamic pressure (q*), psi	Mach number (u/a)
F1.1-9040.01	850					
F1.1-9040.02	1050	470.0	125.0	445.0	240.0	3.3
F1.1-9041.00	1350	275.0	60.0	255.0	150.0	3.6
F1.1-9041.00Nx	1350					
F1.1-9042.01	1650	143.5	31.0	150.0	80.0	2.3
F1.1-9042.02	2000	58.5	23.0x	44.0	35.0	1.3
F1.1-9042.05N	2250	48.0	12.4	36.0	27.0	1.4
F1.1-9042.06	2500	47.0	9.2	38.0	25.0	1.3
F1.1-9042.06Nx	2500	35.0	9.2	28.0	19.0	1.2
F1.1-9042.07	3000	29.0	9.1	20.0	15.1	1.0
F1.1-9042.07Nx	3000	26.5	9.1	20.5	17.0	1.04
F1.1-9042.02	3500	11.2	8.6x	3.4	2.8	0.45
F1.1-9042.08	4000	10.0	9.0	1.3	1.3	0.29
F1.1-9042.08N	4000					
F1.1-9042.04	4500	7.8	6.5x	1.7	1.2	0.29

* N refers to new q gauge. x values are from q gauge. q* = corrected dynamic pressure (see ITR-1401). $(P_p - P_0)^{*\prime}$ = total head Pitot pressure minus ambient preshock static pressure, uncorrected and containing air and dust components.

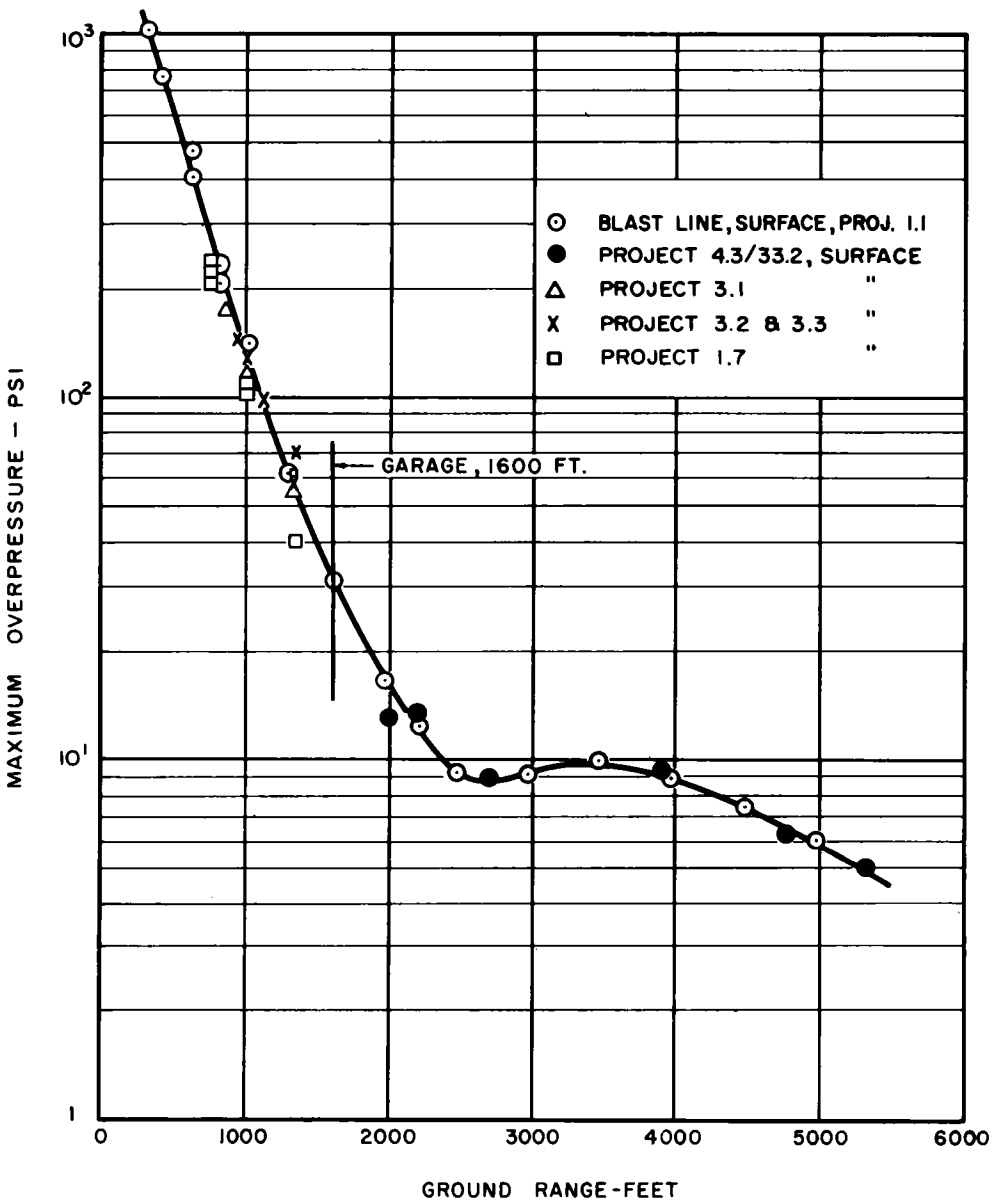

Fig. 3.17 — Free-field maximum overpressure vs. time curve.

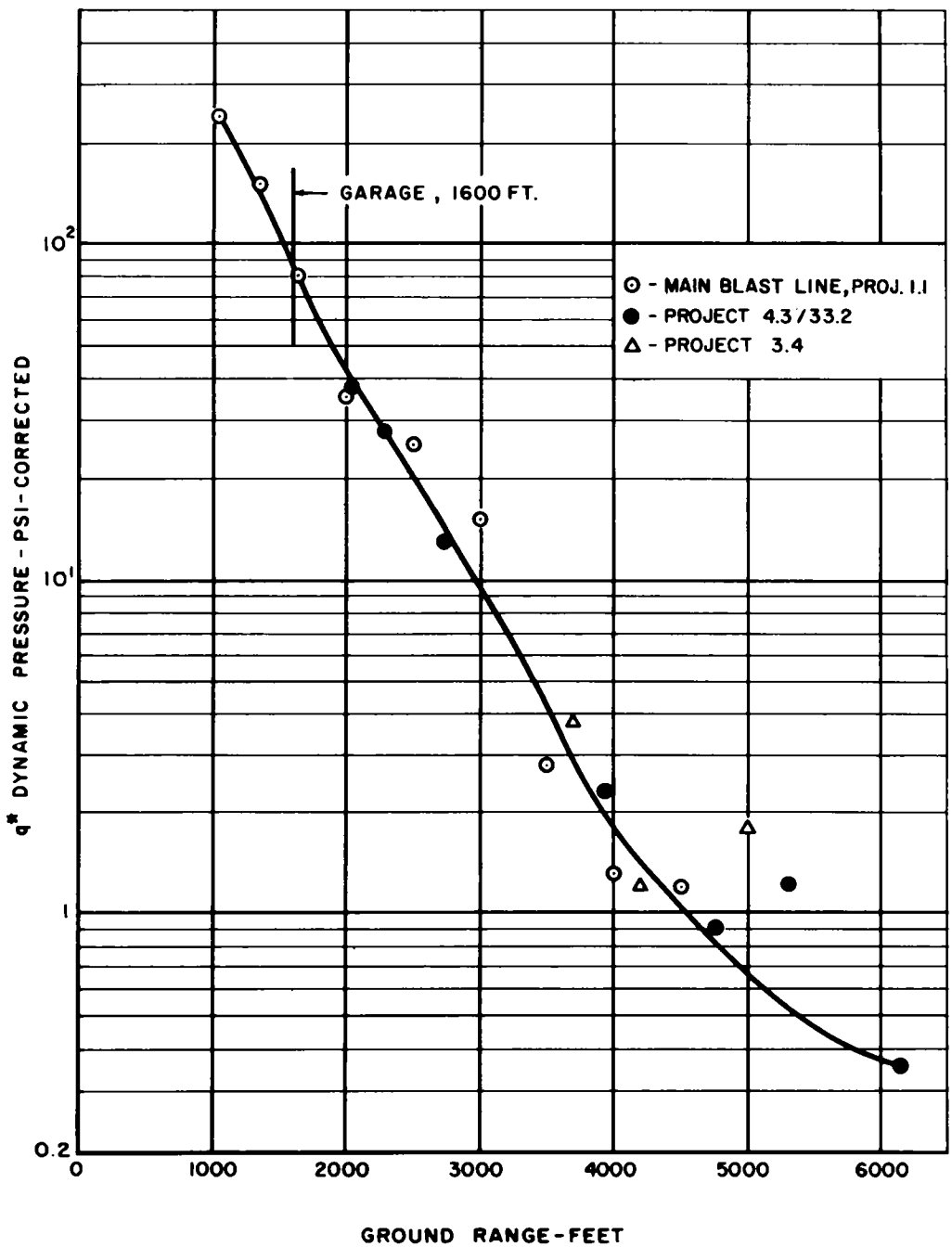

Fig. 3.18 — Free-field corrected dynamic pressure vs. distance curve.

TABLE 3.6—COMPARISON OF FREE-FIELD PRESSURES

	Blast line (Project 1.1)	Garage (Project 30.5)
Peak incident pressure, psi	35	39
Incident-pressure positive-phase impulse, psi-sec	4.0	
Incident-pressure positive-phase duration, sec	0.43	
Peak dynamic pressure, psi (corrected)	89	112

TABLE 3.7—RESULTS OF GAMMA-RADIATION FILM DOSIMETERS

Dosimeter location	Total dosage, r		Dosimeter location	Total dosage, r	
	3 ft	5 ft		3 ft	5 ft
a	0.65	0.65	p	1.6	1.5
b	0.1	0.8	q	1.5	1.6
c	1.2	1.3	r	1.3	1.2
d	1.4	1.3	s	1.4	1.3
e	1.4	1.2	t	1.4	1.3
f	1.2	1.2	u	1.8	1.6
g	1.1	1.2	v	1.2	1.1
h	1.4	1.2	w	1.0	1.0
j	1.4	1.3	x	1.2	1.4
k	1.5	1.6	y	0.01	0.7
l	0.9	0.7	1	12.0 (on concrete-door bumper)	
m	1.0	0.013	2	32.0 (on concrete-door bumper)	
n	1.0	0.95			
o	1.2	1.1			

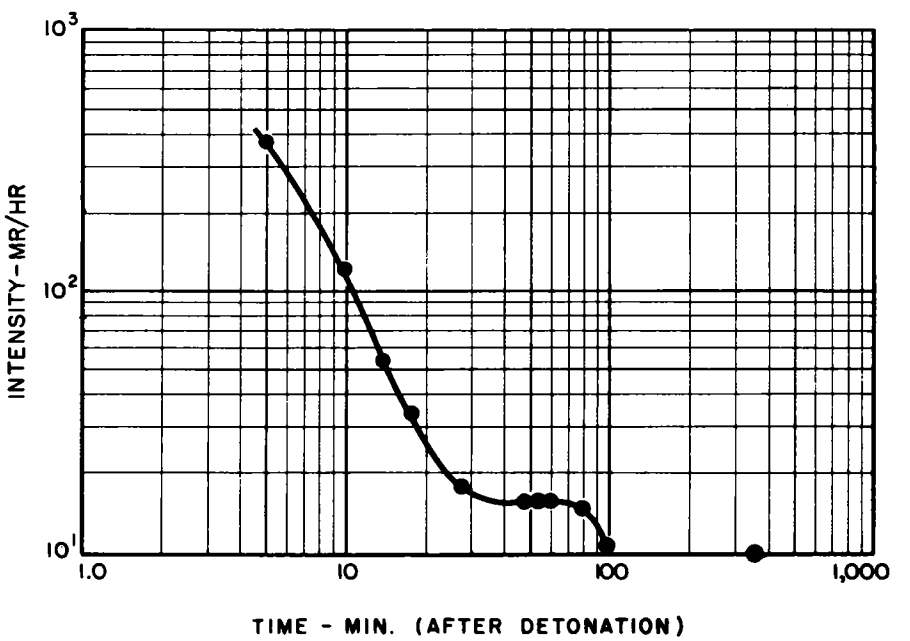

Fig. 3.19—Gamma-radiation decay pattern for telemetering instrument.

The goal-post-line dose–distance curve for the initial gamma radiation obtained with the U. S. Air Force chemical dosimeters (Project 39.1) is indicated in Fig. 3.20. These data for various slant ranges from 410 to 1773 yd are given in Table 3.8. The slant range of the garage is approximately 582 yd. Figure 3.21 is a plot of the stake-line dose–distance measurements obtained from the gamma-radiation film dosimetry of Project 39.1a. The data from which this curve was plotted are shown in Table 3.9.

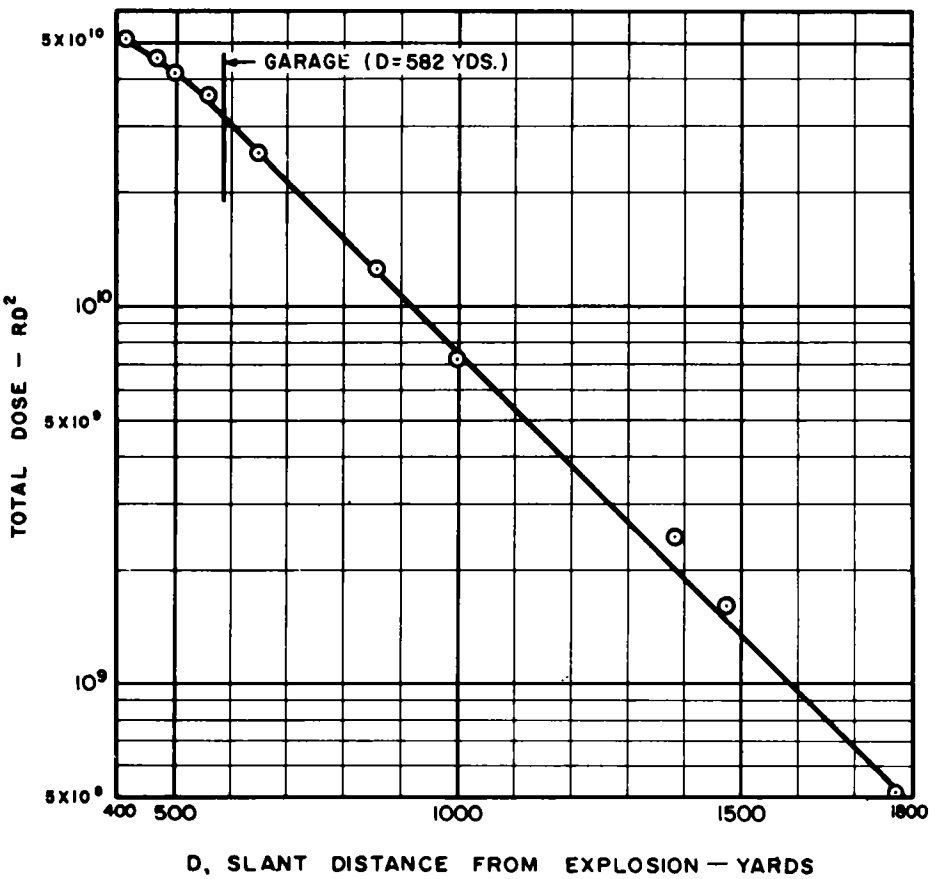

Fig. 3.20—Goal-post line gamma dose-distance curve.

TABLE 3.8—GOAL-POST-LINE GAMMA DATA

Slant range (D), yd	D^2	Dose, r	RD^2
410	1.68×10^5	3×10^5	5.04×10^{10}
470	2.21×10^5	2.05×10^5	4.53×10^{10}
500	2.5×10^5	1.65×10^5	4.13×10^{10}
560	3.14×10^5	1.15×10^5	3.61×10^{10}
650	4.23×10^5	6×10^4	2.54×10^{10}
860	7.40×10^5	1.7×10^4	1.26×10^{10}
1000	1×10^6	7200	7.20×10^9
1383	1.91×10^6	1290	2.46×10^9
1477	2.18×10^6	740	1.61×10^9
1773	3.14×10^6	162	5.09×10^8

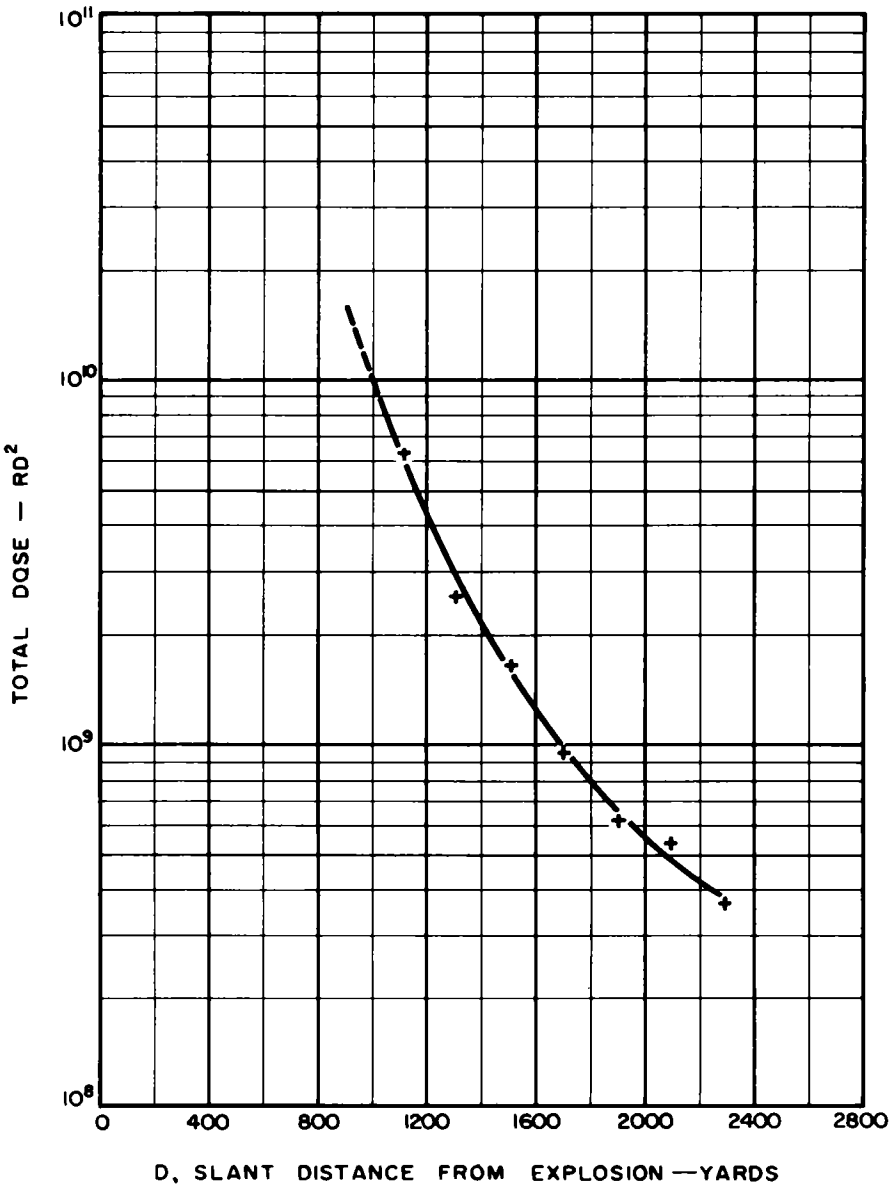

Fig. 3.21 — Stake-line gamma dose-distance curve.

TABLE 3.9—STAKE-LINE GAMMA DATA*

Slant distance (D), yd	D^2	Dose EG&G container,† r	RD^2	No. of EG&G badges per point	Maximum deviation per point, %	Film types read
410	1.68×10^5	NR				
470	2.21×10^5	NR				
500	2.5×10^5	NR				
560	3.14×10^5	NR				
650	4.23×10^5	NR				
800	7.4×10^5	NR				
1000	1.0×10^6	NR				
1104	1.22×10^6	5.2×10^3	6.34×10^9	2	0.0	1112
1296	1.68×10^6	1.5×10^3	2.52×10^9	2	0.0	1112
1383	1.91×10^6	NR				
1477	2.18×10^6	NR				
1496	2.24×10^6	725.0	1.62×10^9	2	0.69	1112
1694	2.87×10^6	327.5	9.4×10^8	2	0.76	606
1773	3.14×10^6	NR				
1892	3.58×10^6	168.5	6.03×10^8	2	3.86	510
2090	4.37×10^6	122.5	5.35×10^8	2	2.04	510
2289	5.24×10^6	69.0	3.61×10^8	2	1.45	510

* Dose vs. distance: RD^2 vs. D.
† NR, not recovered.

Recovery of the goal-post-line and stake-line dosimetry was accomplished at H + 1½ hr and 5 hr, respectively.

A complete description of the radiation-instrumentation test results can be obtained from the Project 39.1, 39.1a, and 39.9 reports, ITR-1500 (Ref. 4), WT-1466 (Ref. 5), and WT-1509 (Ref. 3), respectively.

3.4 SURVEYS

A comparison of the pre- and postshot surveys taken on the survey points located within the underground parking garage and on the access-ramp floor indicated considerable absolute movement of all survey points. The pre- and postshot survey values for the coordinates and elevations of these survey points are given in Tables 3.10 and 3.11, respectively. All coordinates, azimuths, and bearings are referred to the Nevada State Grid North, which is neither true nor magnetic.

Subsequent to the postshot survey, it was learned that the triangulation was of second-order accuracy (1 : 10,000 permissible error) and that the average base-line lengths were over 11,000 ft (Fig. 3.22); therefore this survey cannot be relied upon for estimating the absolute movements of the structure. An inspection of the permanent movements obtained from this survey and shown in Table 3.10 indicated that the structure as a unit moved approximately 0.10 ft toward GZ and 0.50 ft sideways. The relative displacements of the survey points should be fairly accurate, however, and are also included in Table 3.10.

The elevation-survey data summarized in Table 3.11 are also subject to considerable error, although they appear to be quite reasonable. The relative displacements, which are probably fairly accurate, give some indication that the absolute values of the permanent motions were small.

3.5 FREE-FIELD GROUND-MOTION DATA

During shot Priscilla, free-field ground motions were recorded at various depths below the ground surface and various ground ranges in the general vicinity of the test structures.

TABLE 3.10—PRE- AND POSTSHOT COORDINATES

Point	Preshot	Postshot	Absolute movement, ft	Movement relative to point y, ft
w	N 746,555.96	N 746,556.47	0.51 N	0.02 N
	E 714,547.04	E 714,547.15	0.11 E	0.01 E
x	N 746,589.70	N 746,590.18	0.48 N	0.01 S
	E 714,400.53	E 714,400.64	0.11 E	0.01 E
y	N 746,625.36	N 746,625.85	0.49 N	
	E 714,411.85	E 714,411.95	0.10 E	
a	N 746,671.36	N 746,671.85	0.49 N	0
	E 714,428.33	E 714,428.43	0.10 E	0
b	N 746,664.17	N 746,664.67	0.50 N	0.01 N
	E 714,455.24	E 714,455.34	0.10 E	0
c	N 746,658.11	N 746,658.61	0.50 N	0.01 N
	E 714,482.52	E 714,482.62	0.10 E	0
d	N 746,647.77	N 746,648.26	0.49 N	0
	E 714,406.56	E 714,406.66	0.10 E	0
e	N 746,644.09	N 746,644.58	0.49 N	0
	E 714,422.10	E 714,422.20	0.10 E	0
f	N 746,637.92	N 746,638.42	0.50 N	0.01 N
	E 714,447.25	E 714,447.35	0.10 E	0
g	N 746,630.67	N 746,631.17	0.50 N	0.01 N
	E 714,475.35	E 714,475.45	0.10 E	0
h	N 746,626.47	N 746,626.98	0.51 N	0.02 N
	E 714,490.75	E 714,490.86	0.11 E	0.01 E
k	N 746,616.99	N 746,617.48	0.49 N	0
	E 714,414.81	E 714,414.91	0.10 E	0
l	N 746,610.91	N 746,611.41	0.50 N	0.01 N
	E 714,441.85	E 714,441.96	0.11 E	0.01 E
m	N 746,603.70	N 746,604.21	0.51 N	0.02 N
	E 714,469.45	E 714,469.52	0.07 E	0.03 W
n	Not recorded	Not recorded		
o	Not recorded	Not recorded		
p	N 746,620.40	N 746,620.91	0.51 N	0.02 N
	E 714,458.97	E 714,459.06	0.09 E	0.01 W

The closest location, with respect to the Project 30.2 structure, at which ground-motion data were recorded was approximately 250 ft (radially) from the structure (1350 ft from GZ). The recorded peak surface incident overpressure at this ground range was 59 psi. These records include ground-acceleration and -displacement measurements recorded during Projects 1.4 (Ref. 6) and 1.5 (Ref. 7).

Summarized below are the results of the pertinent available free-field data at the 1350-ft ground range. These data consist of surface and below-ground acceleration vs. time and displacement vs. time measurements. Also included are velocity vs. time, displacement vs. time, and shock-spectra ground-motion data computed from the acceleration vs. time records. Although these measurements were not recorded at the same ground range as the structure, they are probably representative of motions which are in the range of values or somewhat higher than free-field ground motions in the vicinity of the structure, consistent with the ac-

TABLE 3.11—PRE- AND POSTSHOT ELEVATIONS

Point	Preshot	Postshot	Movement, ft
y	3061.61	3061.59	0.02 downward
a	3063.67	3063.66	0.01 downward
b	3063.71	3063.69	0.02 downward
c	3063.59	3063.57	0.02 downward
d	3063.55	3063.54	0.01 downward
e	3063.77	3063.74	0.03 downward
f	3063.51	3063.48	0.03 downward
g	3063.62	3063.60	0.02 downward
h	3063.67	3063.66	0.01 downward
k	3063.66	3063.64	0.02 downward
l	3063.59	3063.57	0.02 downward
m	3063.36	3063.34	0.02 downward
n	Not recorded	Not recorded	
o	Not recorded	Not recorded	
p	Not recorded	3062.14	
w	Not recorded	Not recorded	
x	Not recorded	Not recorded	

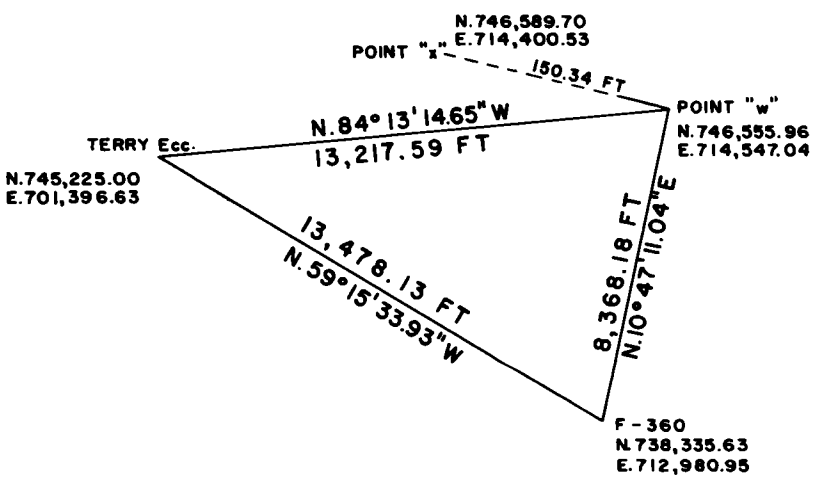

Fig. 3.22—Traverse to point w of structure 30.2.

curacy of the test records. In this regard it should be noted that certain inconsistencies exist, and in some cases the reliability of the test data is uncertain.

The free-field acceleration vs. time ground motions in the horizontal and vertical directions were recorded by accelerometers enclosed in protective canisters that were buried at various depths below the ground surface. Table 3.12 lists the peak accelerations recorded down to 60 ft.

The vertical acceleration curves plotted in references 6 and 7 are mainly characterized by a single sharp peak of acceleration in the downward direction, which becomes less pronounced with depth. These peaks are preceded and followed by minor disturbances. The horizontal acceleration curves show a somewhat similar wave form. However, the first major positive (outward from GZ) peak acceleration is followed by a pronounced negative peak, which in some cases is of greater magnitude than the positive peak.

The acceleration vs. time records of Projects 1.4 and 1.5 were numerically integrated to obtain the particle velocity vs. time. The peak values in the vertical and horizontal directions

are tabulated in Table 3.13. The curves plotted in references 6 and 7 indicate that the wave form is similar to the air pressure, falling off somewhat more rapidly than the pressure and becoming zero before the end of the positive phase of the air pressure. The peak velocities are downward and outward from GZ for the vertical and horizontal directions, respectively.

TABLE 3.12—MEASURED PEAK FREE-FIELD GROUND ACCELERATION

Project 1.4			Project 1.5		
Depth	Vertical	Horizontal	Depth	Vertical	Horizontal
5 ft	9.16 g	No record	Surface	9.1 g	−1.3 g
10 ft	4.84 g	No record	10 ft	5.4 g	2.5 g
Below 10 ft	No record	No record	30 ft	2.2 g	No record
			60 ft	1.8 g	−2.4 g

TABLE 3.13—COMPUTED PEAK FREE-FIELD GROUND VELOCITY

Project 1.4			Project 1.5		
Depth	Vertical	Horizontal	Depth	Vertical	Horizontal
5 ft	2.84 fps	No record	Surface	3.43 fps	No record
10 ft	1.67 fps	No record	10 ft	2.47 fps	1.90 fps
Below 10 ft	No record	No record	30 ft	1.52 fps	No record
			60 ft	1.35 fps	1.45 fps

Displacement vs. time plots were also computed from the double integration of the acceleration records of Projects 1.4 and 1.5. In addition, vertical ground displacements in Project 1.5 were directly measured by relative-displacement gauges. The displacement gauges recorded the displacement vs. time relative to the ground surface motion at various depths below the ground surface. Relative displacements were converted to absolute displacements of the surface and gauge anchors on the assumption that the deepest gauge anchors (200 ft below the surface) were not displaced.[7] The wave forms of the displacement plots[6,7] exhibit a somewhat gradual time of rise to the peak value, which occurs at approximately the end of the positive phase of the air pressure. Displacement measurements and permanent displacements measured at the ground surface by a preshot and postshot first-order survey on a monument located on the ground surface at 1350 ft from GZ were used to record permanent vertical displacements. The computed and measured peak transient and permanent displacements are tabulated in Tables 3.14 and 3.15, respectively. Positive values are downward and outward from GZ for the vertical and horizontal directions, respectively.

As noted in Tables 3.14 and 3.15, the computed displacements are considerably higher than the measured displacements. However, since a good deal of judgment is involved in obtaining meaningful results in the acceleration-integration computations, the measured displacement records are generally considered more reliable. The calculated horizontal displacement (4.30 in.) at the 10-ft depth is unreasonably high and may be in error since it is usually expected that, for certain pressure levels and geological conditions, the horizontal displacement component will be $\frac{1}{3}$ to $\frac{2}{3}$ of the vertical value and perhaps equal to the vertical component, as indicated in other test results.[6–9] It is noteworthy that the recorded permanent displacements were in the upward direction, which is opposite to the peak transient-displacement direction. At the higher pressure ranges for shot Priscilla the permanent displacements were downward. A study of the displacement vs. time curves indicates that the upward permanent displacement may be a result of the relatively large upward rebound (compared to rebound

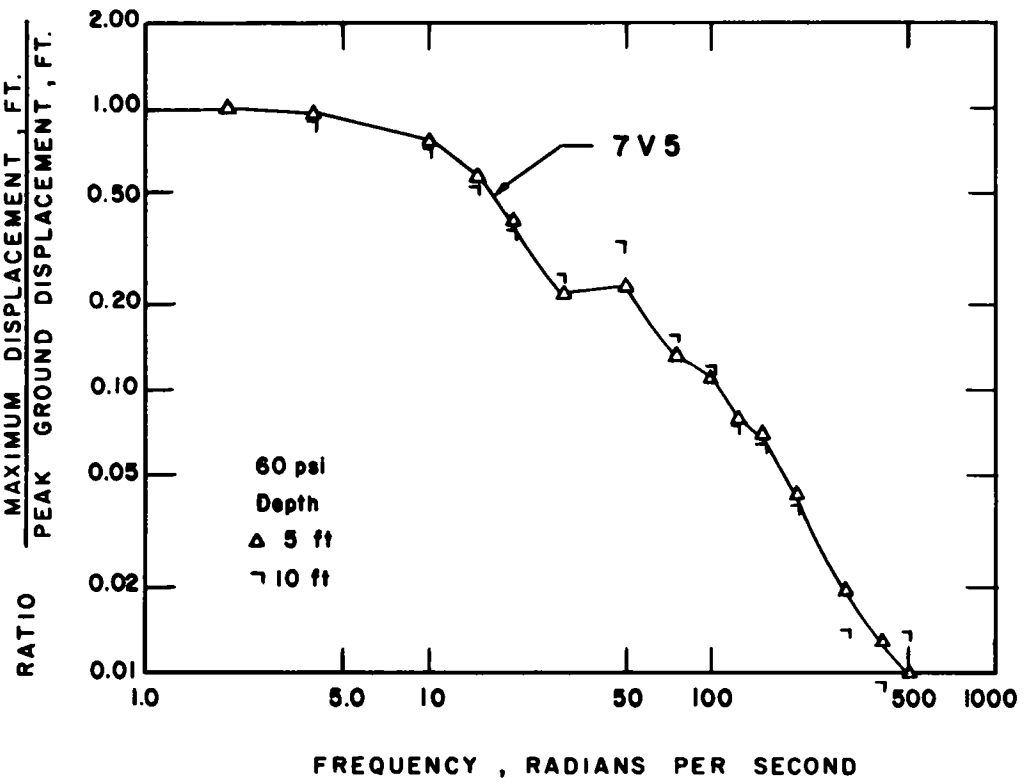

Fig. 3.23—Displacement-response spectra.

TABLE 3.14—COMPUTED PEAK TRANSIENT FREE-FIELD GROUND DISPLACEMENT

Project 1.4			Project 1.5		
Depth	Vertical	Horizontal	Depth	Vertical	Horizontal
5 ft	2.87	No record	Surface	3.69 in.	No record
10 ft	1.85 in.	No record	10 ft	2.39 in.	4.30 in.
Below 10 ft	No record	No record	30 ft	2.07 in.	No record
			60 ft	1.97 in.	0.79 in.

TABLE 3.15—MEASURED VERTICAL FREE-FIELD GROUND DISPLACEMENT (Project 1.5)

Depth	Peak transient	Permanent	Permanent (monument)
Surface	1.4 in.	−0.17 in.	−0.06 in.
10 ft	1.0 in.	−0.05 in.	
30 ft	0.8 in.	−0.18 in.	
60 ft	0.5 in.	−0.03 in.	

at the higher pressure ranges) which followed the downward peak. The large upward rebound and upward permanent displacements may be due in part to reflected and/or refracted ground-shock waves from the lower soil strata.

Response spectra of ground motions[6] were computed for the input ground-motion data recorded during Project 1.4. A response spectrum is defined as the maximum response of a linear single-degree-of-freedom spring-mass system relative to the motion of the ground.[9,10] Figure 3.23 shows the vertical displacement spectrum curve for the 5- and 10-ft depths.[6] This response spectrum corresponds to the input ground-motion data presented for Project 1.4. Corresponding velocity- and acceleration-spectrum curves can be easily determined from shock-spectra theory[10] as outlined below:

$$\text{Velocity spectra} = \omega|X|_{max}$$
$$\text{Acceleration spectra} = \omega^2|X|_{max}$$

where X is the displacement-spectra value at frequency ω, in radians per second, and the velocity and acceleration units are consistent with the unit of displacement.

REFERENCES

1. J. J. Meszaros et al., Instrumentation of Structures for Air-blast and Ground-shock Effects, Operation Plumbbob Report, WT-1452, January 1960.
2. E. J. Bryant, J. H. Keefer, and J. G. Schmidt, Basic Air-blast Phenomena, Part I, Operation Plumbbob Report, ITR-1401, Oct. 25, 1957. (Classified)
3. H. M. Borella and S. C. Sigoloff, Remote Radiological Monitoring, Operation Plumbbob Report, WT-1509, November 1958.
4. S. Sigoloff et al., Regulation Measurements Utilizing the USAF Chemical Dosimeters, Operation Plumbbob Report, WT-1500, November 1953. (Classified)
5. Edgerton, Germeshausen & Grier, Inc., Gamma Dosimetry by Film-badge Techniques, Operation Plumbbob Report, WT-1466, July 1959. (Classified)
6. L. M. Swift, D. C. Sachs, and F. M. Sauer, Ground Acceleration, Stress, and Strain at High Incident Overpressures, Operation Plumbbob Report, WT-1404, May 10, 1960. (Classified)

7. William R. Perret, Ground-motion Studies at High Incident Overpressure, Operation Plumbbob Report, WT-1405, June 20, 1960.
8. L. M. Swift and D. C. Sachs, Ground Motion Produced by Nuclear Detonations, Operation Hardtack Report, ITR-1613, Aug. 14, 1958. (Classified)
9. J. F. Halsey and M. V. Barton, Spectra of Ground Shocks Produced by Nuclear Detonations, Operation Plumbbob Report, WT-1487, Aug. 17, 1959. (Classified)
10. M. V. Barton and Y. C. Fung, Some Shock Spectra Characteristics and Uses, J. Appl. Mechanics, 25: 365 (1958).

Chapter 4

DISCUSSION

4.1 RAMP AND DOOR

The only substantial damage noted in connection with this project was to the retaining wall at the end of the ramp where damage was expected (see Sec. 1.4). The peak average pressure on the end wall was 188 psi (110 psi at the top and 266 psi at the base), considerably higher than the peak free-field side-on pressure of 39 to 40 psi recorded at the ground surface. This was due mainly to reflections and the added effect of the dynamic pressures, which were much higher than the side-on pressures at this range. The dynamic-pressure gauge at the base of the ramp was packed with debris and did not record. However, the dynamic-pressure gauge at the surface did record a peak dynamic pressure (corrected) of 112 psi. A peak pressure of 105 psi was recorded on the door (12 ft from the end wall), and the electronic side-on gauge (25 ft from the end wall) recorded a peak pressure of 54 psi. These gauge records are of appreciable significance; however, gauge P4 had a faulty connection and, as a consequence, the pressure back-up in the ramp was not fully defined. Blast results were not successfully recorded by the Carlson gauges behind the ramp retaining walls or the deflection gauges on these walls.

There is evidence that at the time of detonation the upper several feet of backfill behind the end wall was not compacted in accordance with the specifications because of excavation and backfilling for an instrumentation cable trench after original backfilling had been completed. Such a condition would mean that greater deflection would be required before the maximum passive resistance of the soil was developed. Although the damage to the end wall is not important in connection with this project, the mode of failure is technically interesting. Because of its orientation and high pressure loading, the wall was expected to deflect into the backfill by yielding of the reinforcement; however, the concrete and reinforcement were expected to remain bonded together, although the concrete would be badly cracked. The complete separation of the top half of the end wall from the bottom, disintegration of the lower portion into loose rubble, separations along the planes of the reinforcement, and failure of the splices without yielding of the steel can be partially attributed to the poor adhesive quality of the concrete in place. However, the mode of failure also may have been influenced by the rapid blast loading and the probability that the strength of normal splices under such loading may be much lower than under static loading. Laboratory data to verify splice efficiencies under dynamic loading would be highly desirable. The ductility of the wall would be greatly increased by raising the splice point, welding the splices, using full-length bars (thus eliminating the splice), and by providing a vertical expansion joint at the intersection with the longitudinal wall. High door pressures would have been avoided if the ramp had been of a symmetrical through type without an end wall. However, a through type ramp, although desirable to minimize blast effects, is often not economical or practical.

The recorded peak pressure (22 psi) on the side wall toward the top of the ramp (gauge P5) was lower than the surface pressure, possibly because of the dynamic pressure flow down

the ramp. This less-severe face load, in combination with a positive surcharge load, produced no noticeable damage. Although the side wall of the ramp opposite the garage door was loaded by the backup of pressure, the loading was not as severe as that on the end wall. Therefore the side wall of the ramp was only moderately cracked, although it appears that there may have been some bond failure in the cracked area.

Because of the thickness required for radiation protection, the exposed wall of the garage and the concrete door were more than adequate for the blast effects experienced. No damage was evident.

The as-built clearances between the door and frame were as high as $^{13}/_{16}$ in., more than three times that shown on the plans; therefore the pneumatic seal would have been ineffective even in good working condition. To prevent excessive infiltration of the blast pressures, clearances at the base were reduced prior to the shot by 3- by 3- by $^{3}/_{8}$-in. angles; one leg was inserted vertically into the opening, and the other was bolted to the frame. The blast pressures still entered the joint and forced the gasket toward the interior of the shelter, stripping and tearing it along its entire length. It is not known whether or not the compressed-air cylinder placed prior to the test was adequate to maintain pressure in the gasket up to shot time.

4.2 ROOF SLAB AND WALLS

The peak incident pressure recorded on the ground surface was 39 to 40 psi as compared to a peak pressure range of 21 to 42 psi (31 psi average) recorded by the Carlson gauges on the roof surface 3 ft below the ground surface. With the exception of gauge $\overline{P}11$, the surface-pressure record is consistently larger both in peak pressure and total impulse. This pressure difference, which is partially a smoothing of the surface-pressure oscillations, may be attributed to viscoelastic energy losses in the soil mass, smoothing out of the wave form, and/or inadequate sensitivity of the Carlson gauges. Gauge $\overline{P}9$, for example, may give a fair representation of the peak pressure but does not appear to provide a consistent pressure–time variation.

The friction angle for the earth adjacent to the structure was approximated at 40 deg. Consequently the recorded wall pressures of 2.8 to 5 psi correspond to about a 50 per cent attenuation of the peak surface pressure with depth.

The absence of cracks on the roof slab and walls indicates that the structure was capable of resisting the blast load without appreciable inelastic deformation. Analysis of the roof slab (as built) showed that it had a static flexural capacity of 60.8 psi (5 psi dead load plus 55.8 psi live load) compared to the static design load of 45 psi (dead load plus live load). This difference can be attributed to two factors:

1. There was an increase of 23 per cent in the moment-carrying capacity of the section due to a misinterpretation of the engineering drawings in the detailing and fabrication of the transverse and longitudinal truss bars.
2. In the design computations the lever arm between the load centroid and the axis of rotation was computed with the assumption that the quarter-panel axis of rotation was the chord line of the quarter arc of the column capital, whereas in the postshot analysis the axis of rotation was assumed to pass through the centroid of the quarter arc of the column capital. This resulted in an additional increase in static capacity of approximately 10 per cent.

The peak recorded displacement of the center of the instrumented roof panel averaged 0.50 in. relative to the base of the columns, whereas the top of the center column had a peak displacement of 0.25 in. relative to the reference pile below the floor slab. The peak axial deformation in the column is estimated at 0.14 in., and therefore the peak slab deflection relative to the top of the columns is estimated as 0.36 in. The postshot analysis of the as-built roof slab using the recorded pressure data indicated a peak relative deflection of 0.43 in., which corresponds to a peak response of 45.5 psi (50.5 psi including dead load).

The 12-in. gauge walls, designed to resist a blast pressure of 15 psi, were not damaged by the maximum recorded wall load of 5 psi.

4.3 RADIATION

All ramp dosimeters were blown away or badly damaged; consequently results are not available for review. Based upon the goal-post-line records, the gamma surface-radiation dosage at the radius of the Project 30.2 structure is estimated at 102,000 r. The average interior dose recorded by the dosimeters in the structures was 1.2 r, which corresponds to an attenuation factor of 1.2×10^{-5}. Higher interior doses were recorded on the concrete door bumper (12 and 32 r) where some dust was blown through the torn door seal.

4.4 FOUNDATION MOTION AND GROUND SHOCK

According to the test results, the relative displacement of the foundation with respect to the reference pile was 0.11 in. peak transient and 0.02 in. permanent. Based on the free-field ground-shock environment data, the range of magnitude of the absolute peak motions of the foundation and the structure proper may be roughly estimated since ground motions apparently occurred below the base of the reference pile. In the vertical direction the peak transient displacement of the foundation is estimated to be equal to the free-field ground displacement at a depth corresponding to the base of the reference pile plus the relative displacement of the foundation with respect to the reference pile, i.e., on the order of 0.8 in. Based on the permanent free-field displacements, recorded to be in the upward direction in the range of 0.03 to 0.18 in., and the permanent displacement of the foundation relative to the reference pile of 0.02 in. (downward), it is difficult to estimate the permanent displacement of the foundation, although it is expected that the permanent displacement would not be significantly greater (upward or downward) than the free-field values.

Although the horizontal free-field displacement test data are limited, a reasonable estimate of the peak horizontal-displacement component is one-half the peak vertical component, i.e., on the order of 0.4 in. outward from GZ. The permanent horizontal displacement would also be less than the vertical component.

Previous test data[2,3] have indicated that the peak accelerations for structures are generally attenuated from the free-field accelerations, depending on the structure configuration, mass, and stiffness of its structural components. The peak vertical acceleration of the structure is roughly estimated as the free-field acceleration of the ground at a depth corresponding to the base of the foundation, which could be on the order of 2 to 3 g. In the horizontal direction the peak acceleration of the structure would be less than the vertical direction on the order of one-half the vertical value.

It should be noted that the above estimates of the structure motion are approximate and only indicate the range of magnitude of the motions that the foundation and the structure experienced since the free-field data were not recorded at the same ground range of the structure and, in addition, structure-soil interaction effects during the transient ground-shock motion were not considered. If it were required, the structure–soil interaction could be approximated by a detailed dynamic analysis.[4–6]

In view of the high prestress and the state of over-consolidation encountered in the soil survey, the probable natural static in-place stress–strain relations, failure strength, and shearing strength cannot be less than would be obtained under a lateral stress, p_3, of 40 psi (Table 2.1). The residual lateral pressure of a soil is commonly taken to be 0.3 to 0.7 times the prestress. The residual lateral pressure for the soils encountered here is in excess of 0.4 of the prestress. Theoretical studies and correlations of load-settlement relations from plate-bearing tests and from full-scale footings with triaxial test stress–strain relations obtained from undisturbed soil samples have shown that the estimated static-failure stress under a footing can be at least 2.5 times the comparable laboratory triaxial-failure stress.[7] This results from the natural confinement and restraint conditions afforded to lateral displacements by the natural soil mass surrounding a footing, which cannot be duplicated by a simple stress restraint of the lateral stress in a triaxial test. In addition, the confining and restraint influences of the surrounding earth surcharge above the level of the base may increase this value to 3.0 or more.

Using triaxial data for a lateral stress of 40 psi (2.88 tsf), the static-failure stress on the center footing is computed as 16 tsf × 2.5 = 40 tsf (see Appendix C). These postconstruction analyses indicated that the footing sizes could have been reduced substantially.

REFERENCES

1. S. Sigoloff et al., Gamma Measurements Utilizing the USAF Chemical Dosimeters, Operation Plumbbob Report, WT-1500, November 1958. (Classified)
2. J. F. Halsey and M. V. Barton, Spectra of Ground Shocks Produced by Nuclear Detonations, Operation Plumbbob Report, WT-1487, Aug. 17, 1959. (Classified)
3. W. J. Flathau et al., Blast Loading and Response of Underground Concrete-arch Protective Shelters, Operation Plumbbob Report, WT-1420, June 1959. (Classified)
4. E. Cohen and S. Weissman, Underground Shock Environment Data and Application to the Design of Underground Structures, Proceedings of the 28th Symposium on Shock, Vibration, and Associated Environments, Part III. Bulletin No. 28, held at Washington, D. C., Feb. 9-11, 1960, Office of the Secretary of Defense, Research and Engineering, Washington, D. C., September 1960.
5. E. Cohen and S. Weissman, Nuclear Weapon Ground Shock Effects in Relation to Hardened Design, Symposium on Scientific Research in Protective Construction, Ernst-Mach Institut, Freiburg i. Br., Eckerstrasse 4, West Germany, September 1960.
6. S. Weissman, E. Cohen, and N. Dobbs, Nuclear Weapon Blast and Ground Shock Effects on Dynamic Response of Interior Components and Equipment in Underground Structures, Proceedings of the 29th Symposium on Shock, Vibration, and Associated Environments, Part III. Bulletin No. 29, held at Oakland, California, Nov. 15-17, 1960, Office of the Secretary of Defense, Research and Engineering, Washington, D. C., March 1961.
7. D. M. Burmister, The Importance of Natural Controlling Conditions Upon Triaxial Compression Test Conditions, Am. Soc. Testing Materials, Spec. Tech. Publ. No. 106 (1951).

Chapter 5

CONCLUSIONS AND RECOMMENDATIONS

1. The test structure provided adequate protection from the effects of the test device at the test GZ distance. Despite failure of the door sealing gasket, the rise in pressure in the interior did not exceed 1.0 psi.

2. The flat-slab roof and supporting structure were more than adequate to resist the 39-psi peak incident test loading.

3. The door design was satisfactory; however, the pneumatic seal around the door frame should be replaced by a rigid mechanically operated seal.

4. High pressures that acted on the end retaining wall were the result of the particular orientation of the structure relative to GZ and the site conditions. The damage that occurred under these severe circumstances did not impair the usefulness of the ramp for vehicular use during the immediate postshot period. In addition, an actual shelter–garage structure would probably have alternate vehicular and personnel entrances and exits. For this reason the design strength of the retaining walls need not be increased. However, brittle type failure is undesirable, and therefore in future design the details should be modified to produce a more ductile type behavior.

5. Owing to the factors discussed in Sec. 4.2, the capacity of the as-built structure was larger than intended. Consequently a prototype design could be placed at a higher pressure level. It is estimated that, for a megaton type weapon, such a structure would be adequate for a peak blast pressure of 50 psi (assuming an allowable displacement equal to approximately three times the peak equivalent elastic value). It is recommended that the concrete strength for the columns and roof slab be made 5000 psi, which was the value of the as-built slab and columns of the test structure.

Appendix A

DESIGN DRAWINGS

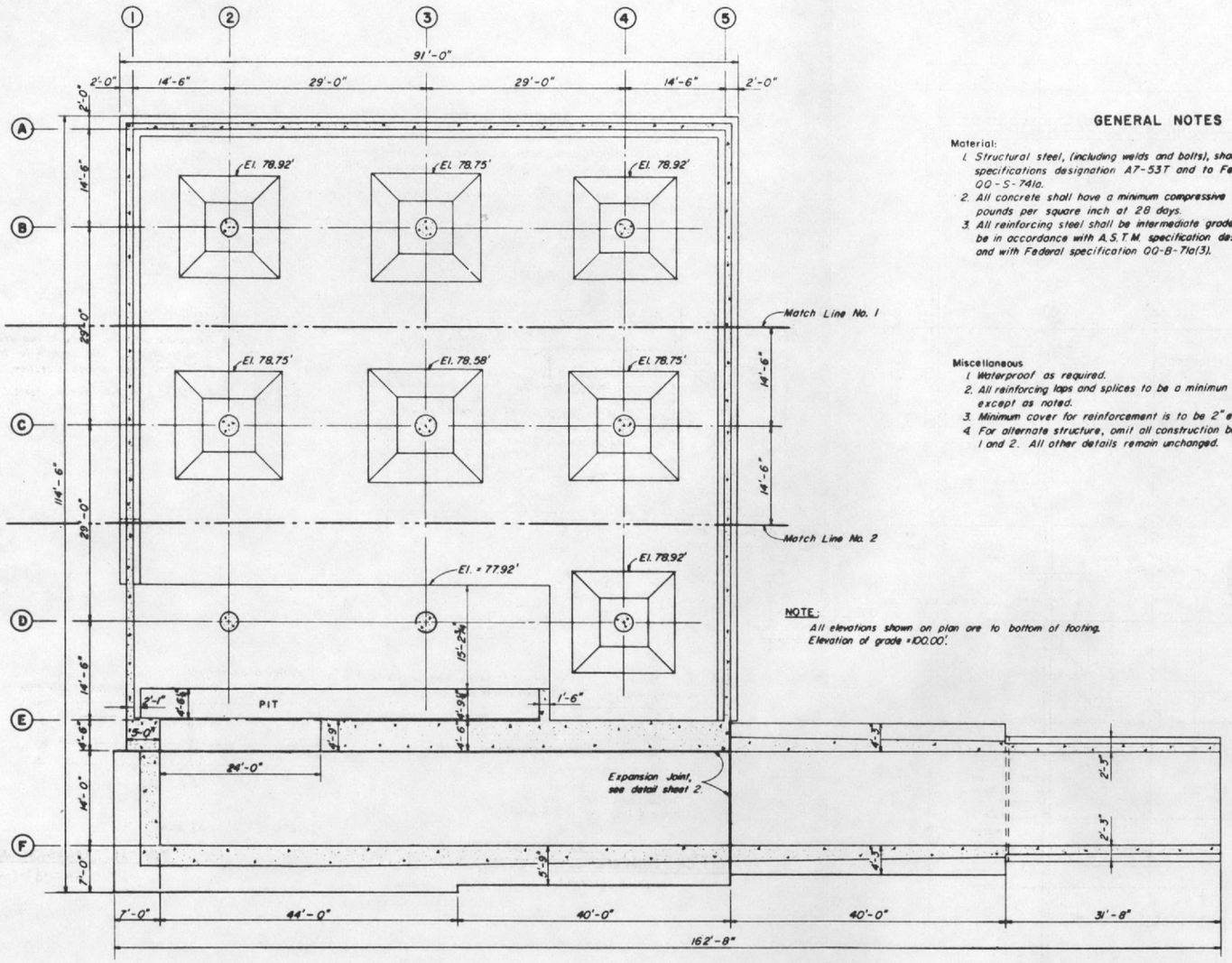

GENERAL NOTES

Material:

1. Structural steel, (including welds and bolts), shall conform to A.S.T.M. specifications designation A7-53T and to Federal specifications QQ-S-741a.
2. All concrete shall have a minimum compressive strength of 4,000 pounds per square inch at 28 days.
3. All reinforcing steel shall be intermediate grade. Deformation shall be in accordance with A.S.T.M. specification designation A305-53T and with Federal specification QQ-B-71a(3).

Miscellaneous

1. Waterproof as required.
2. All reinforcing laps and splices to be a minimun of 30 diameters except as noted.
3. Minimum cover for reinforcement is to be 2" except as noted.
4. For alternate structure, omit all construction between match lines 1 and 2. All other details remain unchanged.

NOTE:
All elevations shown on plan are to bottom of footing.
Elevation of grade =100.00'.

FOUNDATION PLAN
SCALE: $\frac{1}{8}$"=1'-0"

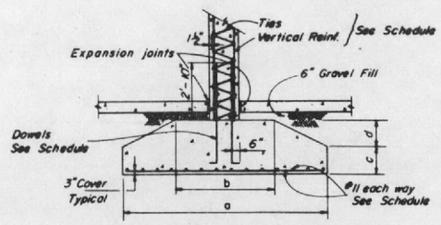

TYPICAL COLUMN FOOTING DETAIL
NTS

COLUMN & COLUMN FOOTING SCHEDULE				
MARK		3C	2B,2D,4B,4D	2C,3B,3D,4C
	Size	36 ϕ	33 ϕ	36 ϕ
	Core	33 ϕ	30 ϕ	33 ϕ
	Vertical Reinf.	20 #9	16 #9	12 #9
	Spiral	#5 @ 3"	#5 @ 3"	#5 @ 3"
	Dowels	20 #9	16 #9	12 #9
FOOTING	a	16'-9"	15'-0"	16'-0"
	b	8'-3"	7'-2"	7'-10"
	c	2'-2"	2'-0"	2'-1"
	d	2'-1"	1'-11"	2'-0"
	Reinf. each way	44 #11	36 #11	41 #11

Notes:

1. Spirals to be held firmly in place and true to line by a minimum of four vertical spacers.
2. 1½ extra turns of spiral rod at each end of spiral to be provided for anchorage
3. Spirals to extend from top of footing to a plane at which the dia. of the capital is twice that of the column
4. Column reinforcing to extend from top of footing to top reinforcing in roof slab.
5. For column footing 2B only, distribute 36 #11 reinforcing bars each way except as follows:
   Middle strip (b=7'-2"): 22 #11
   Outside strip (7'-10"): 14 #11

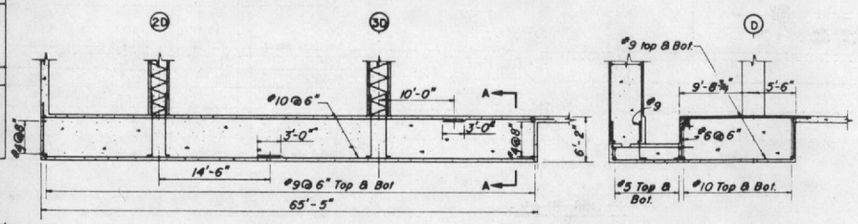

LONGITUDINAL SECTION

SECTION A-A

COMBINED FOOTING
SCALE: $\frac{1}{8}$"=1'-0"

Fig. A.1—Foundation plan.

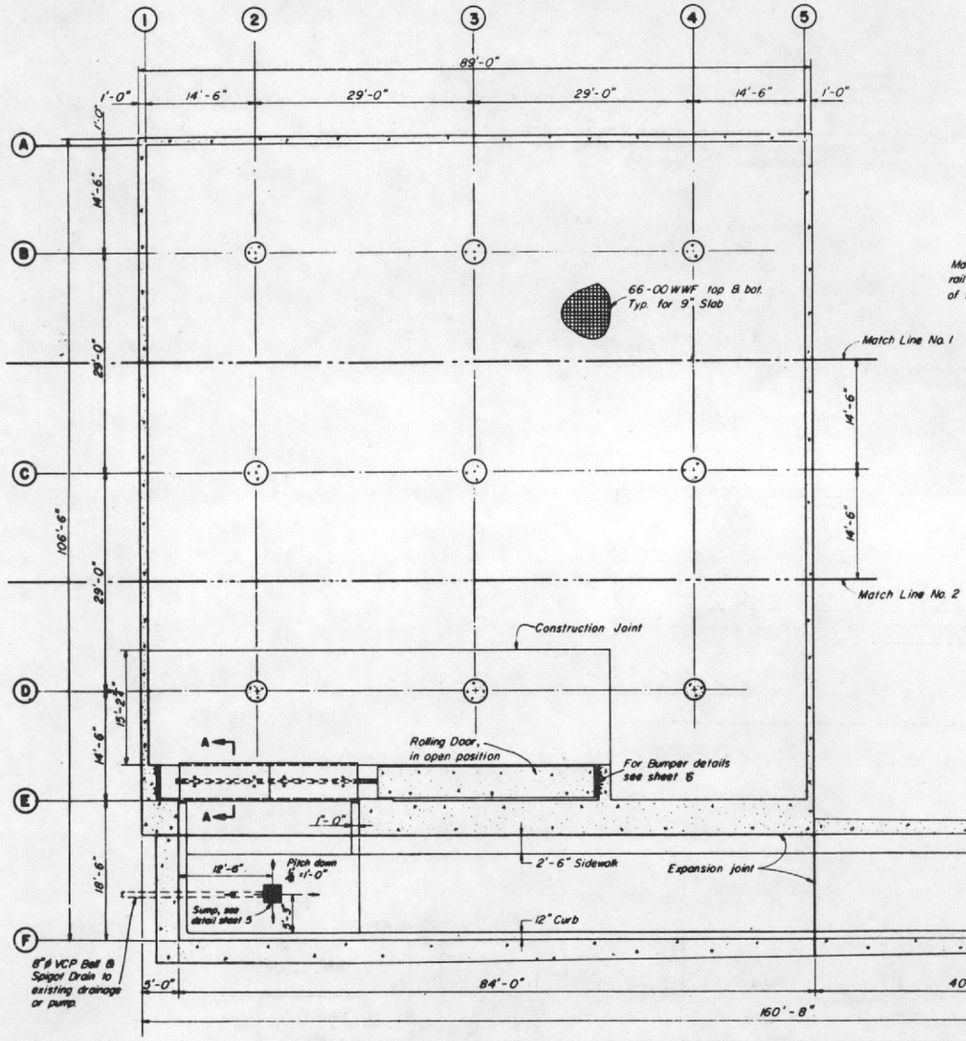

FLOOR PLAN
SCALE: 1/8"=1'-0"

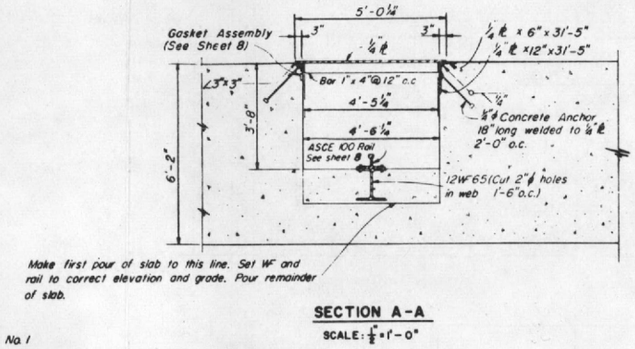

SECTION A-A
SCALE: 1/2"=1'-0"

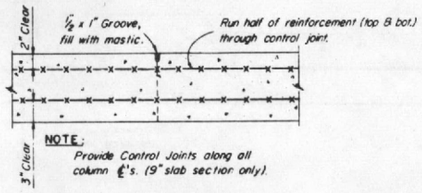

NOTE:
Provide Control Joints along all column ℄'s. (9" slab section only).

TYPICAL CONTROL JOINT DETAIL
SCALE: 1 1/2"=1'-0"

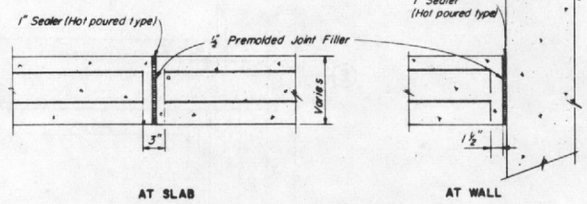

TYPICAL EXPANSION JOINT DETAILS
SCALE: 1 1/2"=1'-0"

NOTE:

1. Removable pit cover to be in two sections 11'-11" long. Provide four 2" diameter holes in each section for lifting purposes. Holes to be located 2'-0" from ends in long direction.
2. Reinforcing not shown, see sheets 1 & 6

Fig. A.2—Floor plan, sections, and details.

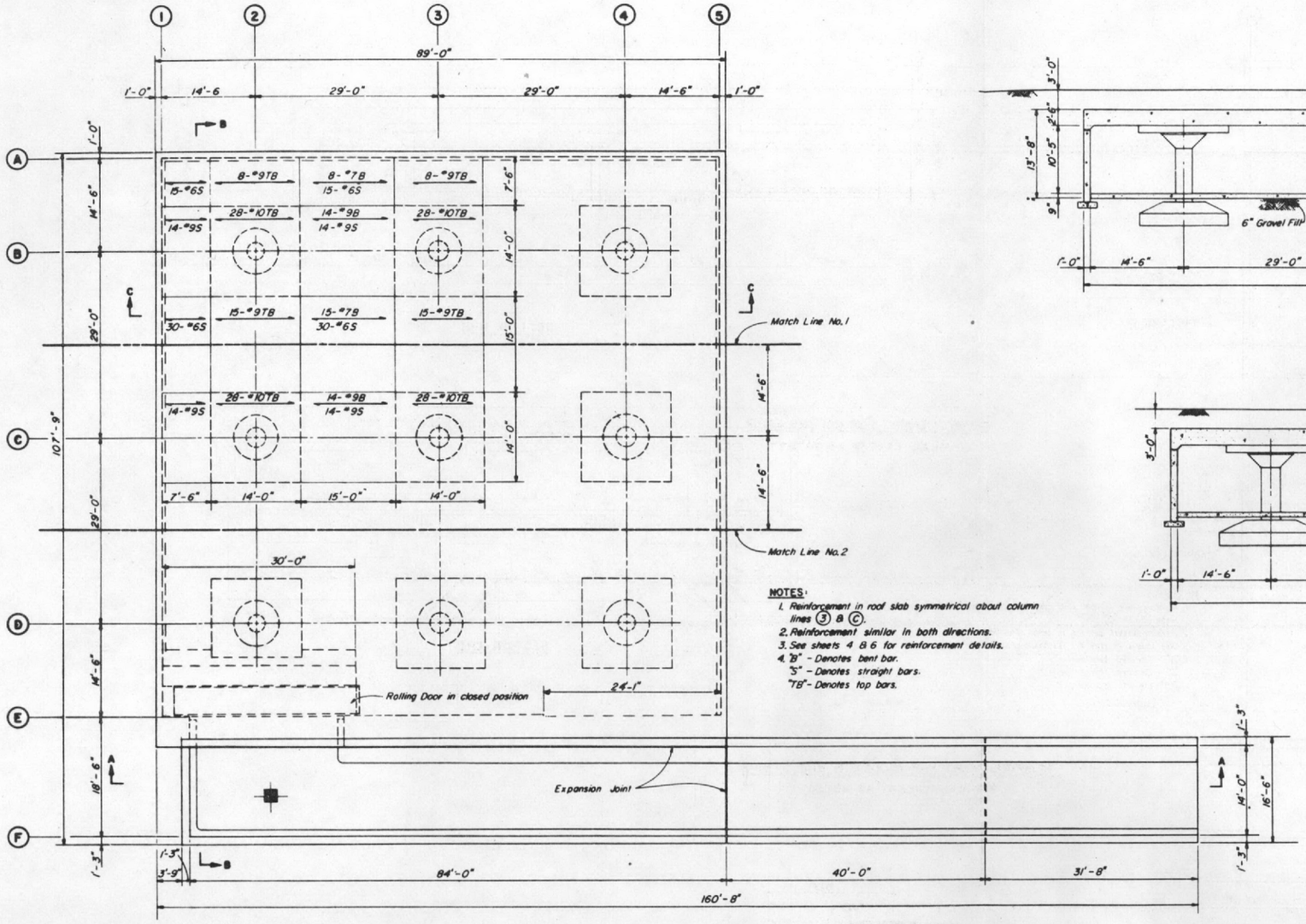

ROOF PLAN

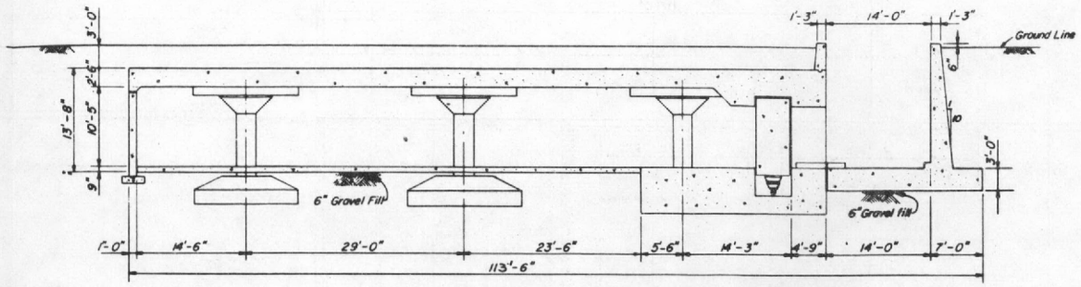

SECTION B-B

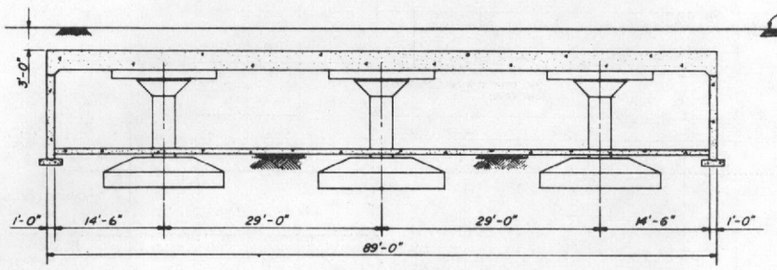

SECTION C-C

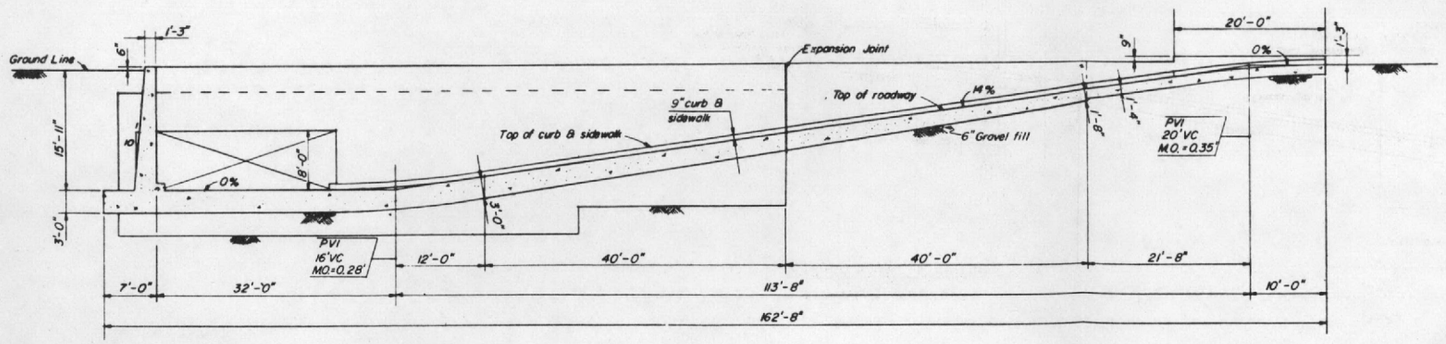

SECTION A-A

Fig. A.3—Roof plan and sections.

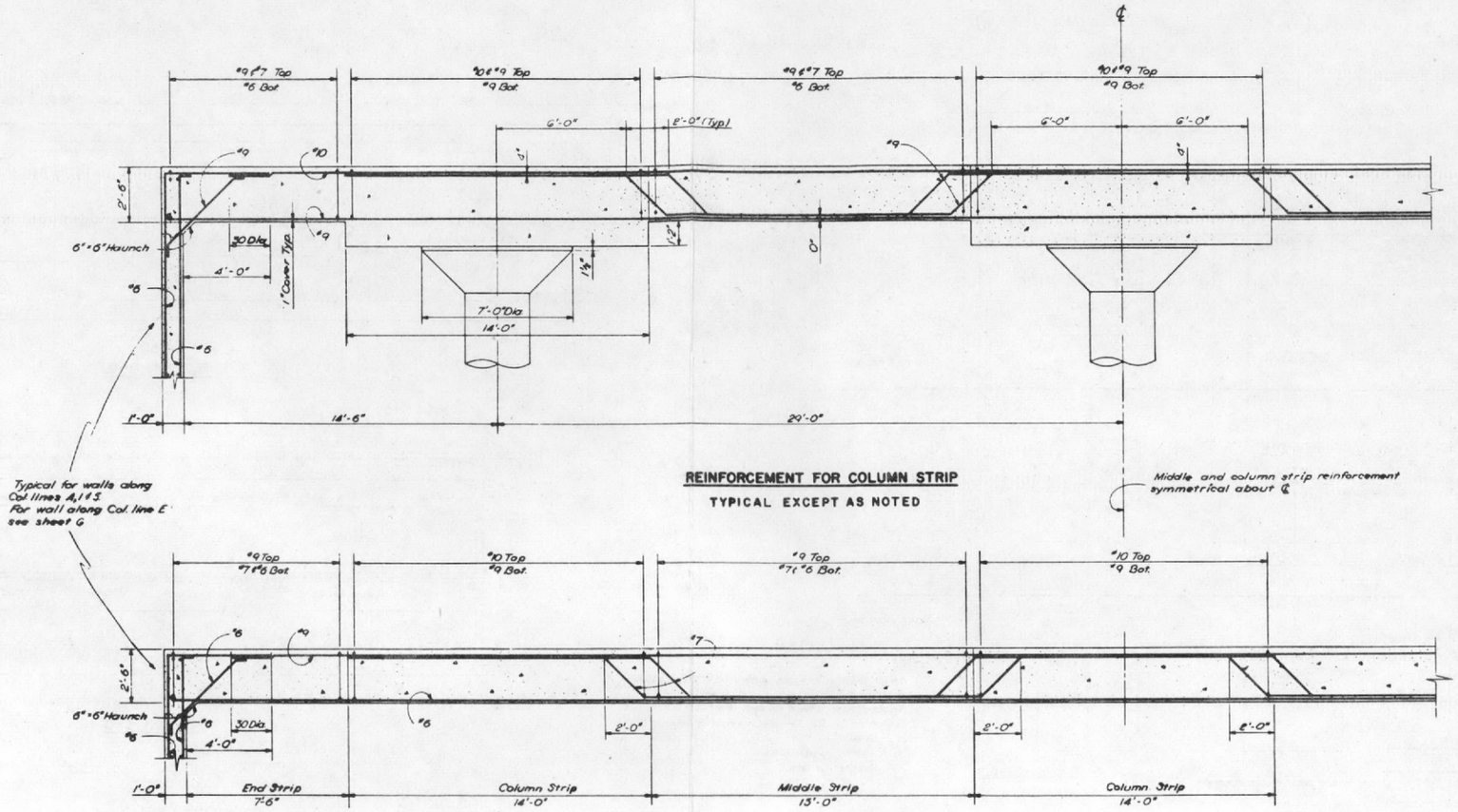

REINFORCEMENT FOR MIDDLE & END STRIPS

TYPICAL EXCEPT AS NOTED

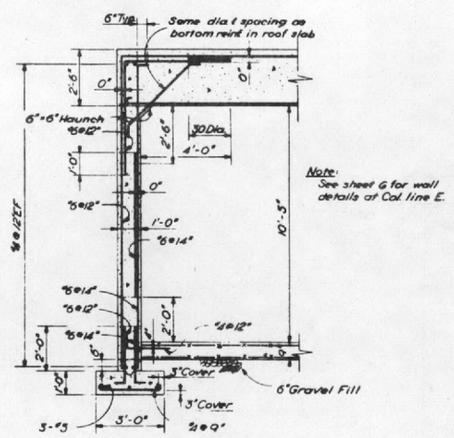

EXTERIOR WALL DETAIL

TYPICAL AT COL. LINES A, 1, & 5

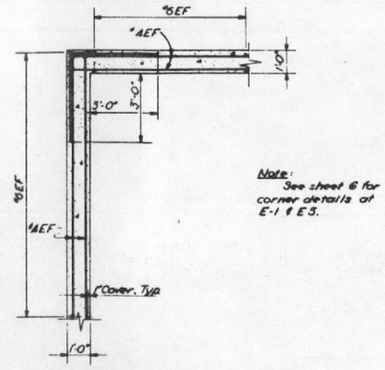

DETAIL AT WALL CORNER

TYPICAL AT A-1 & A-5

Fig. A.4—Typical roof slab and wall details.

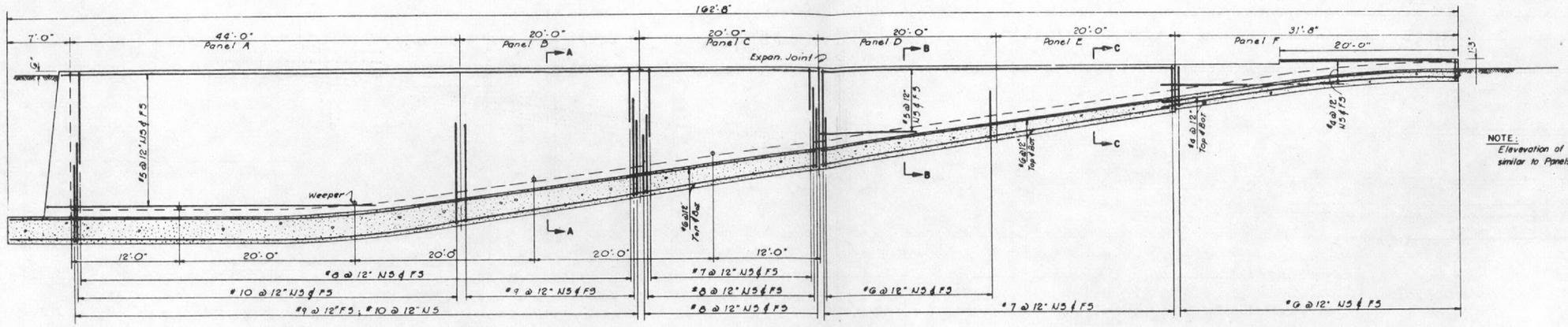

NOTE:
Elevevation of Ramp at column line E similar to Panels D, E, F (opposite hand)

ELEVATION OF RAMP AT COLUMN LINE F
SCALE: 1/16" = 1'-0"

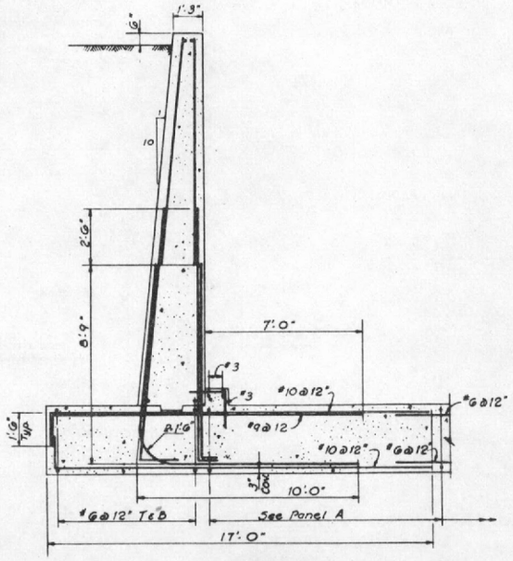

SECTION D-D
SCALE: 1/8" = 1'-0"

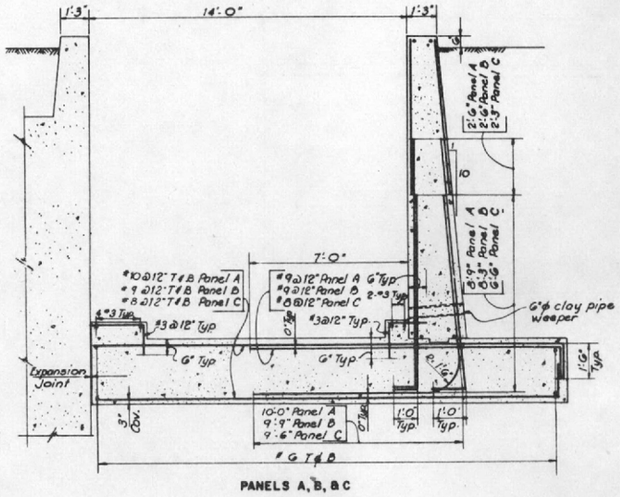

PANELS A, B, & C
SECTION A-A
SCALE: 1/8" = 1'-0"

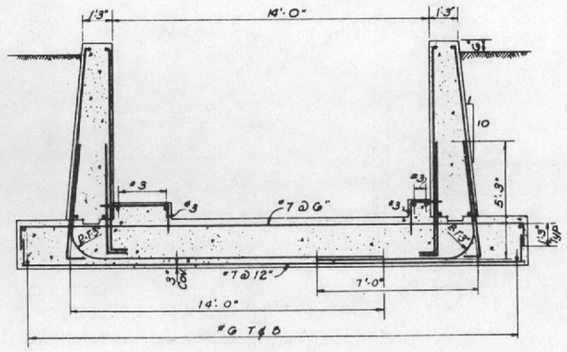

PANEL D
SECTION B-B
SCALE: 1/8" = 1'-0"

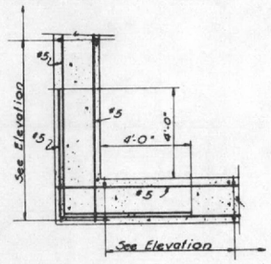

CORNER DETAIL
SCALE: 1/8" = 1'-0"

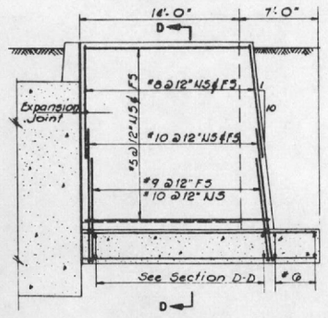

ELEVATION OF RAMP AT COLUMN LINE I
SCALE: 1/16" = 1'-0"

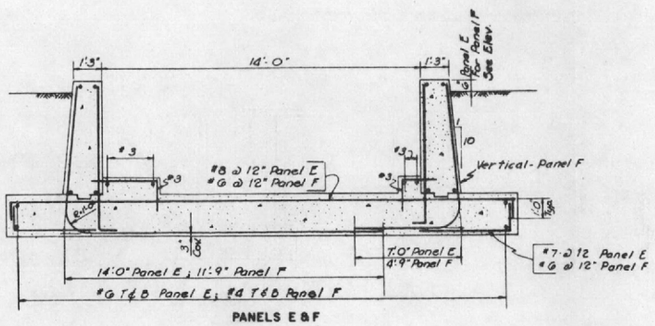

PANELS E & F
SECTION C-C
SCALE: 1/8" = 1'-0"

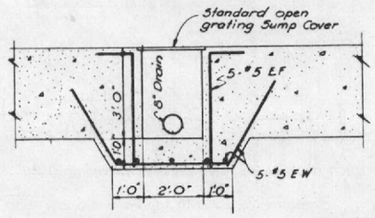

SUMP PIT DETAIL
SCALE: 1/2" = 1'-0"

NOTE:
For vertical alignment of ramp see sheet 3

Fig. A.5—Ramp elevations and sections.

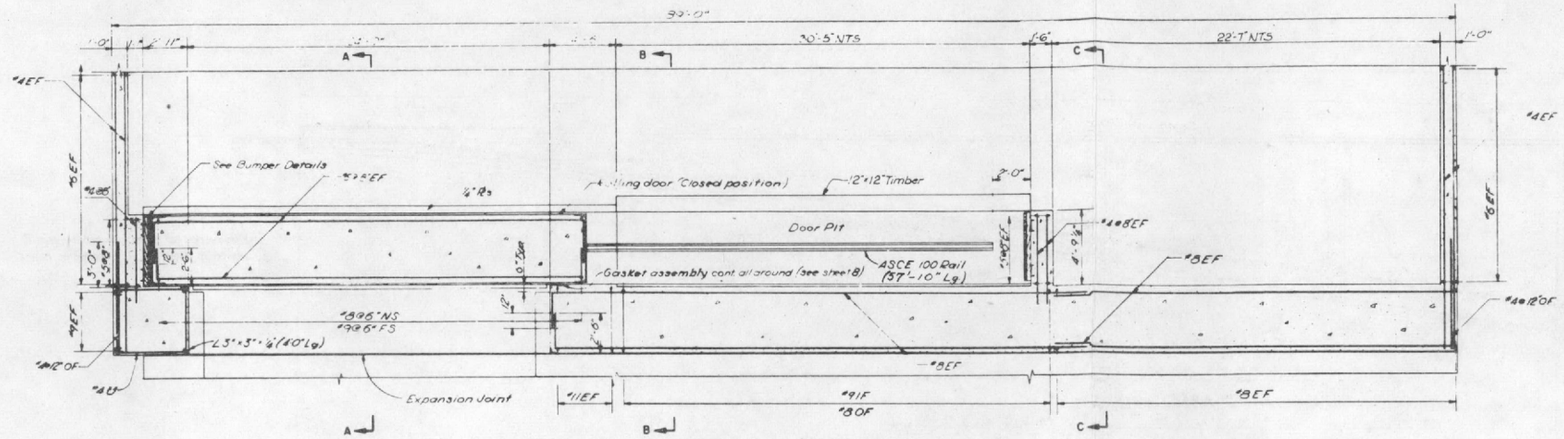

PLAN OF WALL AT COLUMN LINE E

SCALE: $\frac{1}{4}$" = 1'-0"

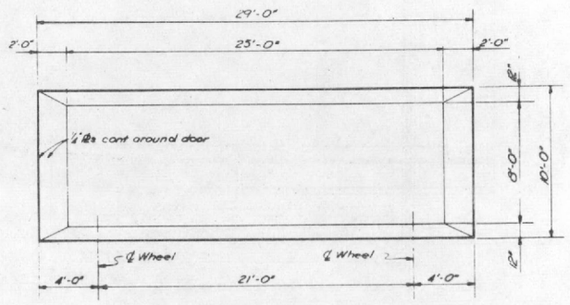

ELEVATION OF ROLLING DOOR

SCALE: $\frac{1}{4}$" = 1'-0"

Note:
See plan and section of wall at Col line E for door reinf. For details of door see sheet 7.

Note:
See Detail a for beam reinf. and stirrups.

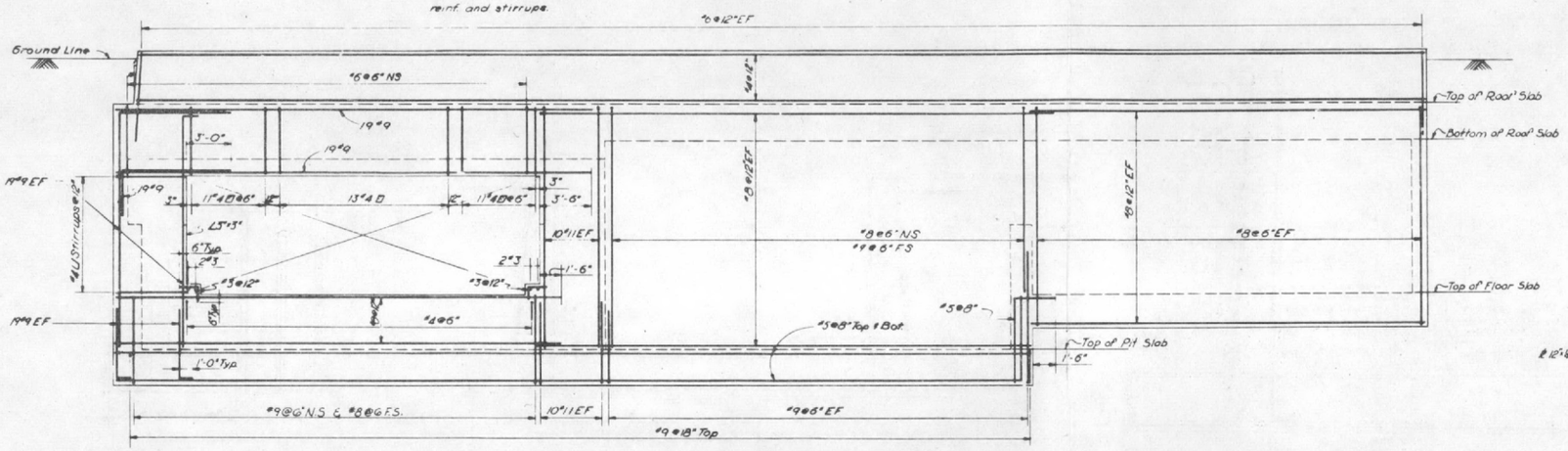

ELEVATION OF WALL AT COLUMN LINE E

SCALE: $\frac{1}{4}$" = 1'-0"

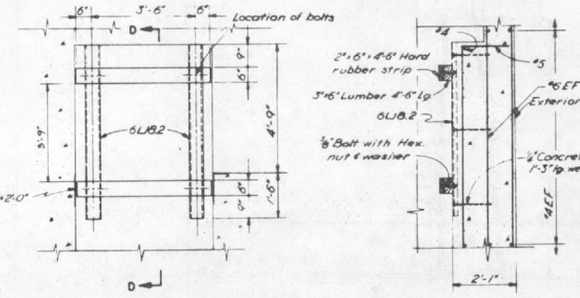

BUMPER DETAIL

SCALE: $\frac{1}{2}$" = 1'-0"

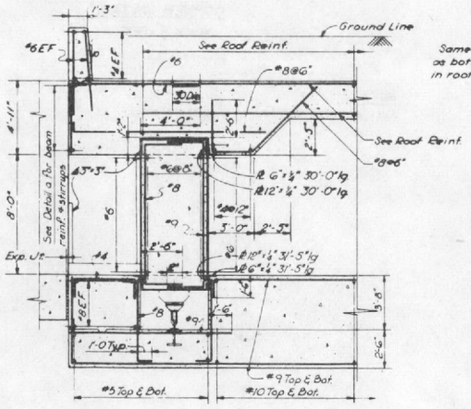

SECTION A-A

SCALE: $\frac{1}{4}$" = 1'-0"

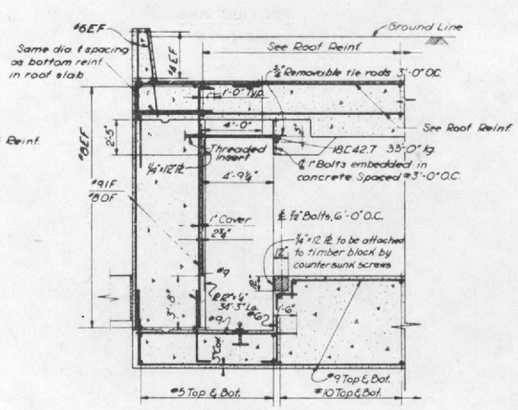

SECTION B-B

SCALE: $\frac{1}{4}$" = 1'-0"

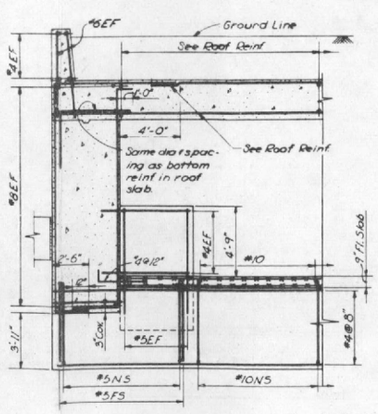

SECTION C-C

SCALE: $\frac{1}{4}$" = 1'-0"

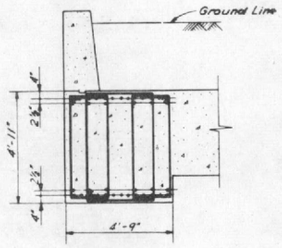

DETAIL a

SCALE: $\frac{3}{8}$" = 1'-0"

Fig. A.6—Column line E, sections and details.

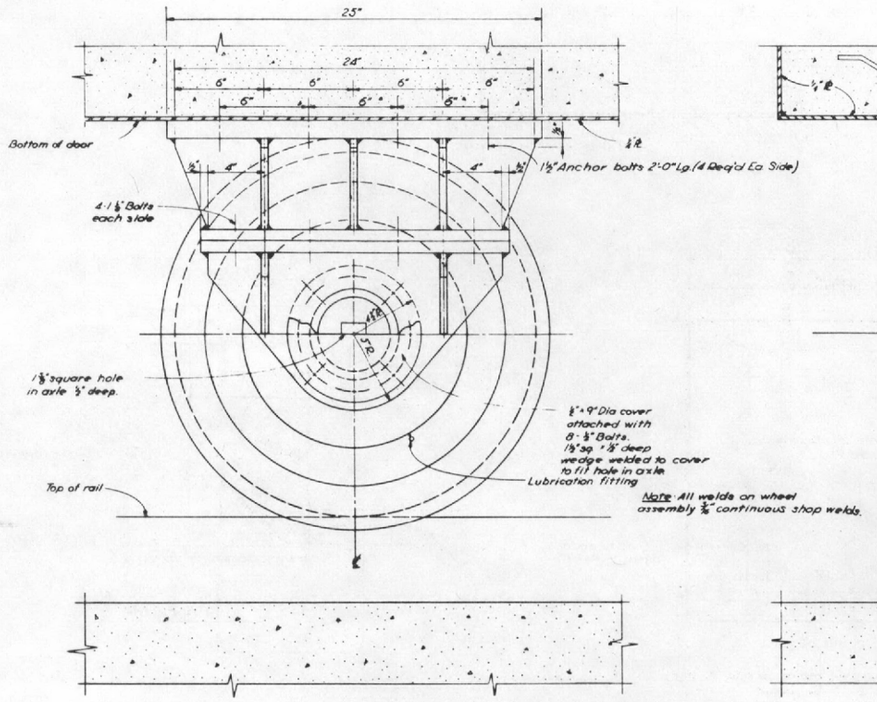

SIDE ELEVATION

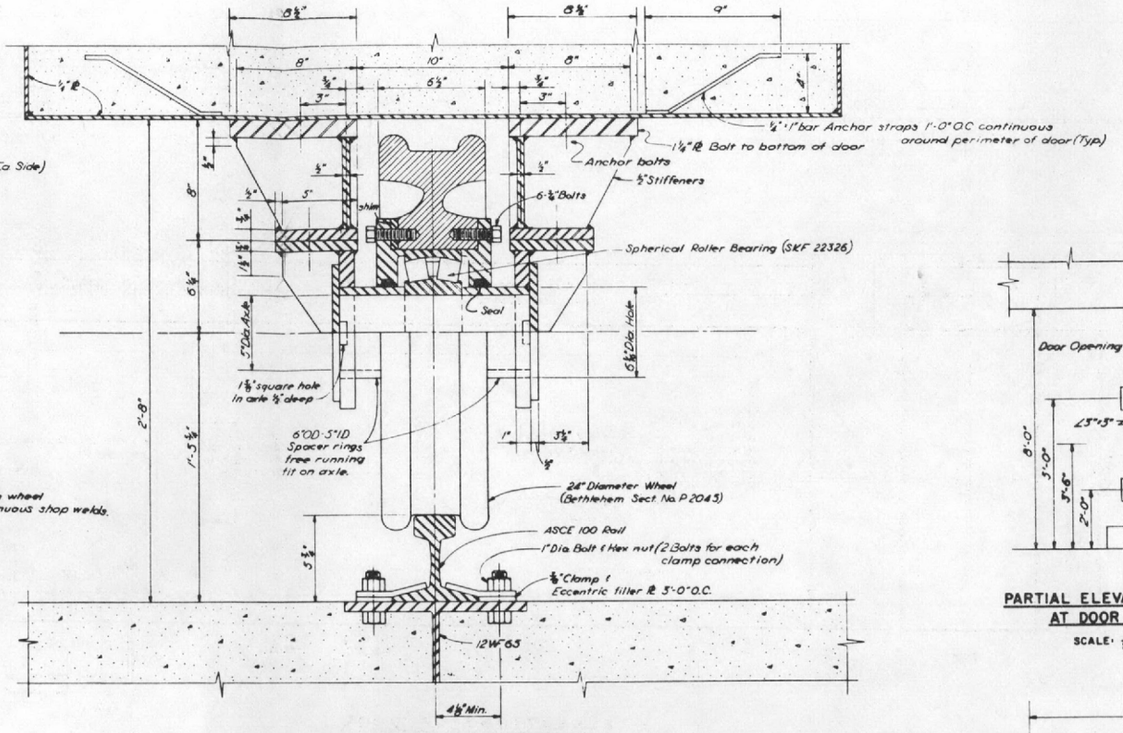

HALF SECTION

WHEEL ASSEMBLY DETAILS

SCALE: 3" = 1'-0"

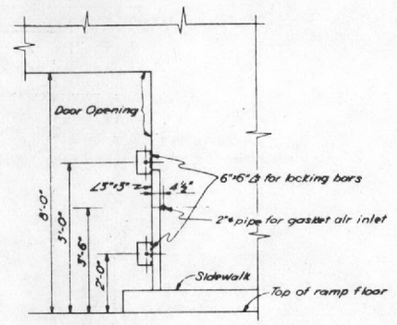

PARTIAL ELEVATION OF WALL AT DOOR OPENING

SCALE: ½" = 1'-0"

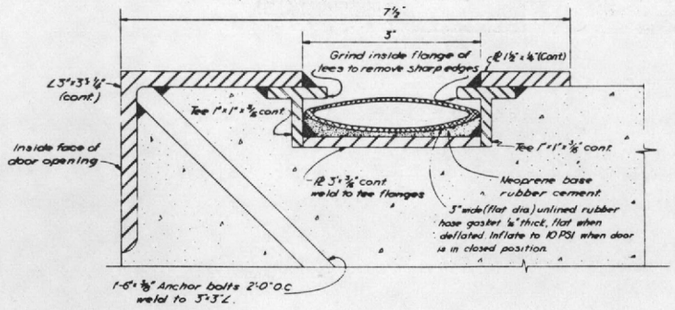

GASKET ASSEMBLY

FULL SCALE

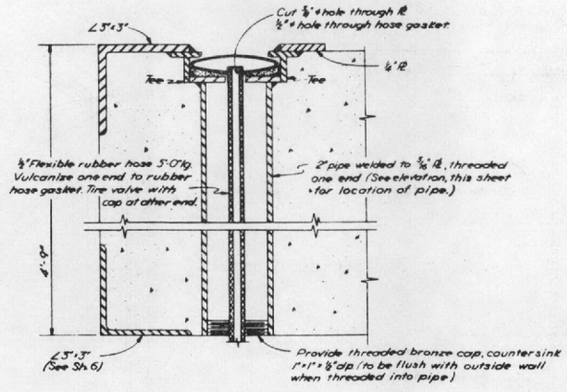

AIR INLET DETAIL

HALF SCALE

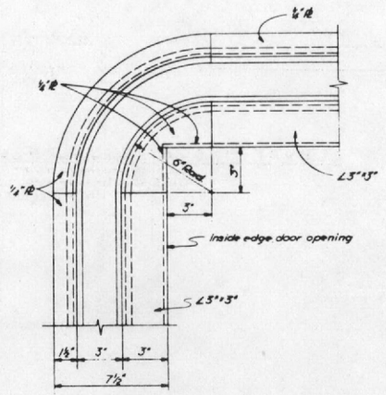

GASKET CORNER DETAIL

SCALE: 3" = 1'-0"

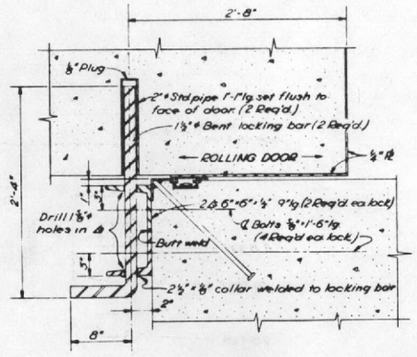

LOCKING DETAIL

SCALE: 1½" = 1'-0"

Fig. A.7—Rolling-door details.

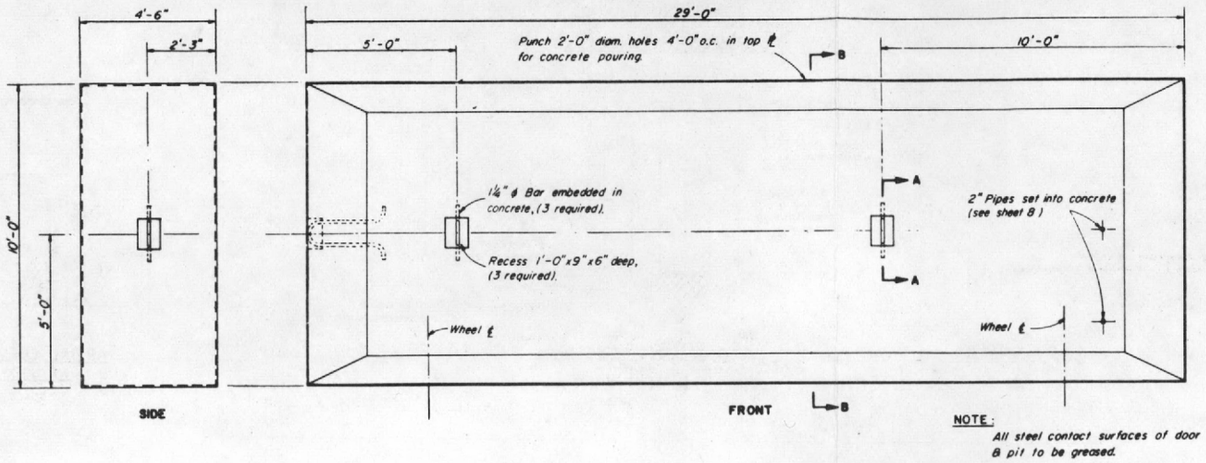

ELEVATIONS OF DOOR

SCALE: $\frac{1}{2}$" = 1'-0"

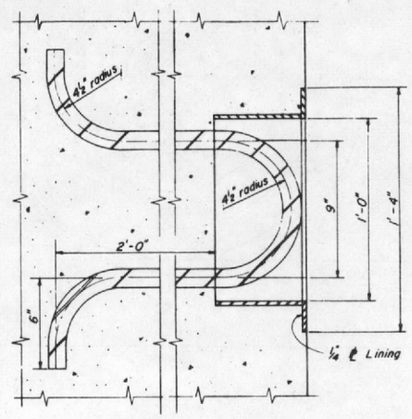

SECTION A-A (TYPICAL)

SCALE: 3" = 1'-0"

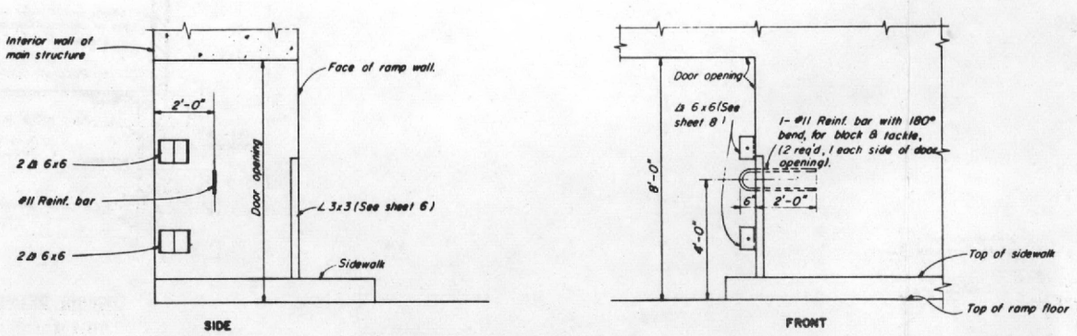

ELEVATIONS AT DOOR OPENING

SCALE: $\frac{1}{2}$" = 1'-0"

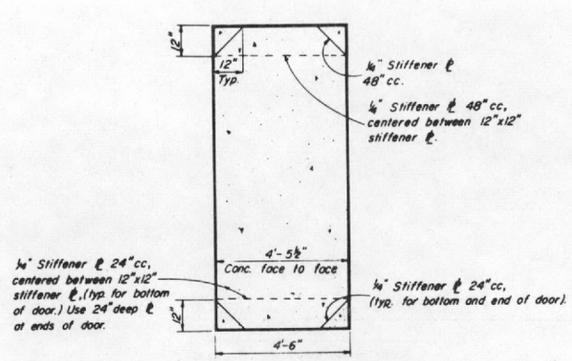

SECTION B-B

SCALE: $\frac{1}{2}$" = 1'-0"

Fig. A.8—Rolling-door details.

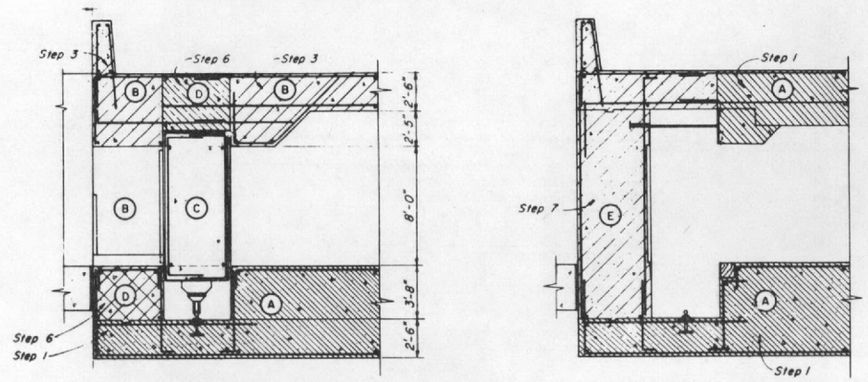

Recomended Erection Procedure at Column Line E

Steps:

1. Pour 2'-6" pit slab, combined footing and floor slab. Roof slab and 4'-6" wall may be poured to the extent indicated. (Sections A)
2. Place door assembly (plates, wheel assembly, etc., on rail) in trench at door opening. Support bottom of door with a sufficient number of blocks and/or jacks to prevent bending of the bottom plate due to the load of the wet concrete.
3. Pour sections B above the door opening along with the pilasters on each side of the door opening.
4. Place reinforcement and forms for door, brace securely and pour concrete. (Section C)
5. After concrete in door has attained sufficient strength, remove blocks and jacks, and roll door to open position.
6. Pour sections D at the door opening.
7. Roll door to closed position and complete pouring of 4'-6" wall and roof slab adjacent to pilaster. (Section E)

SECTION A-A

SECTION B-B
DOOR NOT SHOWN

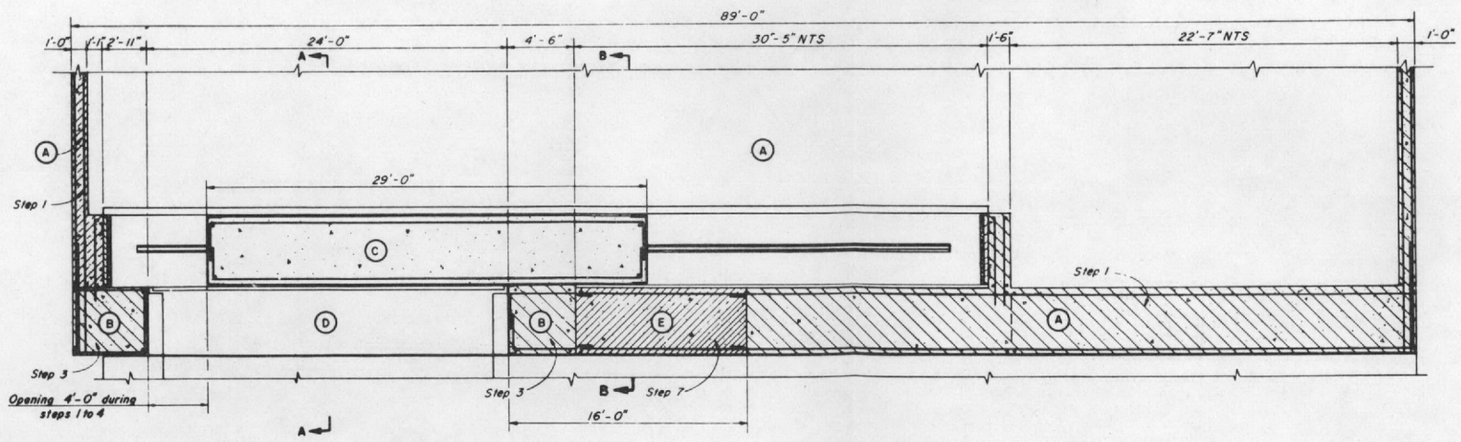

PLAN OF WALL AT COLUMN LINE E

Fig. A.9—Erection procedure at column line E.

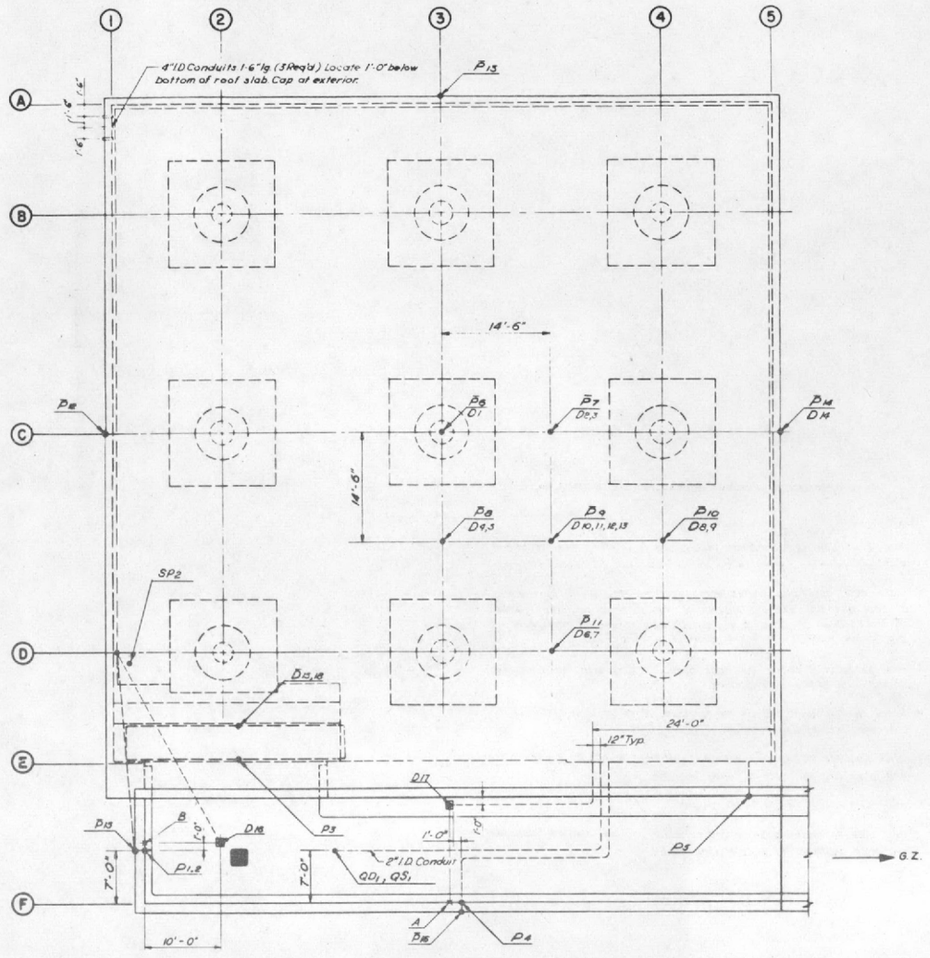

ROOF PLAN

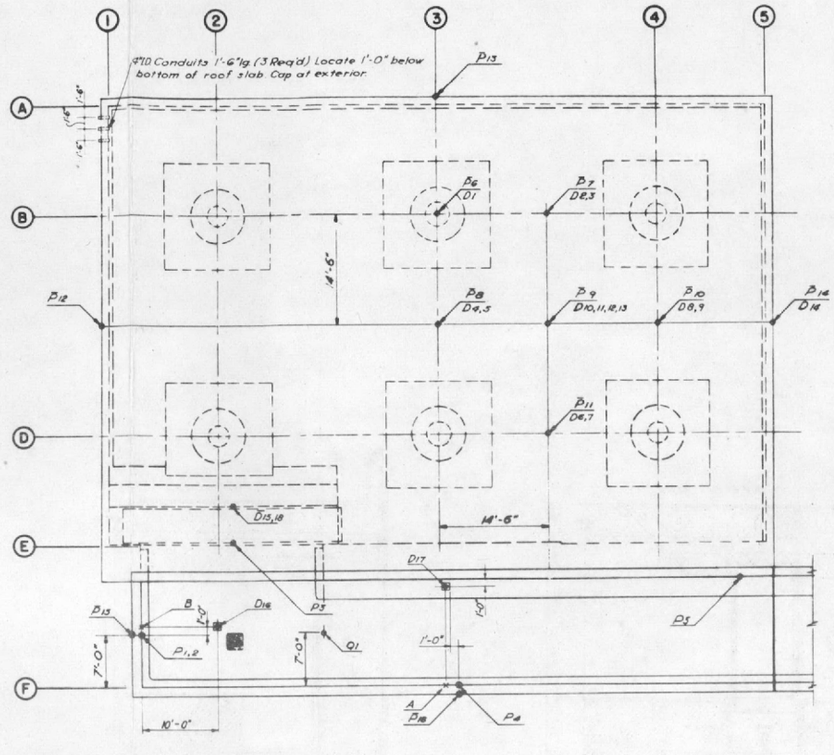

ROOF PLAN — ALTERNATE

NOTE:
Conduits for Alternate Structure Roof Plan similar to Roof Plan conduits

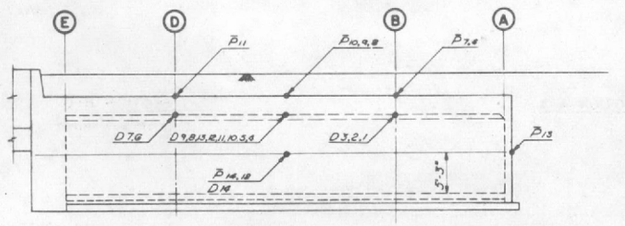

ELEVATION ALONG COLUMN LINE 5 — ALTERNATE

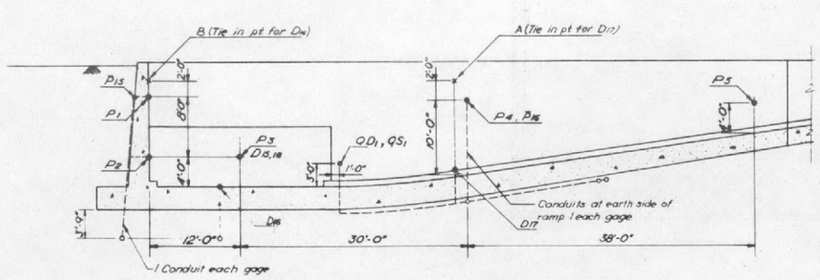

RAMP ELEVATION

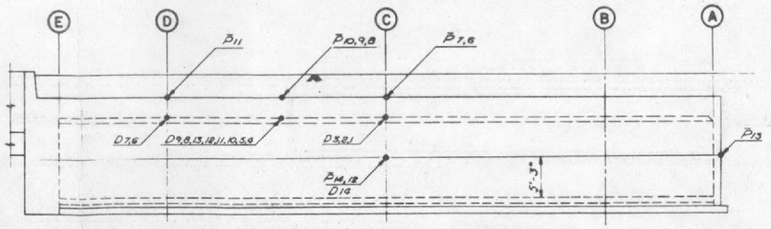

ELEVATION ALONG COLUMN LINE 5

NOTES:
1. BRL will place all instrument cables, (not conduits) install all gages, and provide all ditching required for same.
2. Earth pressure gages (Carlson Type) must be calibrated by BRL prior to backfilling.
3. Dynamic Pressure gages — Q
4. Wiancko Type Pressure gages — P
5. Carlson Type Pressure gages. — P
6. Inductance Type Deflection gages — D
7. BRL Deflection gages — D
8. Conduits with bends to be equipped with pull wire.
9. All conduits to be 1/4" I.D. except as noted.
10. Conduit for P6 is to be taken down through column and bent out 8'-0" above floor level.
11. Gage D1 is to be referenced to the steel pile in the floor slab below P6. (See Sheet #11)
12. See Sheets 11 & 12 for Mount details.
13. BRL Self-Recording Pressure gage — SP

Fig. A.10— Instrumentation.

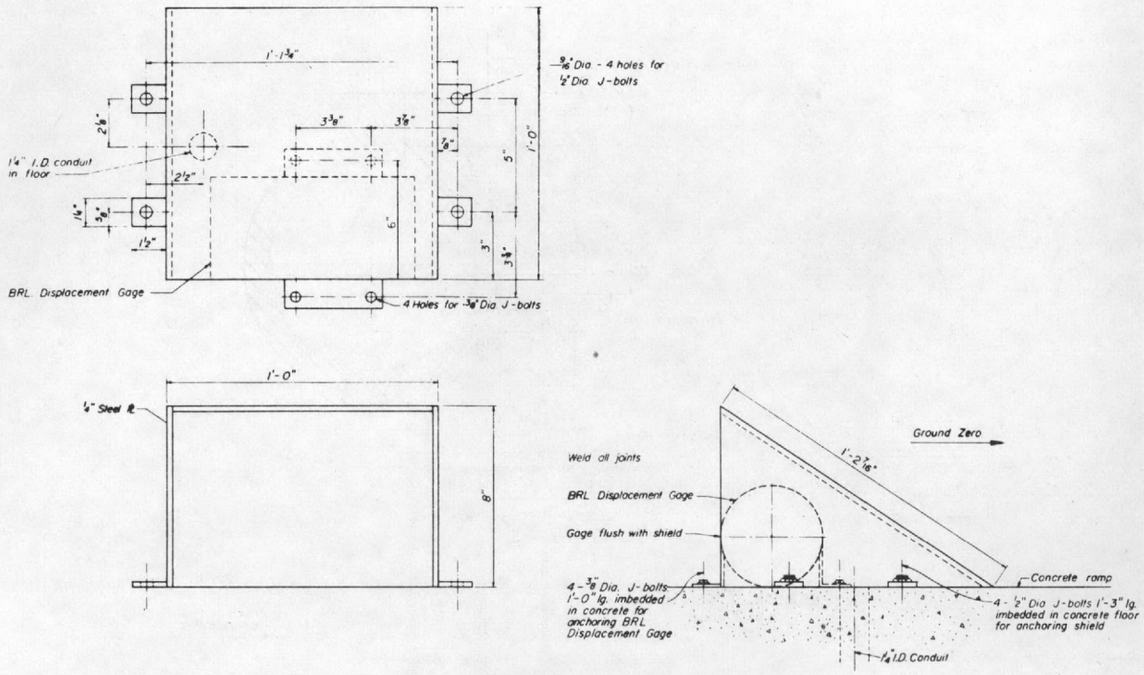

BRL DISPLACEMENT GAGE SHIELD FOR POSITION D_{16}

SCALE: 3/8" = 1"

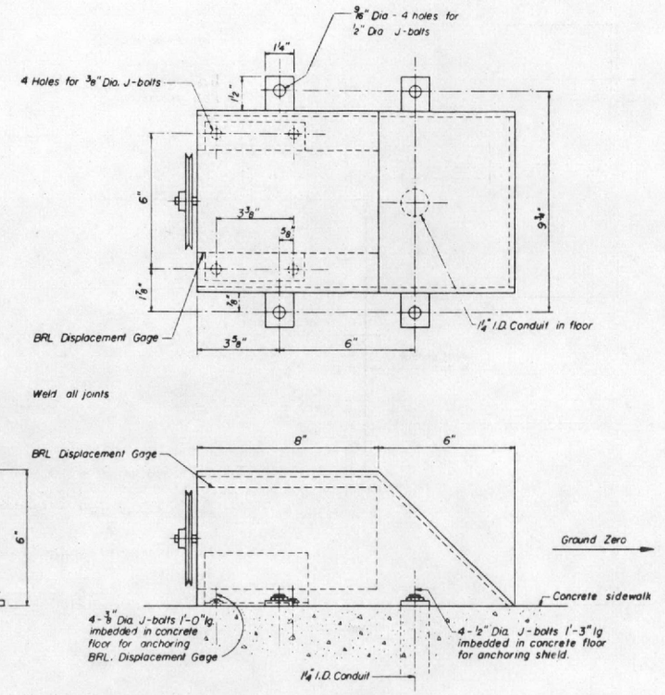

BRL DISPLACEMENT GAGE SHIELD FOR POSITION D_{17}

SCALE: 3/8" = 1"

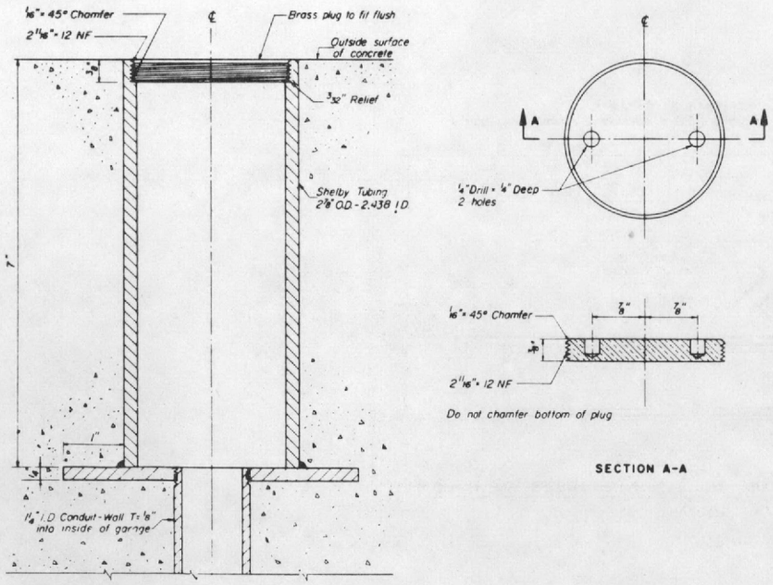

WIANCKO GAGE MOUNT

FULL SCALE

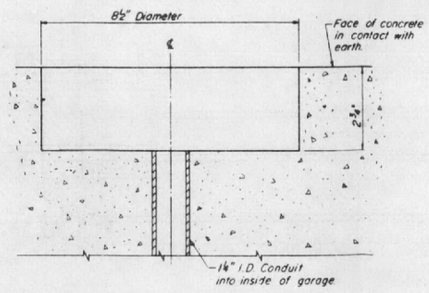

CARLSON (EARTH PRESSURE) GAGE MOUNT

HALF SCALE

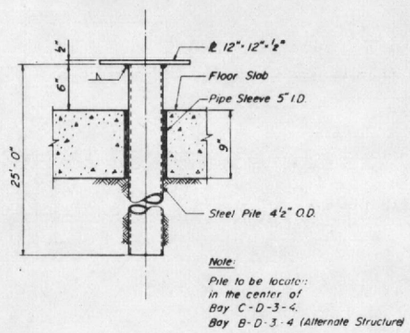

REFERENCE PILE FOR DEFLECTION GAGE D_1

SCALE 1½" = 1'-0"

NOTES:

1. Tie-in points on ramp walls for Gages D_{16} & D_{17} to be ⅜" ϕ bolts anchored into the wall with one inch of thread extending out from the concrete.

Fig. A.11—Instrumentation mounts and details.

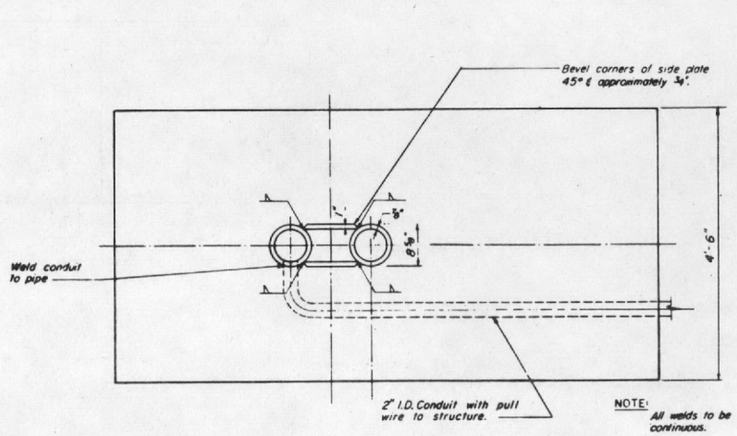

PLAN

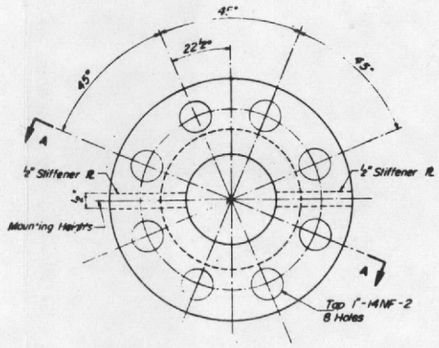

ELEVATION

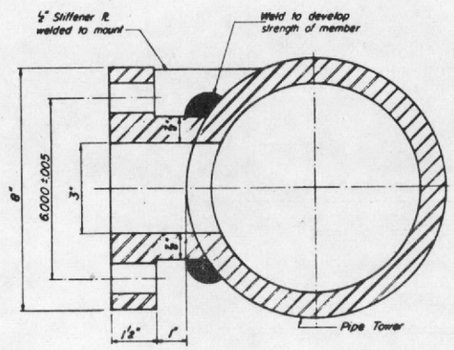

SECTION A-A

Q-GAGE MOUNT DETAIL

HALF SCALE

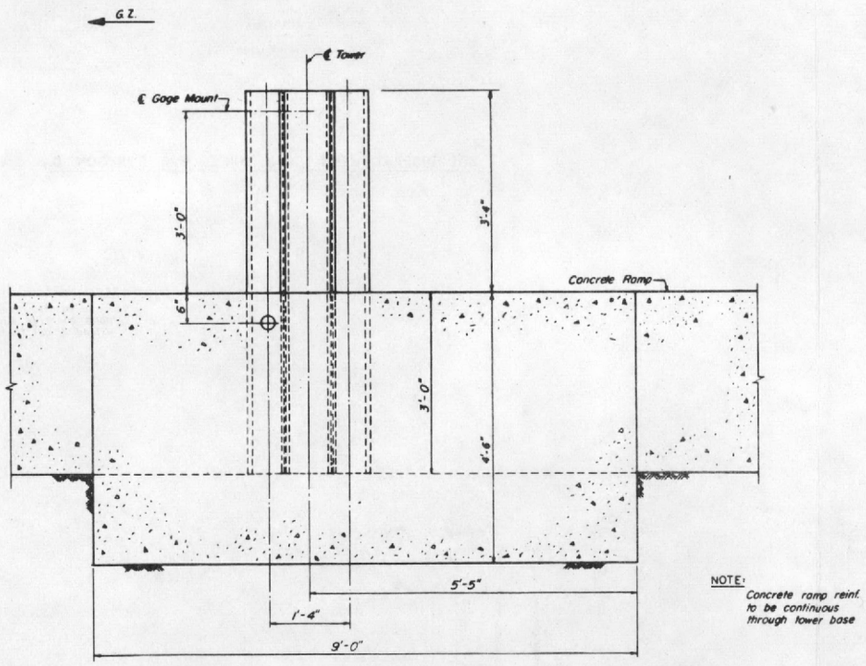

ELEVATION

TOWER & BASE OF Q-GAGE MOUNT AT POSITION Q_1

SCALE: 1" = 1'-0"

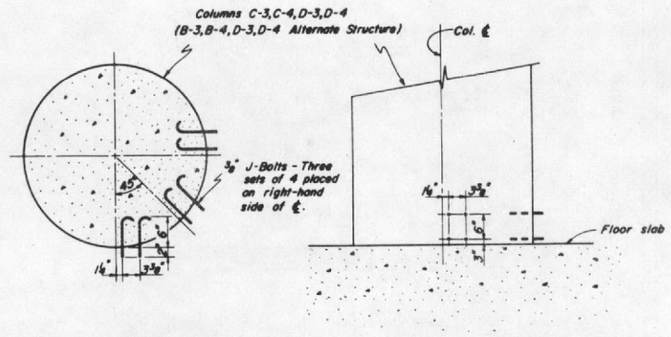

DEFLECTION GAGE MOUNTS FOR GAGES D2 thru D14

SCALE: 1" = 1'-0"

Fig. A.12—Instrumentation mounts and details.

Appendix B

CONSTRUCTION

B.1 GENERAL

All work was done under contract to the U. S. Atomic Energy Commission. The contractor for the construction of the reinforced-concrete dual-purpose underground parking garage and personnel shelter was the Lembke, Clough, and King Construction Company of Las Vegas, Nev. Reynolds Electric and Engineering Company supplied the concrete aggregate and miscellaneous work required to make the structure ready for the test. Holmes & Narver, Inc., provided over-all supervision and coordination as field representatives of the USAEC.

The OCDM, under whose sponsorship the structure was built, was represented at the site by an Ammann & Whitney field representative during the major portion of construction. The representative provided inspection and advisory service for the construction groups. This service was supplemented by visits to the site at critical times by the Project Officer.

Construction, in general, was geared to a very rapid time schedule. This schedule was closely adhered to despite the many difficulties that were experienced. The schedule called for a maximum of 75 calendar days from the scheduled starting date of Mar. 1, 1957. Excavation was started on March 5, and the backfilling was scheduled to be completed on May 15. This schedule could not be completely adhered to because of problems that developed during construction. These problems will be more fully defined in Secs. B.3.1 to B.3.9.

Figures B.1 to B.31 are photographs of the underground parking garage at various stages of construction. Deviations from the drawings and specifications are recorded in Sec. B.3. Tables B.1 and B.2 indicate the schedules adhered to during the construction phase of the operation.

B.2 MATERIALS

B.2.1 Concrete

Concrete was mixed at a central mixing plant operated by Lembke, Clough, and King Construction Company. The plant was a portable batcher type installation and was located approximately three miles from the structure. The concrete was trucked to the structure by conventional transit-mix trucks. During transportation the concrete was in a dry state, and upon arrival at the construction site the mixing water, as predetermined by the concrete-mix design, was added to the dry mix. The concrete was placed by the use of one or more of the three following methods: (1) by dumping into a $\frac{3}{4}$-cu yd bucket and placing by crane, (2) by dumping into concrete buggies and then placing directly, and (3) by placing directly with the use of concrete chutes.

A total of 87 standard 6- by 12-in. cylinders was taken from the structure for 7- and 28-day tests. Also, six preshot and seven postshot 4-in.-diameter cores were taken from the roof slab of the structure.

The results of the concrete strengths, as recorded for the concrete cylinders, are contained in Tables B.3 and B.4. The average values obtained from these tests are summarized in Table B.5.

The concrete strength as recorded from the roof cores is as indicated in Table B.6. Figures B.32 and B.33 show the points at which the pre- and postshot cores, respectively, were drilled; Fig. B.34 indicates the portions of the postshot cores that were tested for their compression strength. The cross sections of the pre- and postshot cores are shown in Figs. B.35 and B.36. Table B.7 gives the typical concrete-mix design used during construction.

B.2.2 Concrete Components

(a) *Cement.* Monolith type II cement was used for the construction of the underground garage. Batching was by bulk.

(b) *Coarse Aggregate.* The coarse aggregate, $1\frac{1}{2}$-in. graded aggregate, was stockpiled near the batching plant. Owing to the handling procedure and transportation methods employed in moving the aggregate from the crusher to the stockpile, segregation of the aggregate was evident in the stockpiled and batched concrete. Site conditions and limited amount of time for construction were the major causes of the poor handling and segregation.

(c) *Fine Aggregate.* The fine aggregate had additional wind-blown fines (primarily because of weather conditions at NTS) not indicated in Table B.7.

B.2.3 Concrete Forms

Wall and roof-slab forms consisted of $\frac{5}{8}$- and $\frac{3}{4}$-in. stock plywood panels. Part of the material used on the OCDM underground parking garage had been used several times before. Stock for the studs was 2 by 4 in. The columns were formed by use of cardboard spiral cylinders reinforced with band wire. Since the manufactured diameter of the cylinder was 36 in., it was necessary to cut down the diameter of the standard cylinders to 33 in. for columns 2B, 2D, 4B, and 4D.

B.2.4 Reinforcing Steel

Reinforcing steel used in the structure was of intermediate grade. The fabrication of the steel was subcontracted by Lembke, Clough, and King to Triangle Steel Company. Specimens of the bars were kept for future tests. The specific location of the bars from which the specimens were taken was noted. These specimens, totaling nine in all, were tested by the Los Angeles Testing Laboratory, Los Angeles, Calif.

All reinforcing steel was cut and bent in the shop and then transported by flat-bed trucks to the structure. On the whole the bending operation was adequate. However, in several sections of the structure the steel was not fabricated, as shown on the drawings, and therefore there are variations between the construction details and those shown on the drawings. The deviations from the drawings will be discussed further in Sections B.3.1 to B.3.9.

The yield and ultimate stresses and the percentage of elongation of 8-in. reinforcement specimens tested by the Los Angeles Testing Laboratory are given in Table B.8.

B.2.5 Structural Steel

The structural steel consisted essentially of miscellaneous items such as steel rail, I-beam support for the rail, face plates, gauge mountings, anchor bolts, and protection angles for corners of concrete. Several items were damaged in shipment from the fabrication shop. These items will be discussed in the following sections.

B.3 CONSTRUCTION OF THE STRUCTURE THROUGH ITS COMPONENT ITEMS

B.3.1 General

The following sections deal with the procedures used in construction of the component items of the structure and the conditions that existed at the completion of the construction

phase of the operation. Also included in this section are all deviations from the drawings and specifications and any additions that were deemed necessary to complete the structure in a satisfactory manner.

B.3.2 Excavation

The soil condition that existed at the forward site was of a clayey silt material. A full description of the soil is given in Appendix C. The predominant characteristic of the soil, in relation to the excavation, was its ability to maintain a vertical cut without shoring. This characteristic made it possible to excavate a minimum working area with conventional backhoeing equipment. Excavation was begun on the ramp and proceeded downward in stages until a depth of 17 ft 2 in. below the ground surface was reached. This placed the depth of the machine excavation 6 in. below the bottom of the proposed 9-in. floor slab. All additional excavation for the wall and column footings was by hand.

B.3.3 Foundation

The footings for columns 2B, 3B, 4B, 2C, 3C, 4C, and 4D and for the walls on column lines 1, A, and 5 were completed before the Project representatives arrived at the site. It was therefore impossible to ascertain whether any deviation from the contract drawings had occurred. The footings for columns 2D and 3D were changed by the designer from individual footings to a combined footing. However, the excavation for the individual footings had been completed prior to receipt of the change order calling for the combined footing. It was therefore necessary to backfill the excavated area of the individual footings with lean concrete to bring the bottom elevation up to that required for the combined footing. See Fig. B.37 for the backfilled area. There were several deviations between the design drawings and the actual reinforcement placement in the combined footing. However, these were minor and had negligible effect upon the structural capacity of the footing.

B.3.4 Columns and Walls

Columns 2B, 3B, 4B, 2C, 4C, and 4D were also erected before the Project Officer's representatives arrived at the site. It was therefore impossible to observe any deviations from the drawings for the actual construction of these columns. Columns 3C, 2D, and 3D were supervised during their construction and found correct.

The 1-ft walls along column lines 1, 5, and A and a section of the 4-ft 6-in. wall on column line E between column lines 3 and 5 were poured at the same time. The horizontal reinforcement at the intersection of the 1-ft walls was not placed as shown on the design drawings. A corner splice bar was used to make the joint continuous around the corner in place of the detail shown in Fig. A.4.

B.3.5 Floor Slab

The concrete for the floor slab was poured in two separate operations. The first pour was bounded by column lines 3, 5, A, and E. The remainder of the floor slab was poured the next day. One deviation of the actual construction from the design drawings was observed. At the intersection of the columns and the floor slab, kraft paper was used in place of mastic as a joint fill.

B.3.6 Roof Slab

The entire roof slab, including haunches, was poured in one continuous operation. The pouring of the concrete began about 9:00 p.m. on May 3 and continued through the next day and night until 7:30 a.m. on May 5. The total elapsed time of the operation was approximately 34.5 hr. The concrete placement, once the dry mix arrived at the structure, was performed by the three methods (and/or a combination thereof) described in Sec. B.2.1. A maximum of four transit-mix trucks was used during the pouring. Two trucks were usually in transit between the batching plant and the structure while the remaining two trucks were unloading, one by buggies, the other by crane and/or chutes.

Because of the unfavorable conditions that prevailed, such as climate conditions, time schedule, inconvenient location for obtaining desired equipment, etc., the predetermined construction results could not be fully attained by the above operation. Innumerable shrinkage cracks of a random nature developed over a major portion of the roof slab approximately 10 to 12 hr after the completion of the pour. Three main areas of the roof slab seemed to be appreciably cracked, each consisting of an area about 10 ft square. One area was near the northwest corner, one at the west side, and one on the north side. Single and double cracks, along with transverse cracks, developed in the roof slab above column 2B over an area of approximately 48 sq ft. Cracks with a depth up to 1 in. were observed at various locations in the slab. At several locations where double cracks were observed, the concrete was chipped out to determine the thickness of the reinforcement cover. The cover at one location was about $\frac{1}{8}$ in., whereas at the other there was approximately $\frac{3}{4}$-in. cover.

The roof-slab concrete was placed in strips, 10 to 15 ft in width, starting at the 4-ft 6-in. wall on column line E and proceeding toward the opposite side of the structure. Pour joints, the length of the structure, were apparent between adjacent strips. At each joint the later pour tended to lap over the surface of the earlier pour. It was indicated by the contractor and the inspectors that the strips were poured at approximately 4-hr intervals. At the east edge of the slab there was a rock pocket along the feathered slope of one of the slab pour joints.

After completion of the roof-slab concrete placement, a conference was held by the participating organizations involved in the construction. It was recommended at this meeting that an earth dam be formed around the roof slab and then, by flooding with several inches of water, to cure the concrete for several days. Owing to the time element involved in the test program, it was found impossible to perform the above curing process. A photograph of a typical crack pattern present at various locations in the roof slab is shown in Fig. B.29.

Before the concrete of the roof slab was placed, the reinforcement was checked for correct placement and size. Minor deviations were noted but were not serious enough to effect the structural capacity. Upon completion of the roof-slab pour, a rough leveling survey was performed on the slab. The results of this survey indicated a variation of approximately 3 in. in elevation at various points on the slab.

B.3.7 Rolling Door and Door Frame

Prior to the erection of the roof-slab formwork, the pilasters and upper beam supports for the door were poured. After placement of the reinforcement but prior to the pouring of the roof, six 2-ft-square openings were boxed out of the roof slab above the closed position of the door to facilitate the pouring of the door. The reinforcement across the openings was cut off 2 in. inside the openings. Upon completion of the pouring of the door, reinforcing bars were welded to the 2-in. extensions. Figure B.38 indicates the location of the access openings.

The structural-steel elements of the door were assembled in three stages. The bottom section, with the wheels prewelded to it, was placed on the steel rail. This section of the frame was then positioned under the openings in the roof slab and shored at 2-ft intervals. The two side sections were then lowered into position and welded to the lower section. The top section was subsequently placed and welded to the sides. The placement of the reinforcing steel and the erection of the formwork were then completed. The door was finally poured through the access openings in the roof slab.

Allowable clearances around the door were generally greater than the maximums specified. The width of the door pit and the door clearances are indicated in Figs. B.39 and B.40, respectively.

B.3.8 Ramp Slab and Walls

The floor slab of the ramp was poured in two sections. The first pour consisted of panels A, B, and C, inclusive (see Appendix A, Fig. A.5). The remaining portion of the slab (panels D, E, and F) was poured approximately seven days later. The walls of the ramp were poured in a sequence similar to the floor slab but at a later date. At several places along the ramp, honeycombed areas were observed at the intersection of the walls and floor slab. All the honeycombed areas were grouted prior to the completion of the structure.

B.3.9 Miscellaneous Items

The face plates for the rolling door and all corner protection angles were poured integral with the various concrete members they framed into. The face plates were not made continuous the entire length of the door pit. This deviation from the design drawings caused some postshot door-operating difficulty.

To operate the door preshot, it was necessary to chip the pilaster concrete. The specific areas where chipping was required are shown in Fig. B.39.

All anchor bolts that were not placed prior to pouring were ramset upon completion of the structure.

The gasket assembly shown in Fig. A.7 of Appendix A was found to be out of alignment when delivered to the site. Before installation the entire assembly was placed in good working order. The specified 3-in.-wide (flat diameter) rubber-hose gasket was replaced by one having a 2-in. diameter (round).

The reference pile detail for deflection gauge D1 (shown on Fig. A.11) was revised at the site to utilize an existing 16-in. steel pile used in the boring survey. The revised detail is shown in Fig. B.41.

B.4 SUMMARY OF CONSTRUCTION

When the backfilling had been completed, the instrumentation, as described in Sec. 2.3, was installed. The face plates for the rolling door were lubricated, and the door as a whole was placed in good working order. All construction debris was removed from the site.

TABLE B.1—SCHEDULE OF CONSTRUCTION*

Items	Concrete pours: Date	Concrete pours: Quantity, cu yd	Forms: Placed	Forms: Stripped	Steel placed	Remarks
Column footings						
2B	3/18/57	27	3/15/57	3/22/57	3/16/57	
3B	3/18/57	32	3/15/57	3/22/57	3/16/57	
4B	3/15/57	27	3/13/57	3/22/57	3/14/57	
2C	3/19/57	32	3/16/57	3/23/57	3/16/57	
3C	3/18/57	35	3/15/57	3/22/57	3/15/57	
4C	3/19/57	32	3/15/57	3/23/57	3/16/57	
4D	3/19/57	27	3/15/57	3/23/57	3/16/57	
Combined footings	4/3/57	250	4/2/57	3/6/57	4/2/57	
Walls on column lines						
1	4/9/57	47	4/4 to 4/8	4/11/57	4/4 to 4/8	
5	4/9/57	55	4/4 to 4/8	4/11/57	4/4 to 4/8	
A	4/9/57	55	4/4 to 4/8	4/11/57	4/4 to 4/8	
E	4/9/57	242	4/4 to 4/8	4/11/57	4/4 to 4/8	
Floor slab	4/18/57	220			4/16/57	One-half of slab poured 4/17/57
Roof slab	5/3 to 5/5	950	5/3/57	5/18/57	5/3/57	Opening left for door erection
Parapet on roof	3/29/57	15	5/28/57	6/1/57	4/4 to 4/8	
Rolling door	5/24/57	48	5/24/57	5/27/57	5/23/57	

*Excavation started 3/15/57, finished 3/28/57; backfilling started 6/1/57, finished 6/7/57.

TABLE B.2—SCHEDULE OF CONSTRUCTION

Items	Concrete pours: Date	Concrete pours: Quantity, cu yd	Forms: Placed	Forms: Stripped	Steel placed
Columns					
2B	3/27/57	1.8	3/26/57	4/11/57	3/25/57
3B	3/27/57	2.2	3/26/57	4/11/57	3/25/57
4B	3/27/57	1.8	3/26/57	4/11/57	3/25/57
2C	3/27/57	2.2	3/26/57	4/12/57	3/25/57
3C	4/15/57	2.2	4/15/57	4/20/57	4/15/57
4C	3/27/57	2.2	3/26/57	4/12/57	3/25/57
2D	4/15/57	3.3	4/15/57	4/20/57	4/15/57
3D	4/15/57	3.2	4/15/57	4/20/57	4/15/57
4D	3/27/57	1.8	3/26/57	4/12/57	3/25/57
Ramp walls					
Panel A	5/17/57	82	5/13/57	5/18/57	5/10/57
Panel B	5/17/57	20	5/13/57	5/22/57	5/10/57
Panel C	5/17/57	15	5/13/57	5/22/57	5/10/57
Panel D	5/23/57	21	5/20/57	5/25/57	5/16/57
Panel E	5/23/57	13	5/20/57	5/25/57	5/16/57
Panel F	5/23/57	8	5/20/57	5/25/57	5/16/57
Ramp, panel ABC	5/1/57	197	4/29/57	5/8/57	5/1/57
Slab, panel DEF	5/7/57	100	4/29/57	5/8/57	5/6/57

TABLE B.3—LABORATORY TEST RESULTS
(CYLINDERS)

Member	Test results, psi	
	7 Days	28 Days
Column and wall footings	4040	4910
		3960
		4310
		4320
		3360
		3880
		4450
		3960
		3140
		4430
		3600
		3870
		4080
		4120
Columns B-2, B-3, B-4, C-2,	3090	4420
C-4, and D-4		4200
Foundation line E	2350	3470
	2850	3450
	3200	3710
		3320
		3610
		4000
Walls		3620
		3540
		3960
		4350
		3650
		3540
		4010
		3650
		4310
		3740
		3920
		3250

TABLE B.4—LABORATORY TEST RESULTS
(CYLINDERS)

Members	Test results, psi	
	7 Days	28 Days
Floor slab	2390	3170
	2530	3520
	2320	3600
	2160	3530
		3980
		3890
		3400
		3370
Roof slab	3040	3580
	2970	4090
	2780	3420
	2460	3820
	2780	3510
	3330*	3650
		4180
		4340
		3200
		4370
		3770
		3940
		4350
		3650*
		4220*
Ramp slab	3350	3680
		4210
		3910
		4240
		4930
Ramp walls	2740	3800
	2740	3380
		3630
		3180
Door	3040	4640
		3720

*Cylinders from area of roof slab filled in after pouring the rolling door.

TABLE B.5—AVERAGE VALUES OF CONCRETE STRENGTH

Member	Average test results, psi	
	7 Days	28 Days
Column and wall footings	4040	4030
Columns B-2, B-3, B-4, C-2, C-4, and D-4	3090	4310
Foundation line E	2800	3590
Walls		3800
Floor slab	2350	3560
Roof slab	2800*	3860*
Ramp slab	3350	4190
Ramp walls	2740	3500
Door	3040	4180

*Does not include cylinders from filled-in area of roof slab.

TABLE B.6—LABORATORY TEST RESULTS (4-IN.-DIAMETER CORES)

Core No.	Depth of slab, in.	Diameter of test sample, in.	Length of test sample, in.	Strength, psi
Preshot				
1	29 1/2	4	8	3980
2	29 7/8	4	8	3810
3	29 5/8	4	8	4575
4	30	4	8	3130
5	28 1/4	4	8	4950
6	29 3/4	4	8	3530
Postshot				
1	27 3/4	4	8 5/8	4970
2	45	3 11/16	8 11/16	5525
3	31	3 11/16	8 11/16	5920
4A	44 1/2	3 11/16	8 3/4	3790
4B	44 1/2	3 11/16	8 5/8	4680
5	30 1/4	4	8 9/16	5230
6A	46 1/2	4	8 3/4	5450
6B	46 1/2	4	8 5/8	3680
7	30 1/4	4	8 5/8	4820

TABLE B.7—TYPICAL CONCRETE-MIX DESIGN

Sieve size	Per cent passing U. S. standard sieve: Fine aggregate	Coarse aggregate	Combined
1.5 in.		100.0	100.0
¾ in.		59.0	76.4
⅜ in.		11.6	49.2
#4	100.0	1.4	43.3
#8	78.8		33.5
#16	57.0		24.2
#30	32.9		14.0
#50	17.9		7.8
#100	4.3		1.8
F.M.	3.091	7.280	5.498
Specific gravity (S. and S.D.)	2.47	2.665	

Mix design for one cubic yard of concrete is 4500 psi.
Absolute volume of aggregate in one cubic yard of concrete—19.22 cu ft.
Weight of one cubic yard batch of aggregate—3243 lb.

	Per cent	Batch wt., lb		Absolute vol., cu ft
Gravel			2100	12.11
Sand, dry	38	1095		7.11
Free water in sand, 5.76 gal	4.35	48		0.77
		1143	1143	
Water, added 27.4 gal			228	3.66
Cement, 7.0 sacks			658	3.35
			Total	27.00

Maximum slump = 5 in.

TABLE B.8—LABORATORY TEST RESULTS OF REINFORCEMENT

Nominal size	Deformation	Yield* stress, psi	Ultimate stress, psi	Per cent† elongation, in.
3	Columbia	48,182	75,455	14.9
4	Columbia	52,296	79,081	20.4
5	Bethlehem	45,928	73,941	23.5
6	Columbia	48,189	80,315	21.9
7	Columbia	49,551	77,405	23.5
8	Bethlehem	47,695	77,338	19.5
9	Bethlehem	46,470	75,600	23.0
10	Bethlehem	46,375	75,657	20.4
11	Bethlehem	47,102	78,113	21.5

* Average yield stress = 47,976 psi.
† Per cent of elongation is based on an 8-in. specimen.

Fig. B.1—Placement of wall concrete using tremies.

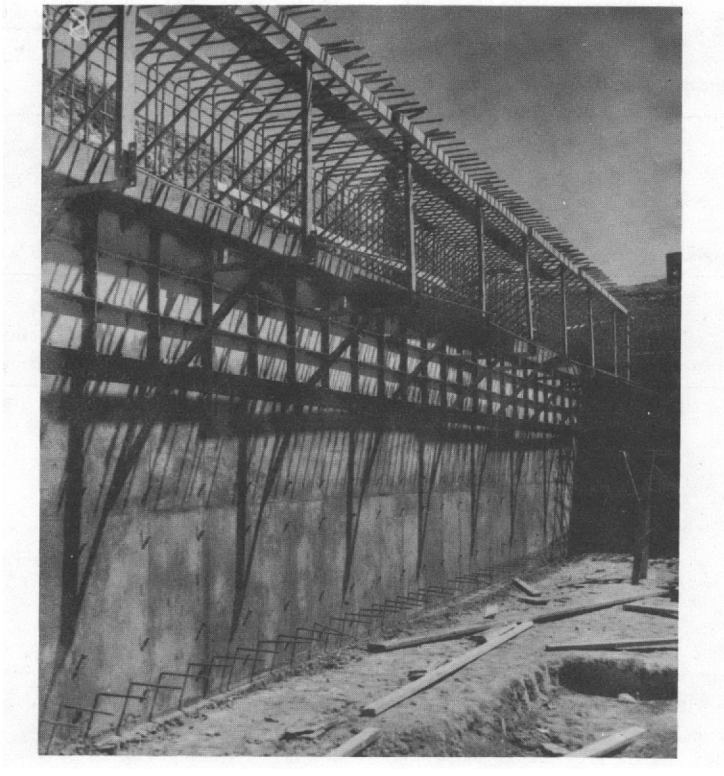

Fig. B.2—North wall with roof reinforcement shoring in place.

Fig. B.3—Grading of sub-base gravel.

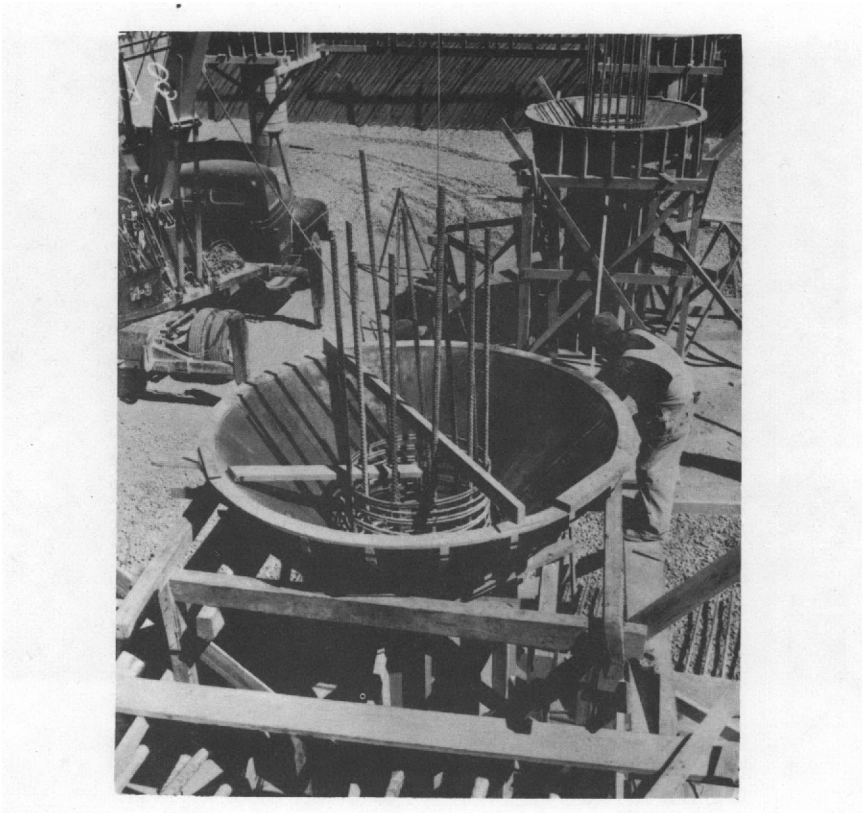

Fig. B.4—Erection of column and capital formwork.

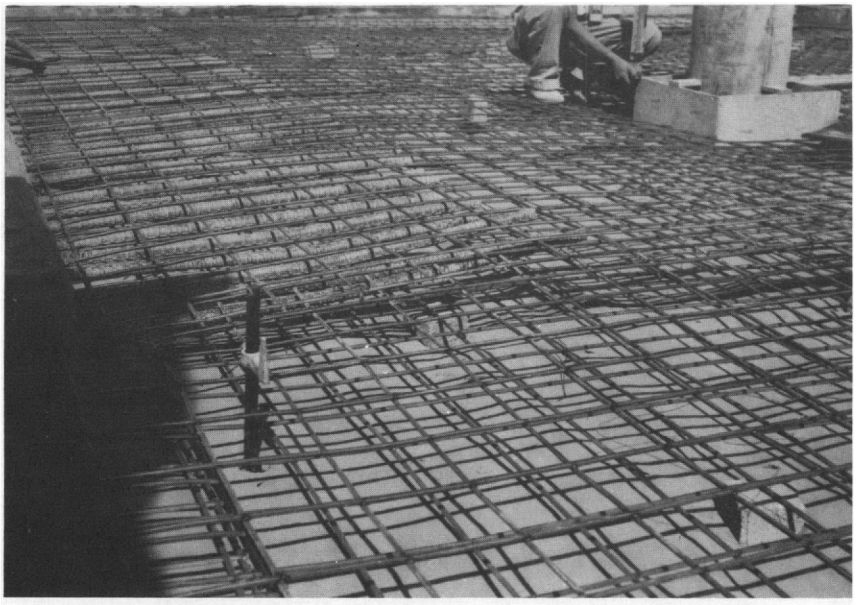

Fig. B.5—Placing floor-slab reinforcement.

Fig. B.6—Placement of floor-slab concrete.

Fig. B.7—Puddling and finishing of floor slab.

Fig. B.8—Reinforcement and incomplete formwork for west door pilaster.

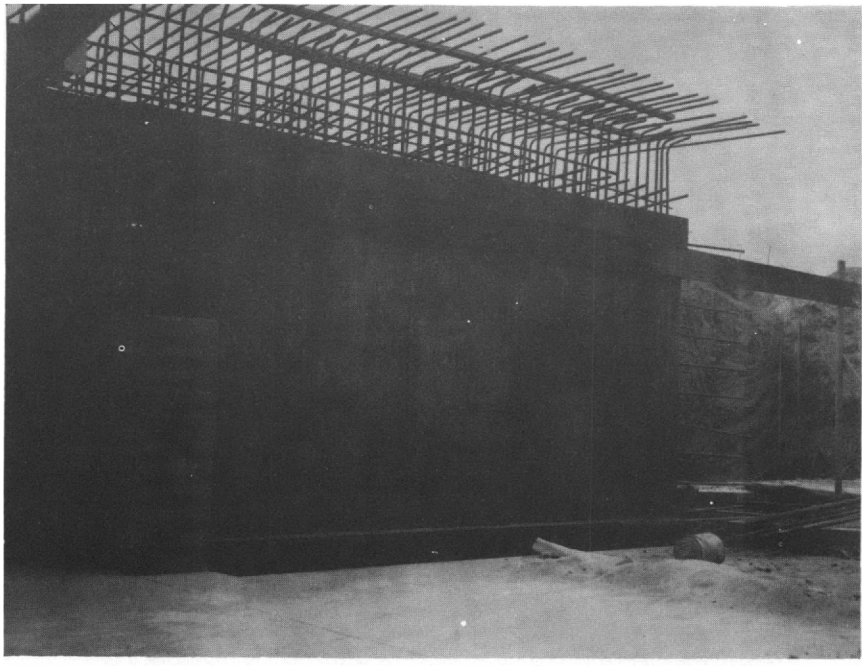

Fig. B.9—Guide plates and bumper for rolling door.

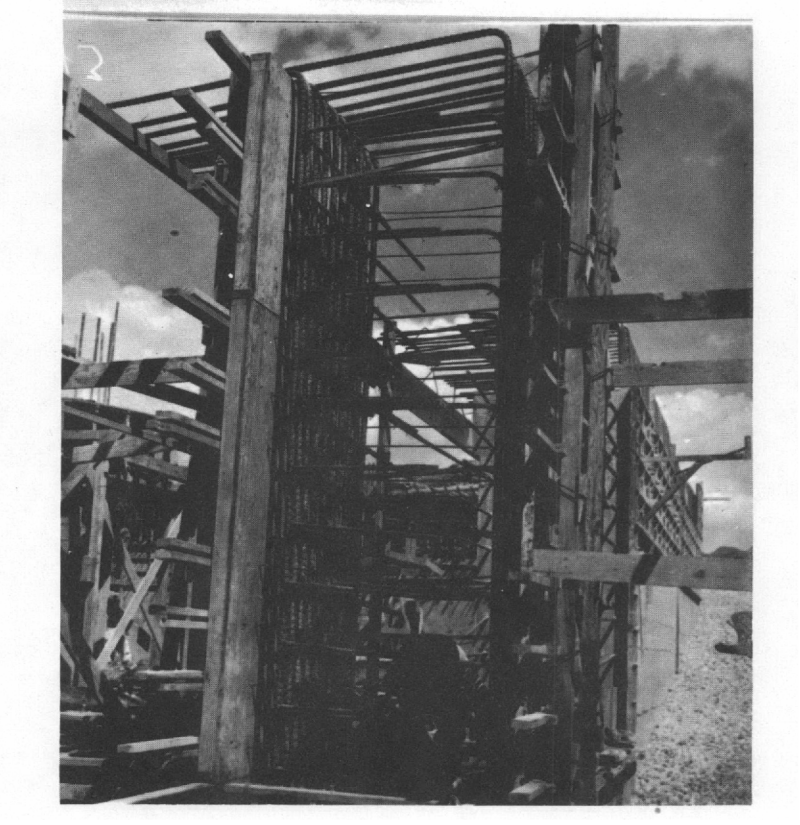

Fig. B.10—Partial reinforcement and formwork for east door pilaster.

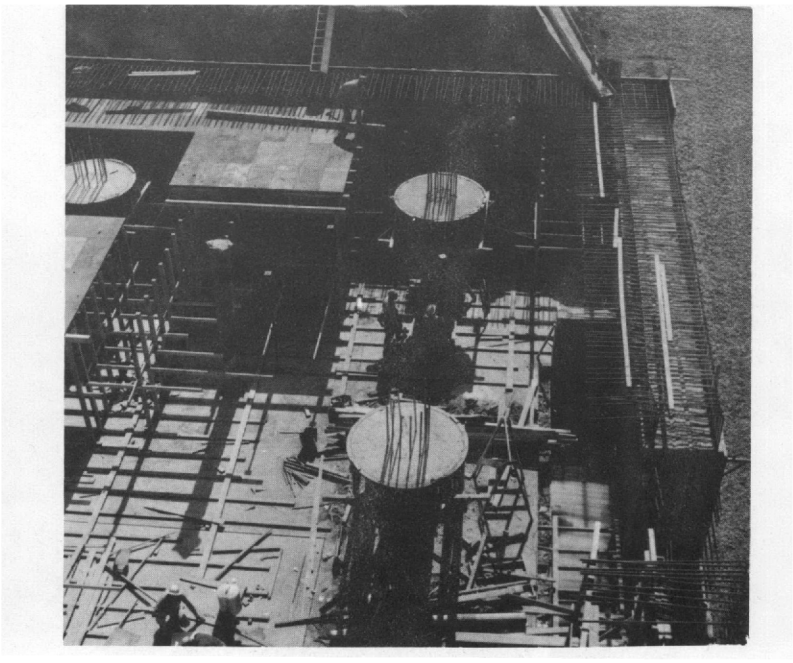

Fig. B.11—Aerial view of structure while erecting roof-slab formwork.

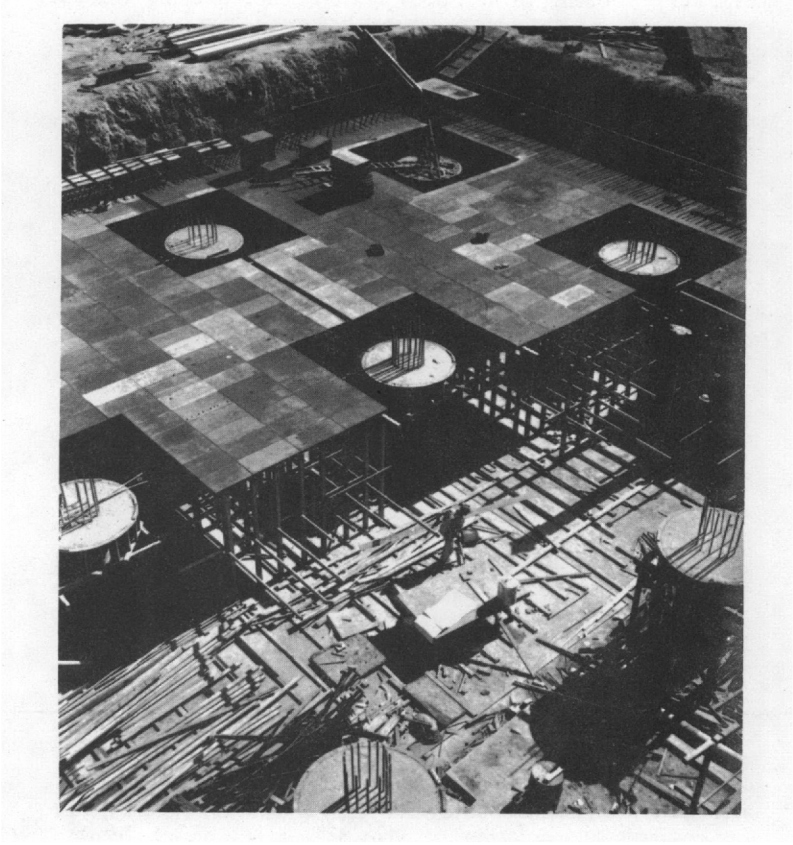

Fig. B.12—Aerial view of structure while erecting roof-slab formwork.

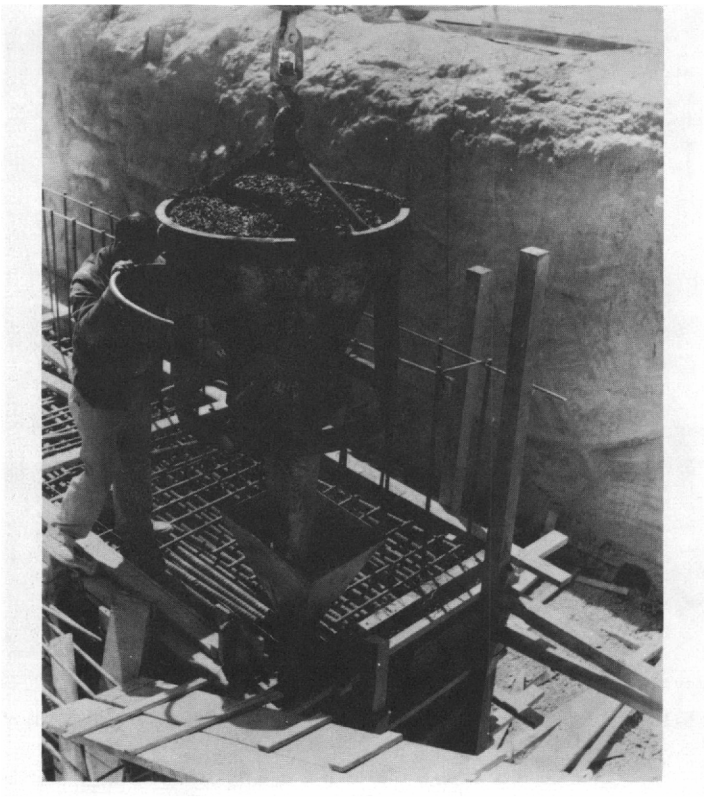

Fig. B.13—Pouring of west door pilaster concrete using tremies.

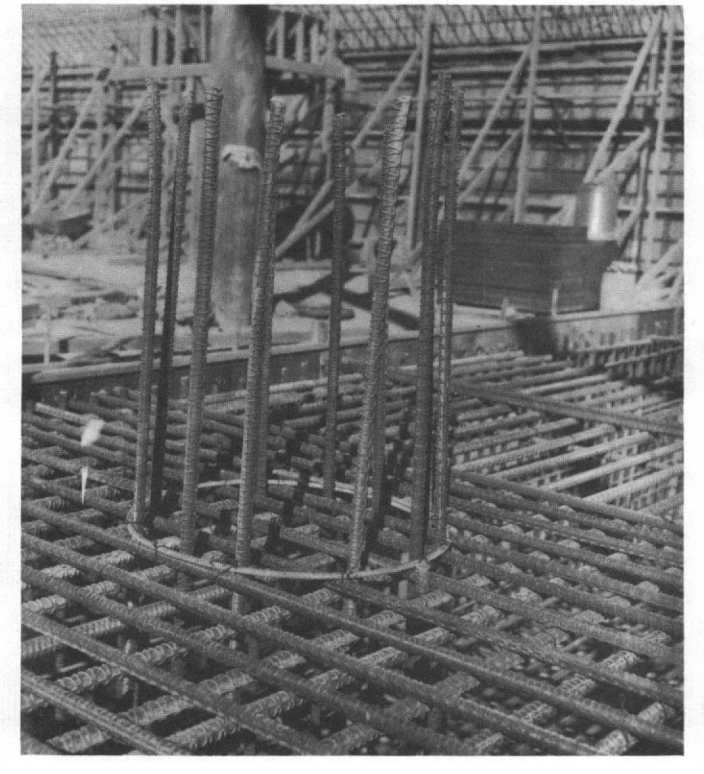

Fig. B.14—Column dowel detail at combined footing.

Fig. B.15—Partial roof-slab reinforcement at northeast corner.

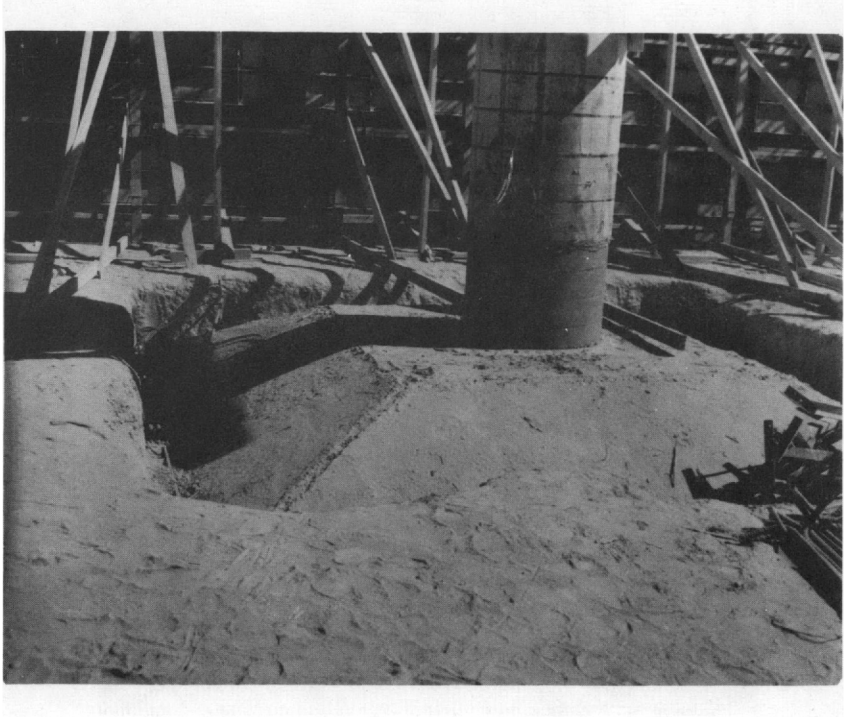

Fig. B.16—Typical individual column footing before backfilling.

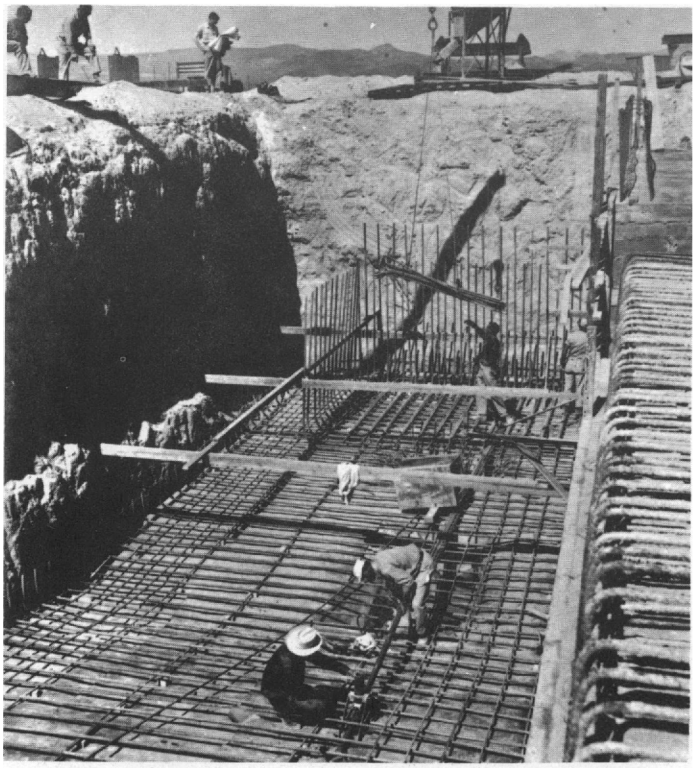

Fig. B.17—Placement of entrance ramp reinforcement.

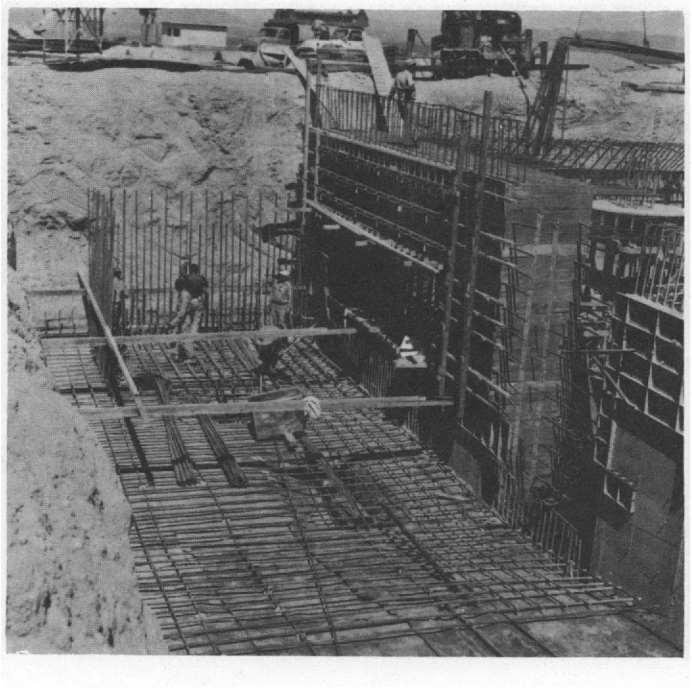

Fig. B.18—Placement of entrance ramp reinforcement.

Fig. B.19—Garage roof-slab formwork erected.

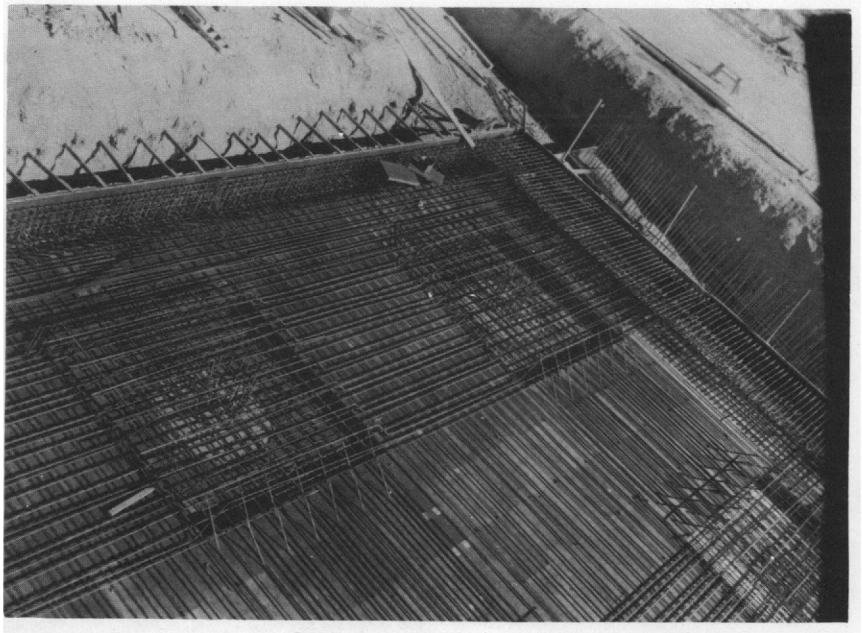

Fig. B.20—Bottom-mat roof-slab reinforcement partially placed.

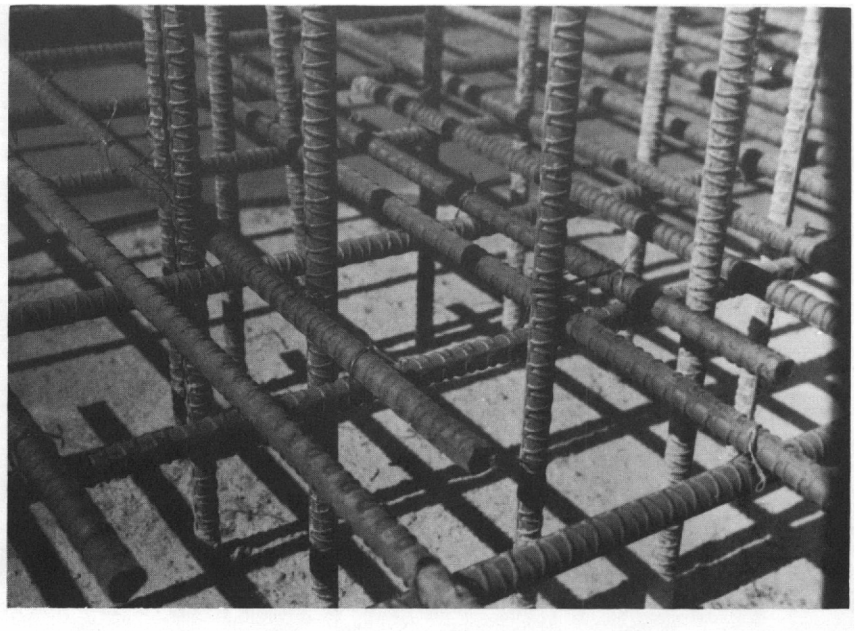

Fig. B.21—Typical bottom-mat reinforcement details at column.

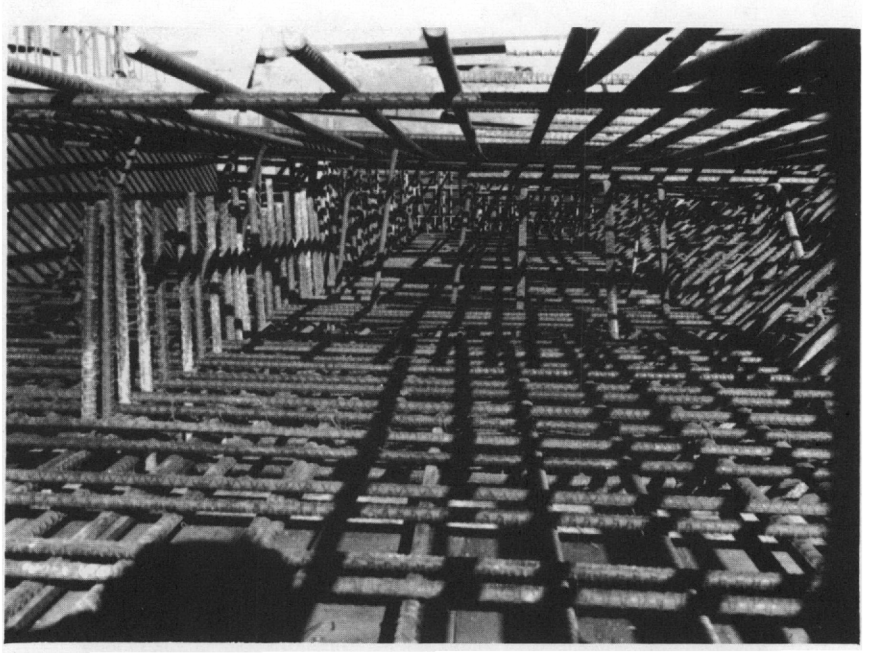

Fig. B.22—Bottom-mat reinforcement details over rolling door.

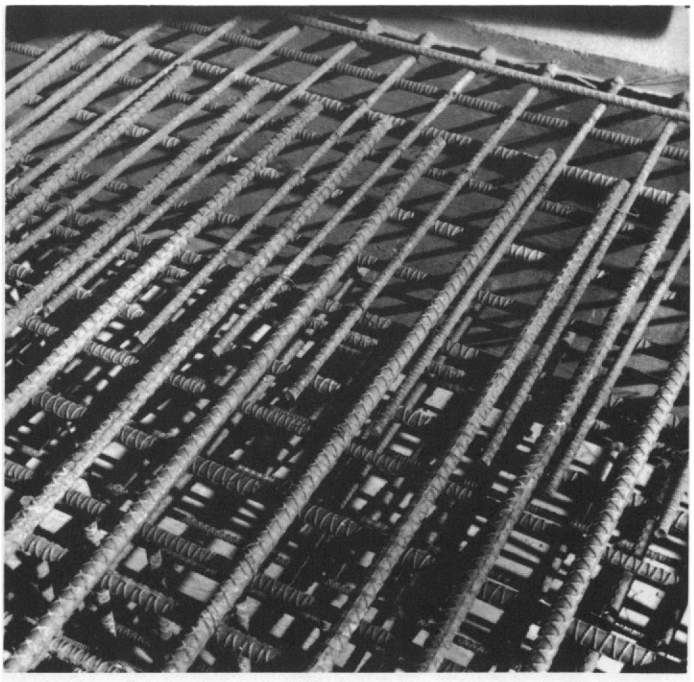

Fig. B.23—Top-mat reinforcement details over rolling door.

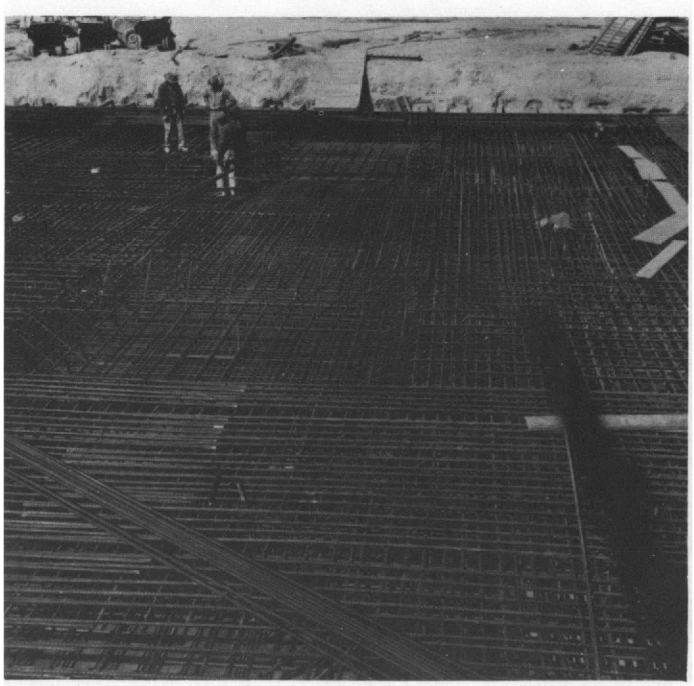

Fig. B.24—Partially completed roof-slab reinforcement.

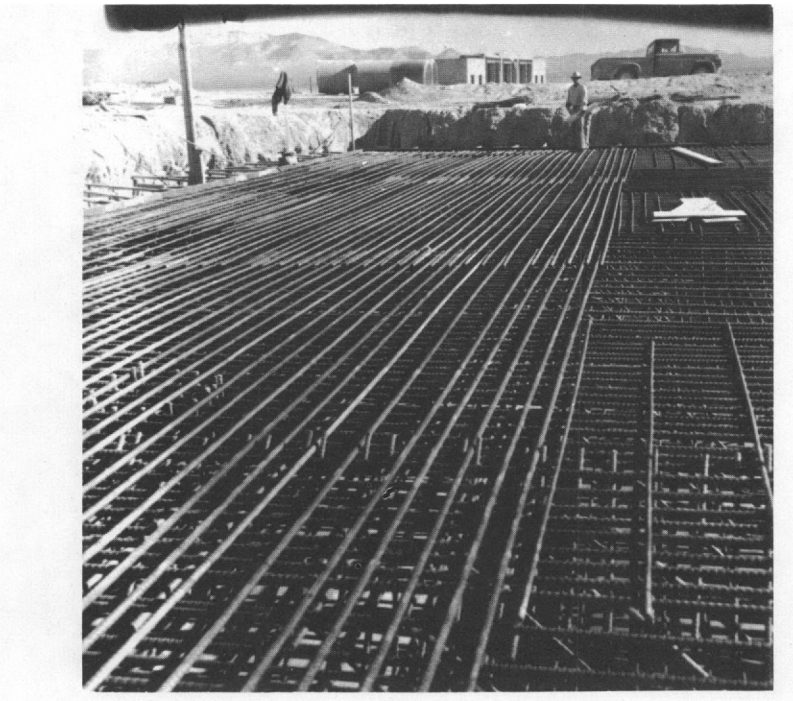

Fig. B.25—Partially completed roof-slab reinforcement.

Fig. B.26—Reinforcement details at typical lap.

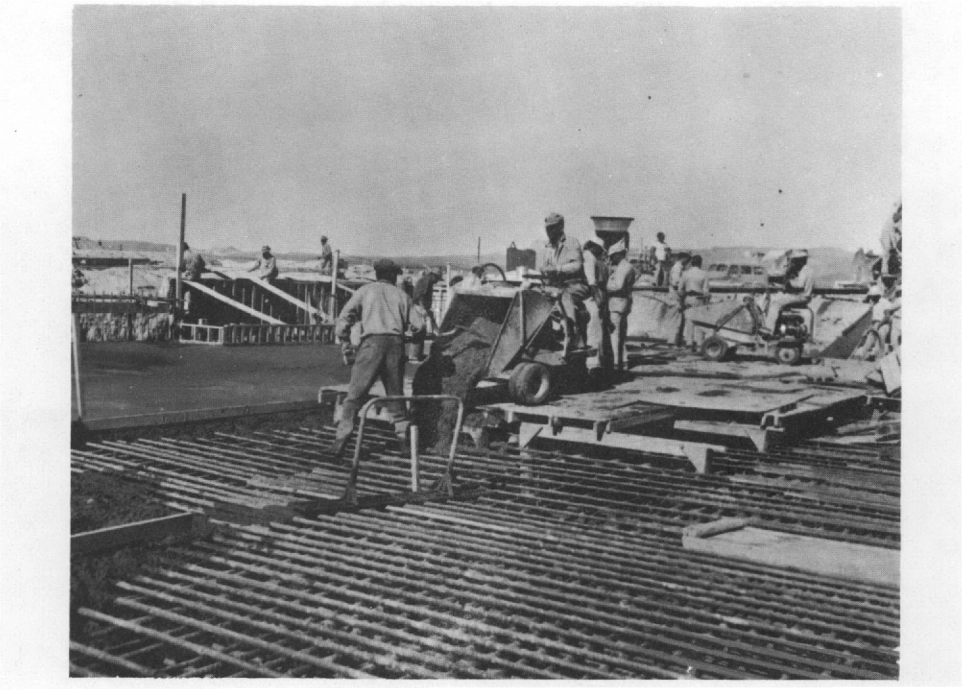

Fig. B.27—Placement of roof-slab concrete using buggies.

Fig. B.28—Roof-slab concrete placement completed. Note strip pattern of placement.

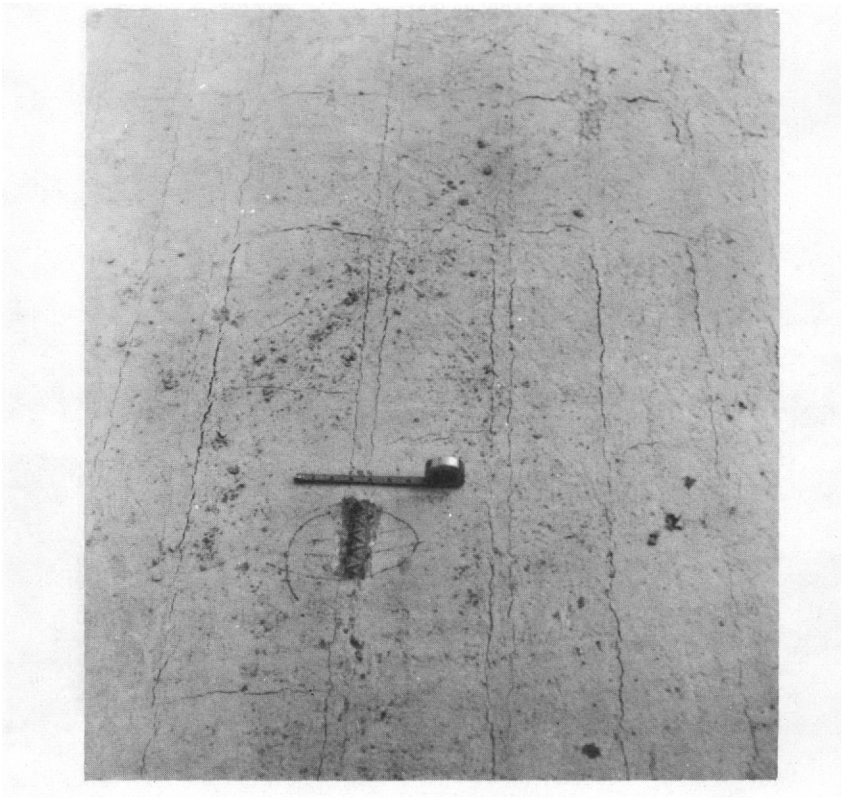

Fig. B.29—Shrinkage cracks in roof-slab concrete.

Fig. B.30—Honeycombed area on underside of roof slab.

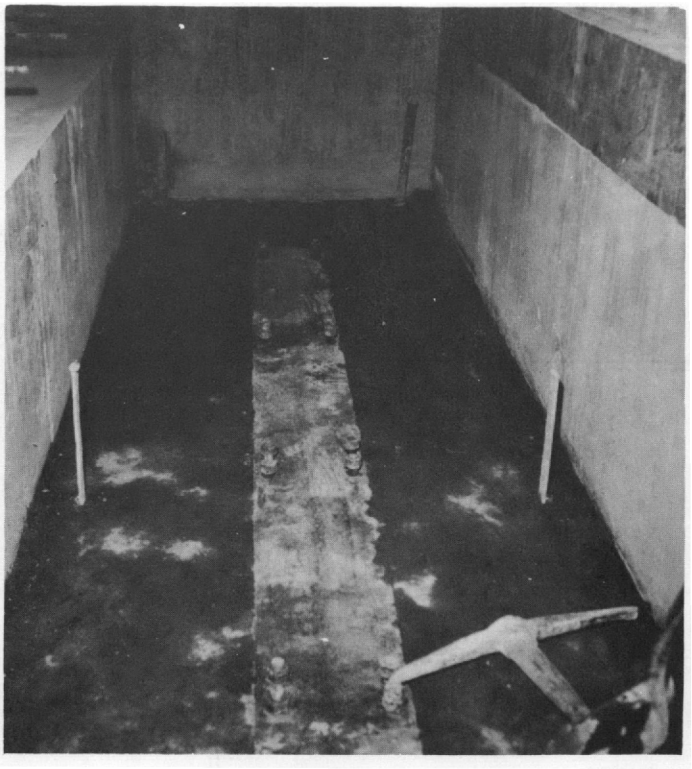

Fig. B.31—Rolling-door pit before installation of rail.

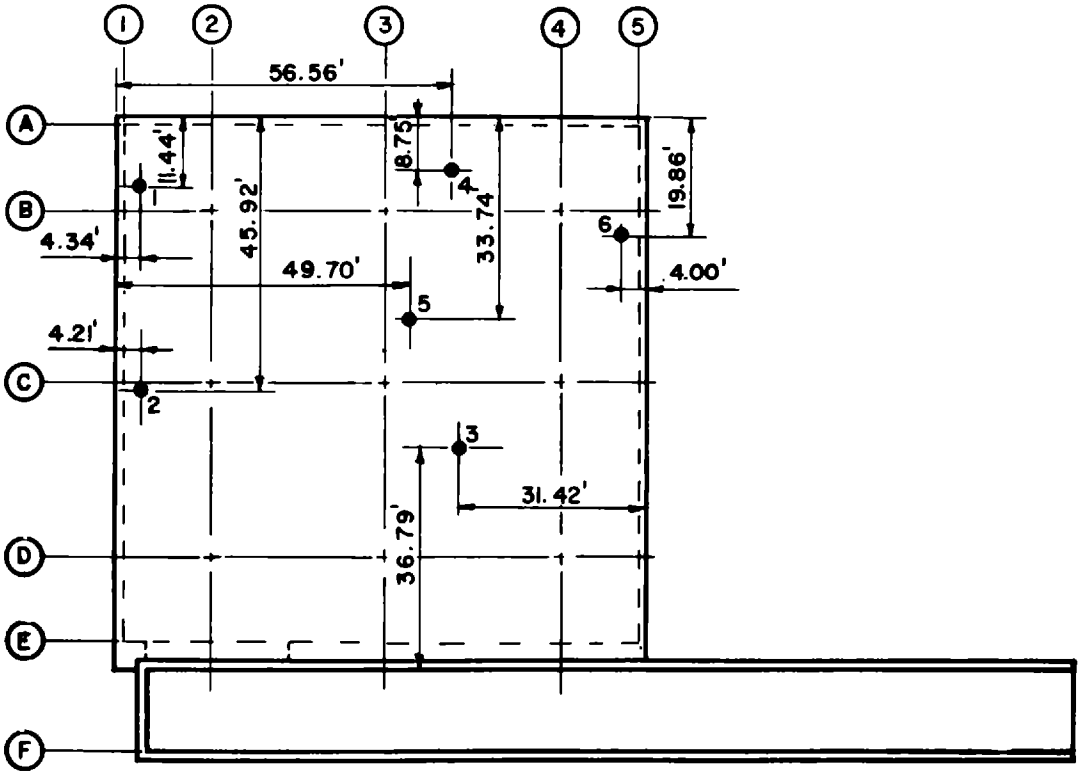

Fig. B.32—Location of preshot core holes in roof slab.

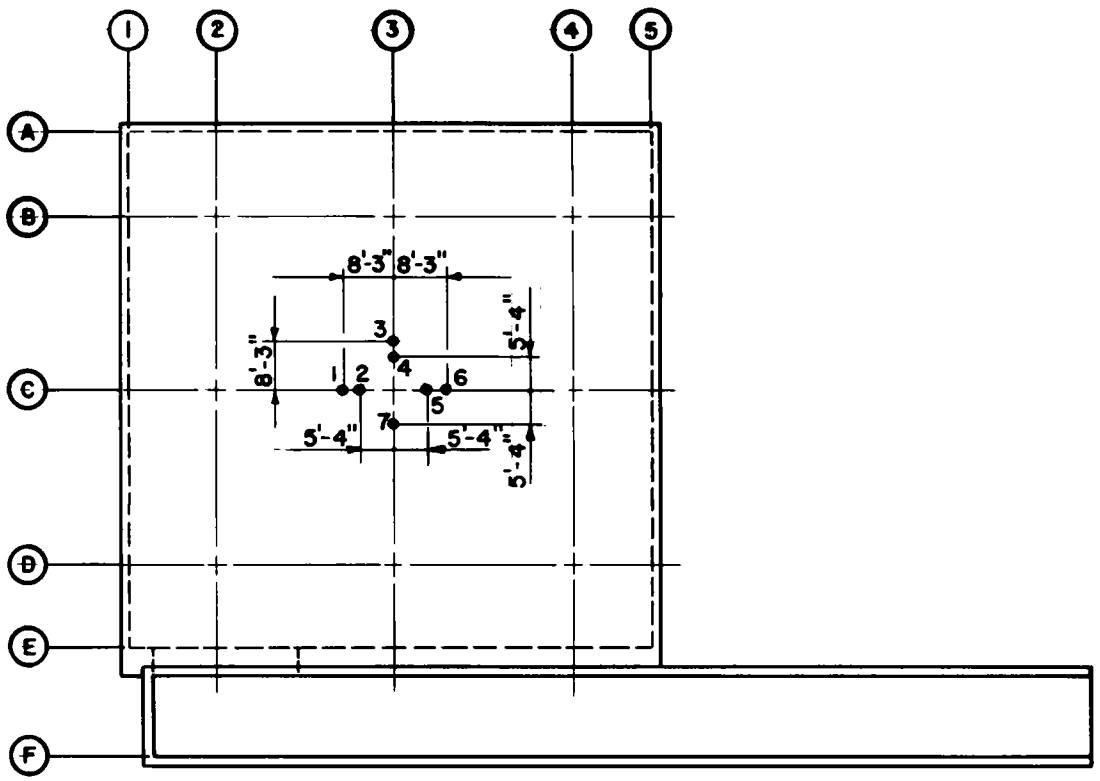

Fig. B.33—Location of postshot core holes in roof slab.

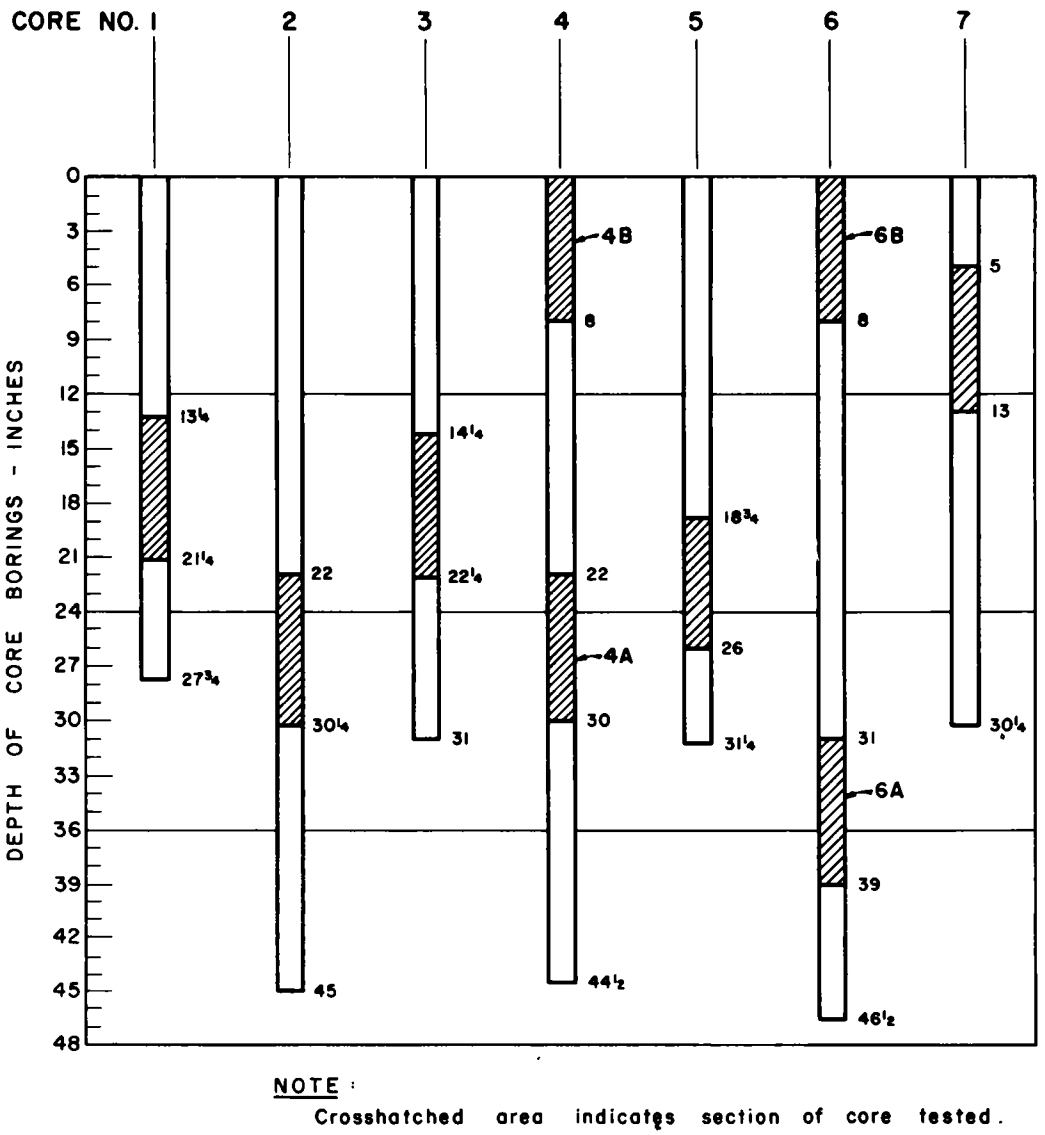

Fig. B.34 — Postshot core compression-test specimens.

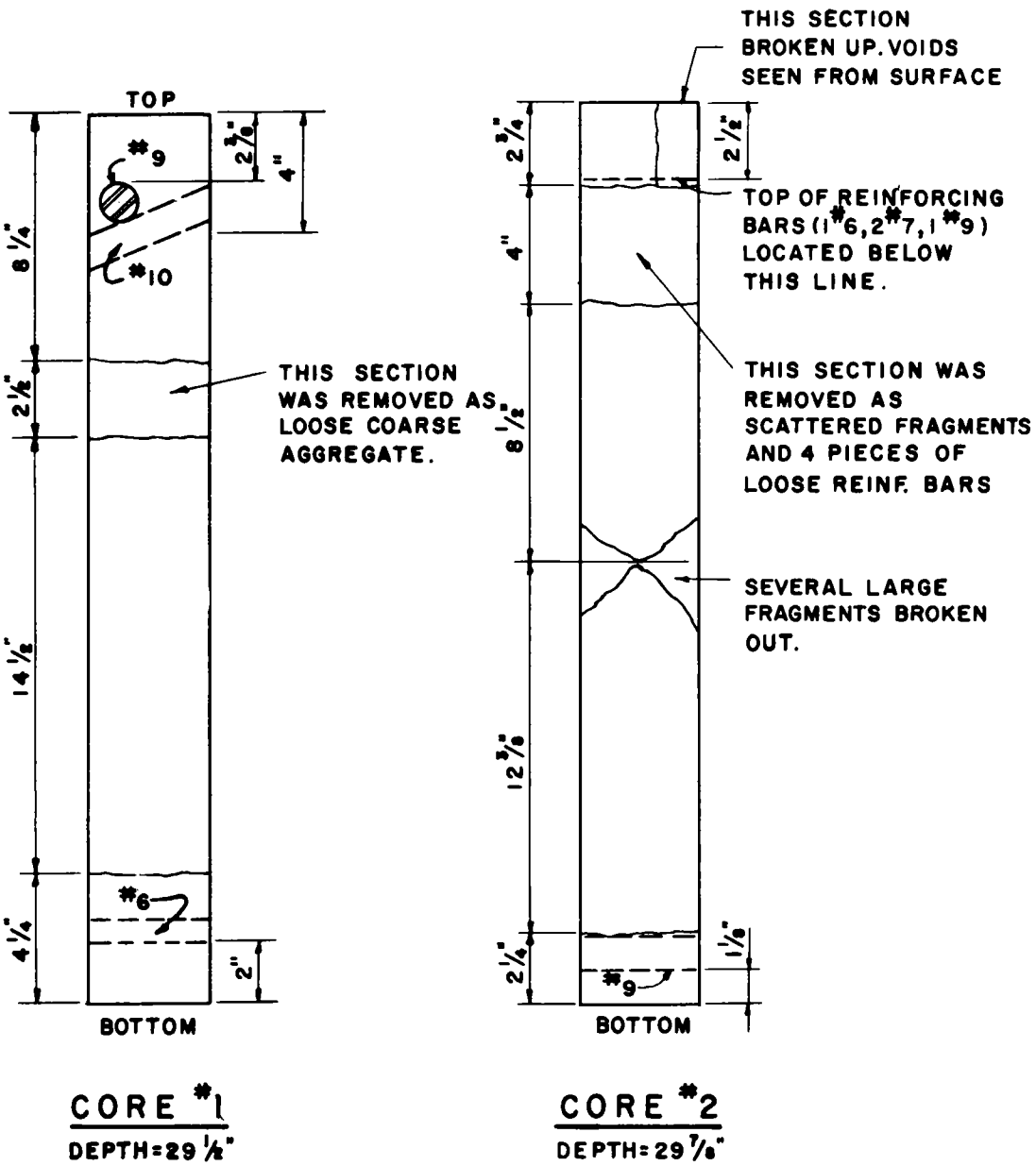

Fig. B.35—Preshot cores.

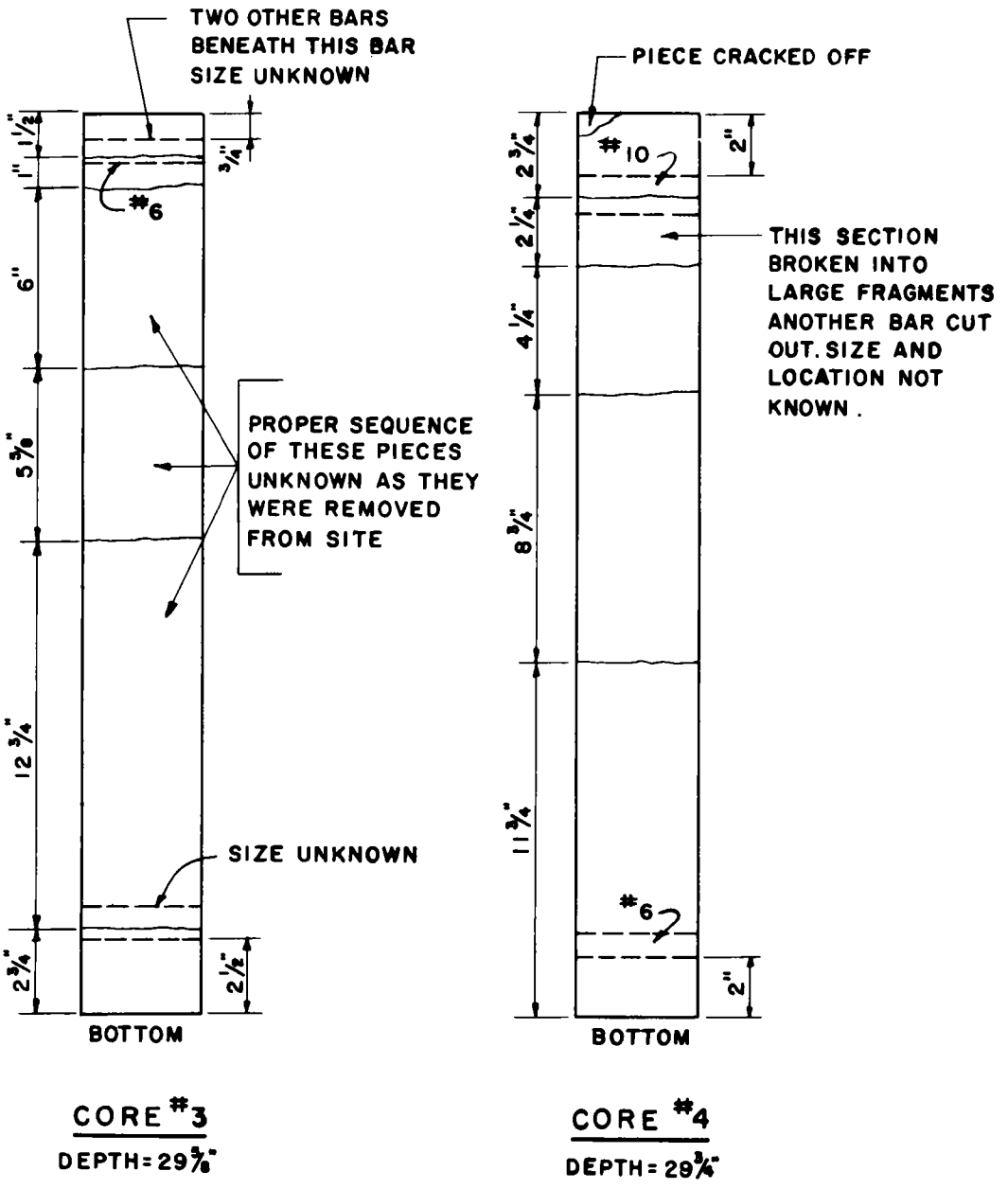

Fig. B.35—(Continued)

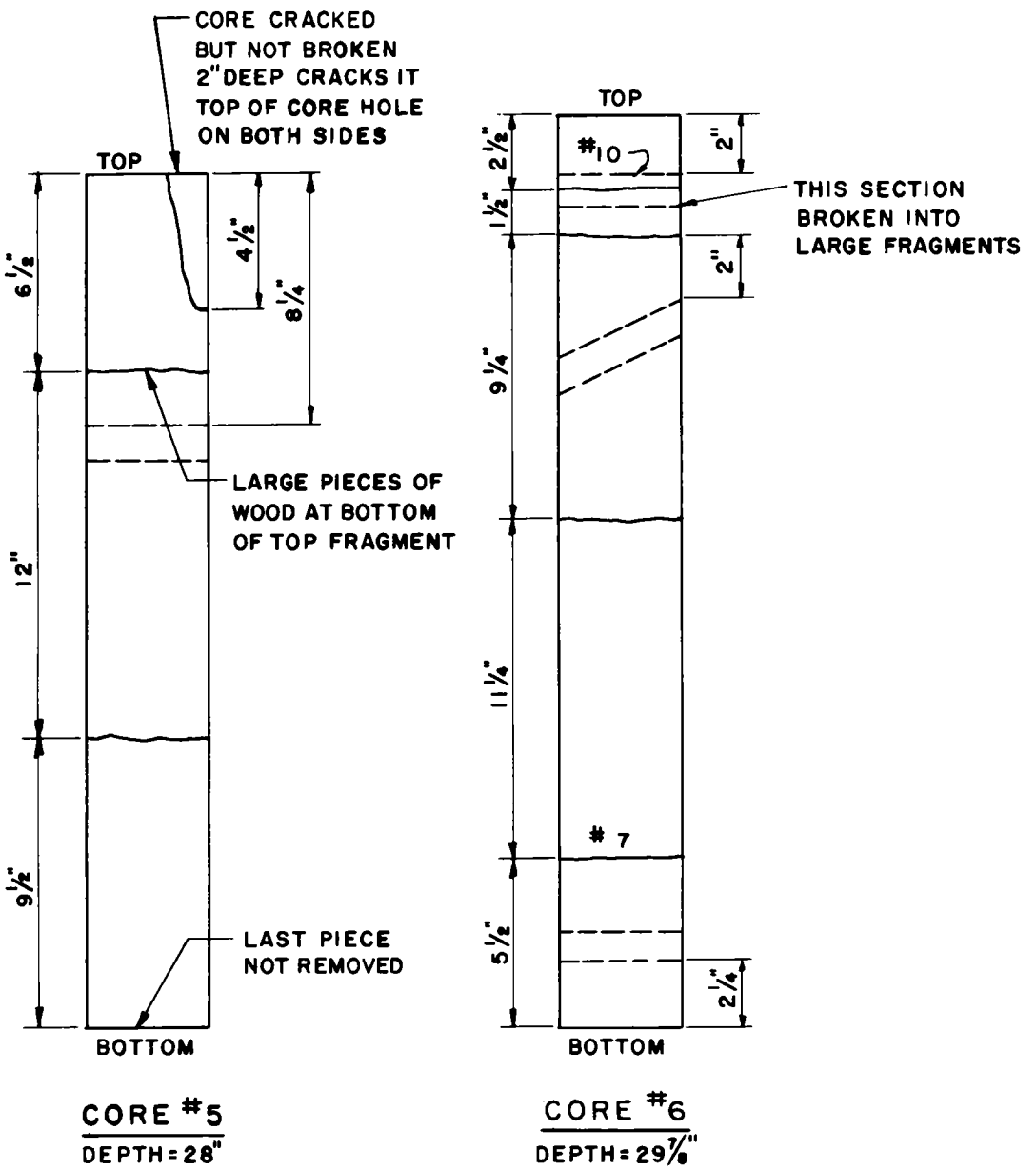

Fig. B.35—(Continued)

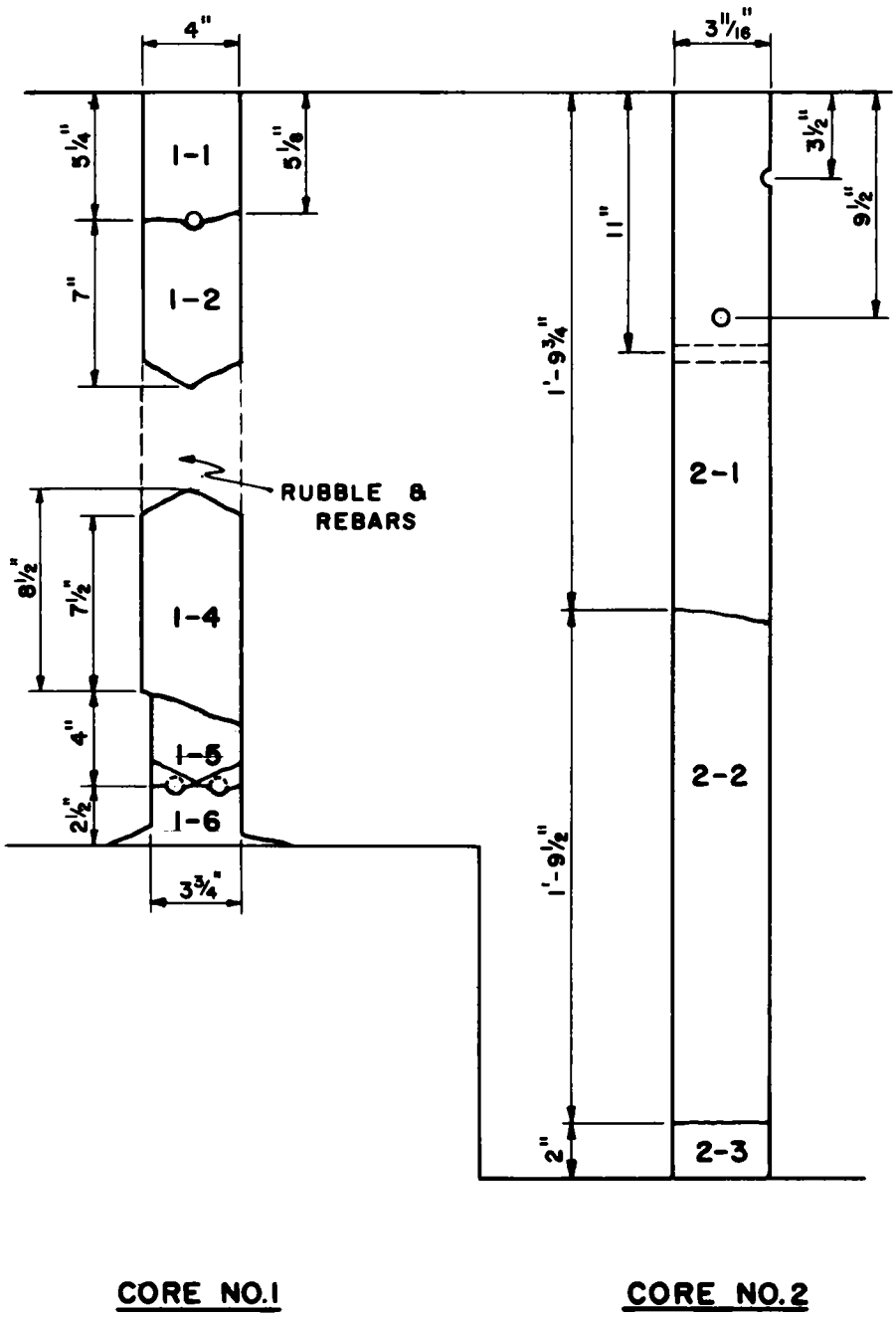

Fig. B.36—Postshot cores.

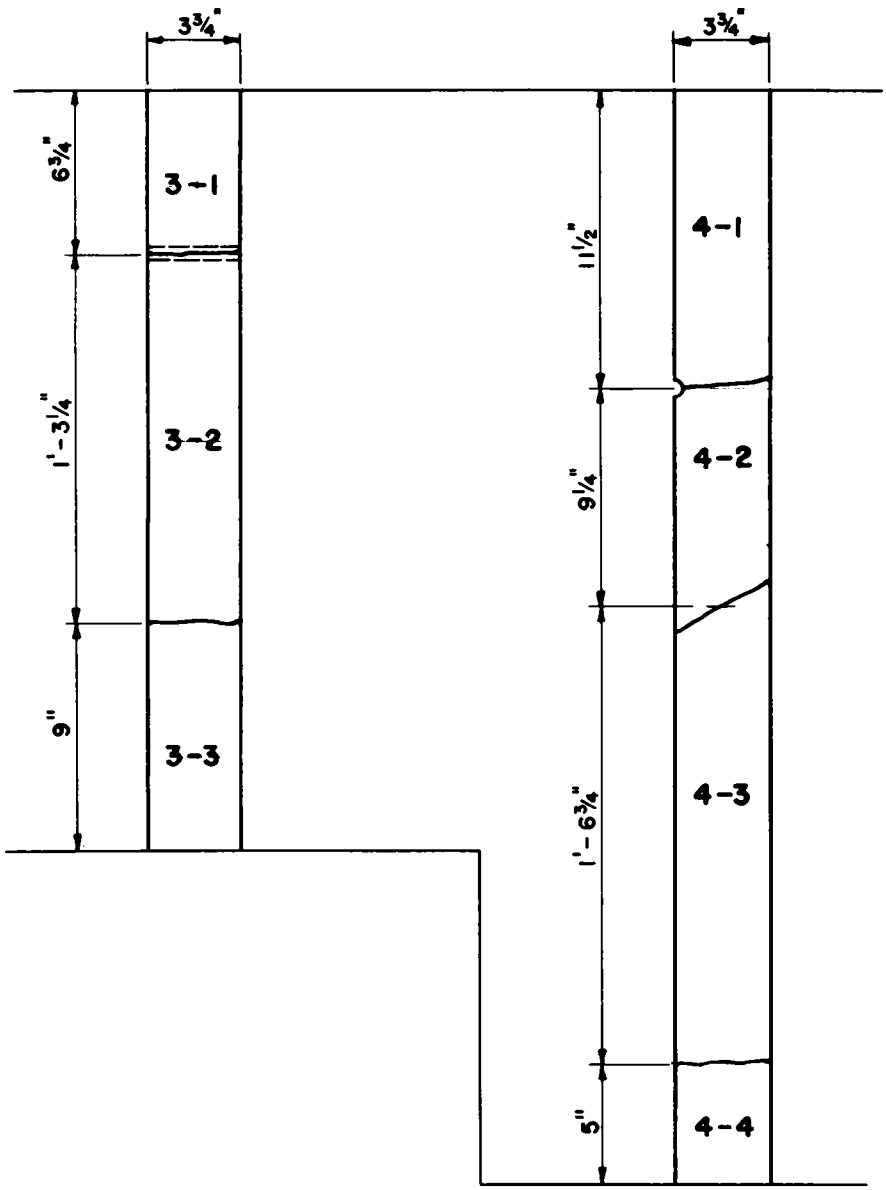

Fig. B.36—(Continued)

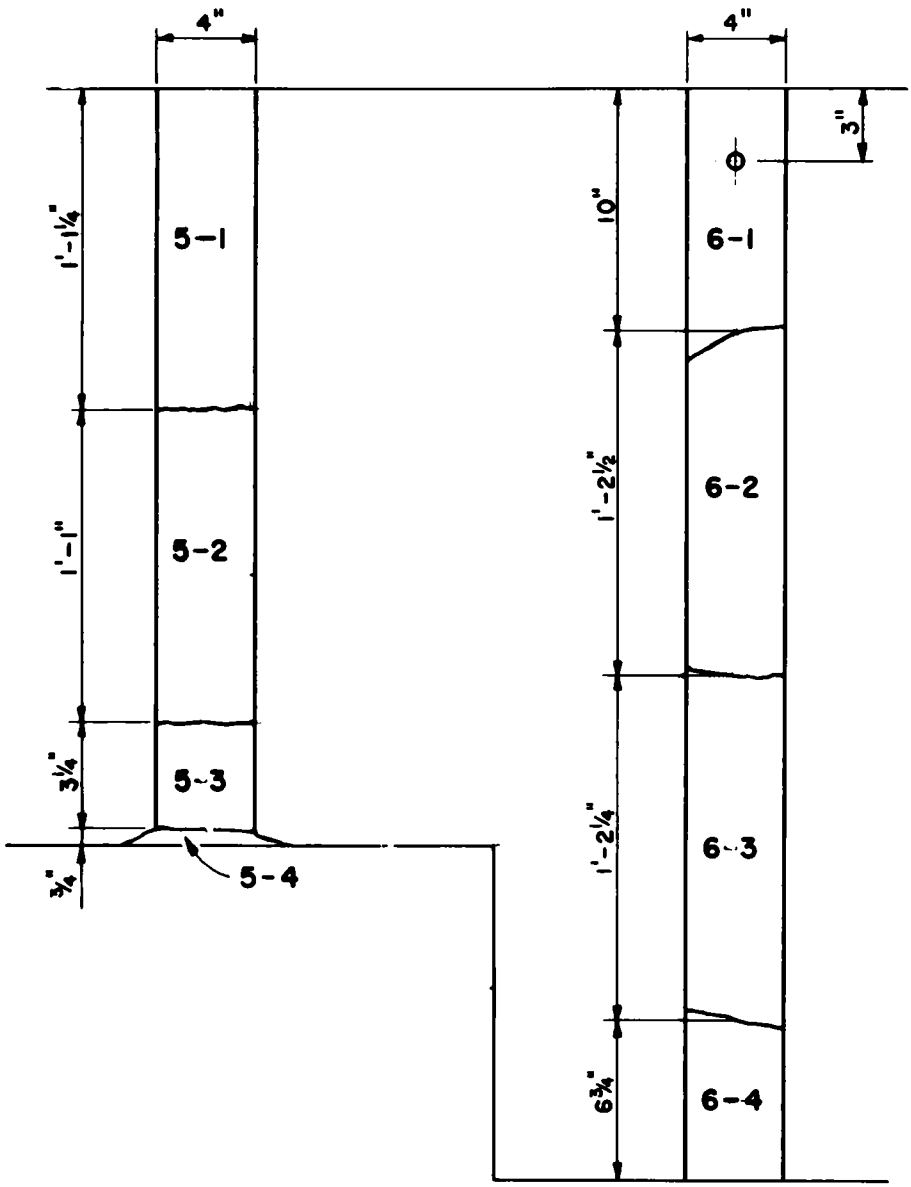

Fig. B.36—(Continued)

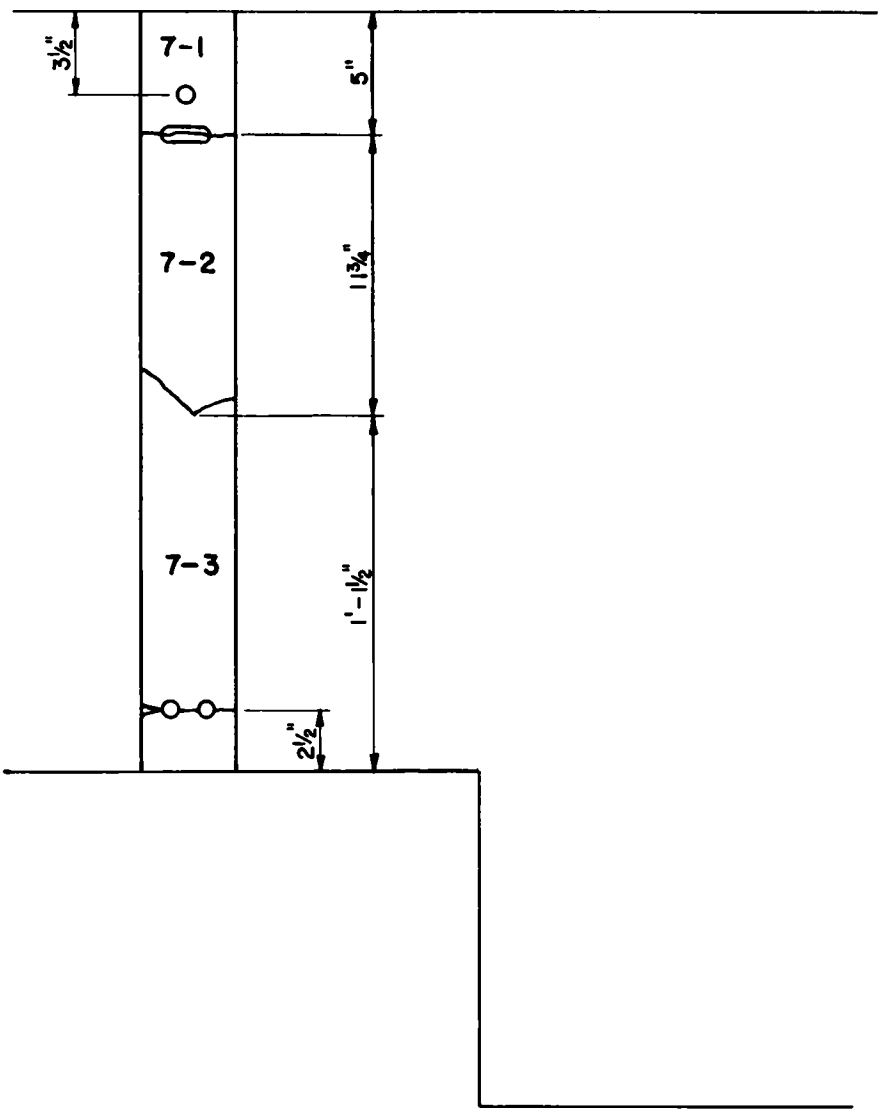

CORE NO.7

Fig. B.36—(Continued)

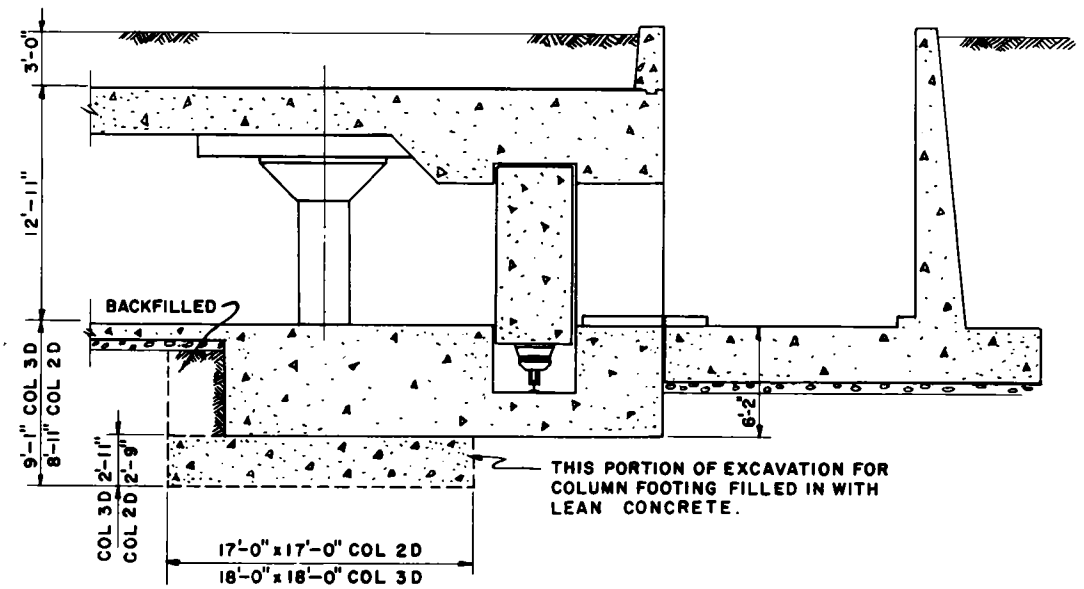

Fig. B.37 —Backfilled area under combined footing.

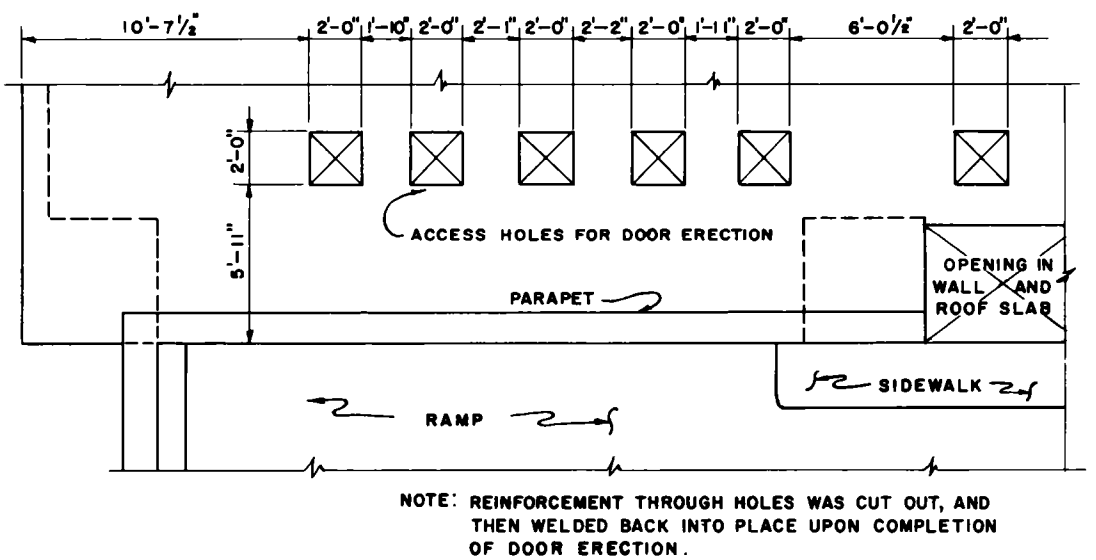

Fig. B.38 —Access holes for door erection.

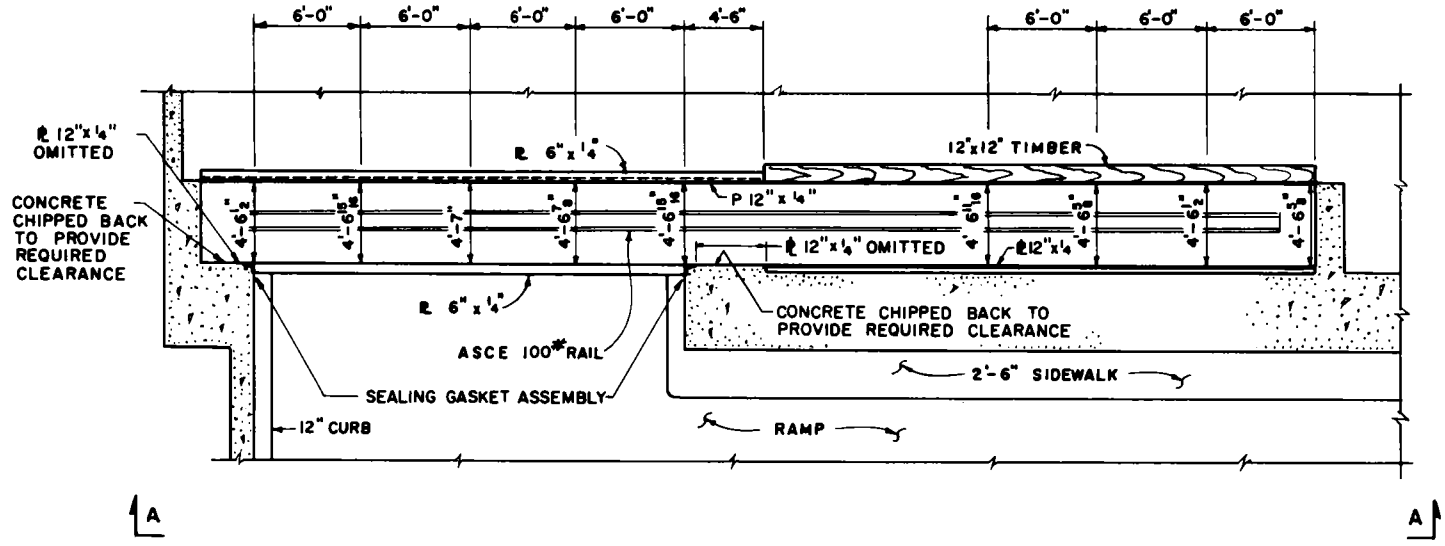

NOTE:

1. HORIZONTAL PIT DIMENSION SHOULD BE 4'-6¼"
2. DOOR NOT SHOWN
3. MEASUREMENTS TAKEN AT FLOOR LEVEL

Fig. B.39 — Plan of garage rolling-door pit.

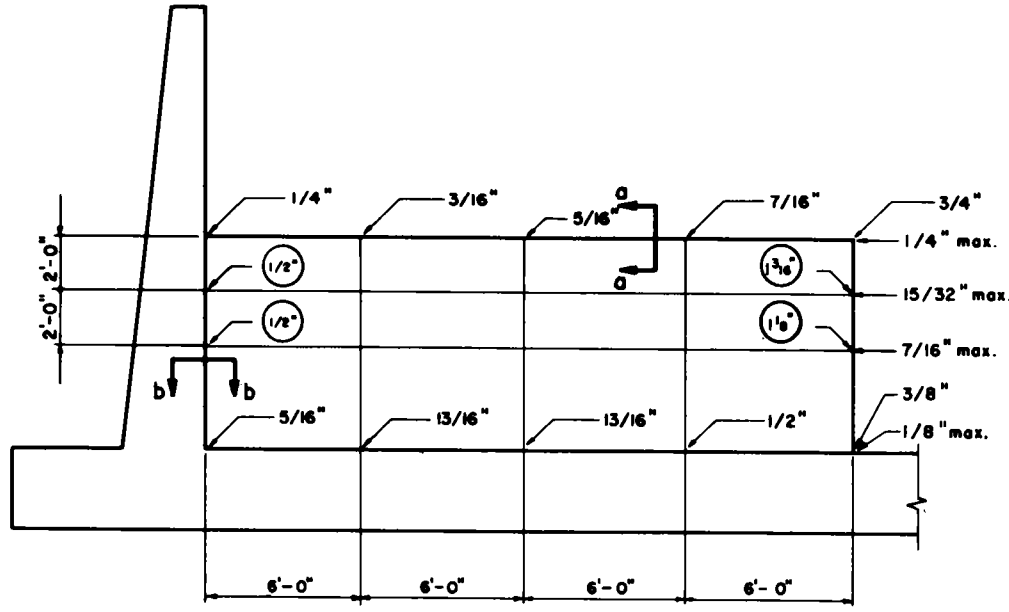

ELEVATION A-A

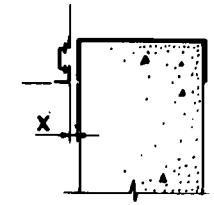

SECTION a-a

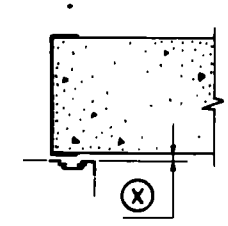

SECTION b-b

⊗ - FROM GASKET FRAME TO CONCRETE OF DOOR
X - FROM GASKET FRAME TO STEEL FRAME OF DOOR

NOTES:

1. DIMENSIONS AT T & B OF DOOR ARE HORIZONTAL DIMENSIONS MEASURED FROM FACE OF DOOR R. TO FACE OF 3"x 3"x ¼" GASKET ANGLE. ALLOWABLE MAXIMUMS ARE INDICATED. OTHER DIMENSIONS ARE MEASURED FROM CONCRETE FACE OF DOOR TO FACE OF 3"x3"x¼" GASKET ANGLE. THE CLEARANCES ARE NOT TRUE MINIMUM OR MAXIMUM OPENINGS AS THE GASKET ASSEMBLY WAS NOT TRULY VERTICAL & THERE WAS A VARIATION IN CLEARANCE BETWEEN THE INDICATED POINTS & THE INSIDE EDGE OF DOOR.
2. DIMENSIONS WITH DOOR IN CLOSED POSITION.

Fig. B.40 —Door clearances, door closed.

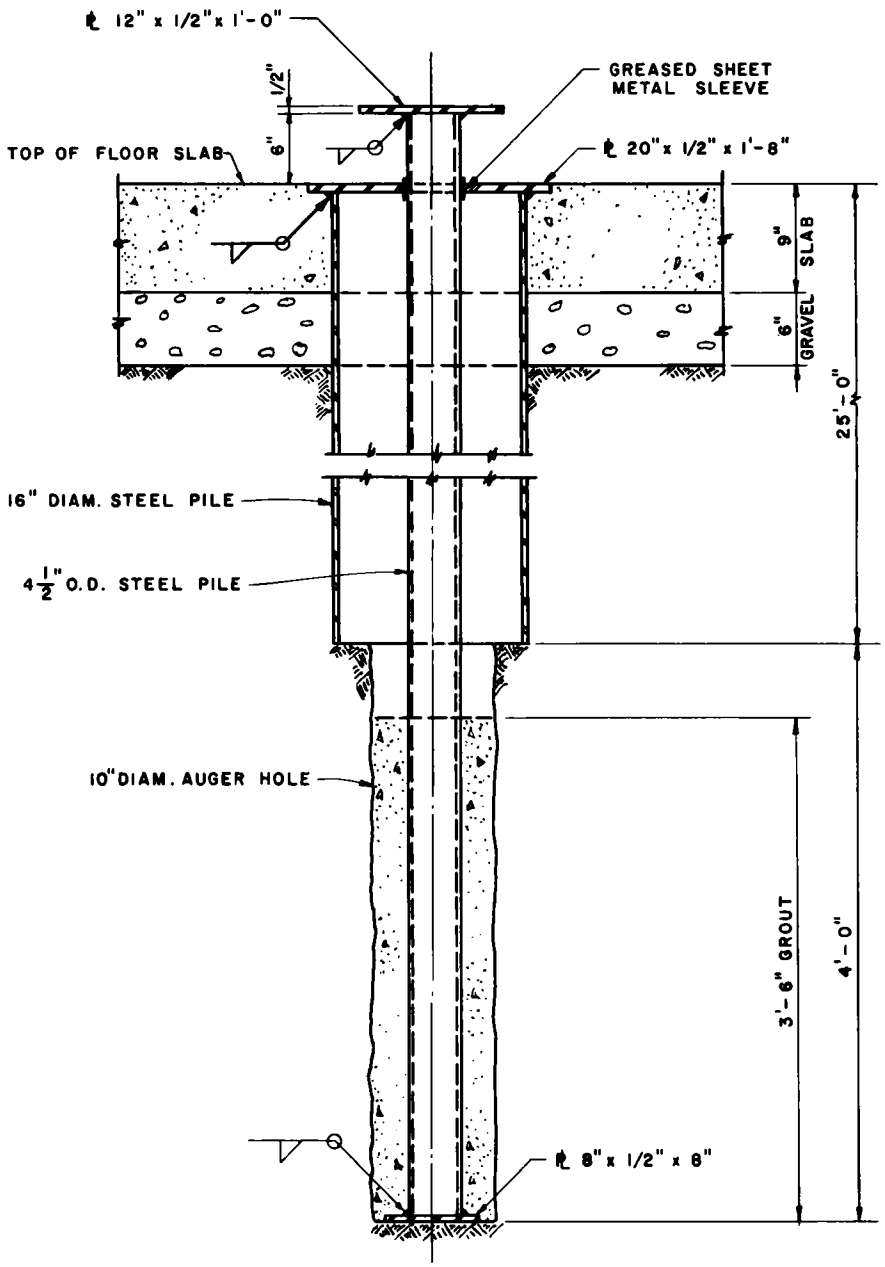

Fig. B.41—Revised detail of reference pile for deflection gauge D1.

Appendix C

SOILS INVESTIGATION

C.1 TEST BORINGS

Test borings consisted of three 16-in.-diameter holes, ranging from 42 to 46 ft deep, and one 48-in.-diameter boring 40 ft deep. The boring locations are shown in Fig. 2.1.

C.2 OBTAINING SOIL SAMPLES

A rotary-bucket rig was used to drill the 16- and 48-in. borings. Disturbed samples were recovered at 2-ft intervals from the 16-in. boring. Undisturbed samples were obtained from the 48-in. boring.

Three types of samples were taken: (1) disturbed bag samples were obtained from the rotary bucket; (2) driven samples were taken in thin-wall brass liners with a split-spoon sampler; and (3) undisturbed block samples were cut by hand in the borings and sealed in paraffin.

The driven samples were found to be badly disturbed as a result of the heavy driving necessary to obtain them. Because of the high resistance to driving, driven samples could only be taken within a few feet of the surface. Recovery was poor, and the thinly stratified material could not be extracted from the brass tubes without further disturbance of the material. Extraction of the samples by cutting the tube was only partially successful and did not eliminate further disturbance of the sample. The driven samples were therefore set aside.

Owing to the friable nature of the soil, difficulty was encountered in preparing test specimens from the block samples.

C.3 TEST PROCEDURE

C.3.1 Liquid and Plastic Limits

Liquid-limit tests were performed in accordance with the requirements of American Association of State Highway Officials (AASHO) Designation T-89, "Standard Method of Determining the Liquid Limit of Soils," mechanical method. Plastic-limit tests were performed in accordance with the requirements of AASHO Designation T-90 "Standard Method of Determining the Plastic Limit of Soils." No unusual difficulties were experienced in the liquid- and plastic-limit testing program.

C.3.2 Sieve Analysis

The sieve analyses were performed in accordance with requirements of the American Society for Testing Materials (ASTM) Designation D-1140, "Standard Method of Test for Amount of Material in Soils Finer than the No. 200 Sieve," except that the No. 40 sieve was

not utilized and the No. 270 and No. 400 sieves were used. The small amount of material that was occasionally retained on the No. 8 sieve was an angular chip-like light-gray material, probably largely calcium carbonate.

Soaking the samples did not produce the normally expected results. Even after prolonged soaking and vigorous agitation (with the mechanical stirring apparatus), the quantity and size of clumps was not greatly reduced. The clumps were broken down by very lightly rubbing the material under running water on the No. 200 sieve.

C.3.3 Field Density

(a) *Wax Method.* The field density of undisturbed samples was determined in accordance with the method described in AASHO Designation T-147, "Standard Method of Test for the Field Density of Soil In-Place," except that when samples of proper size were waxed in the field, the weight of the soil and the weight of the paraffin were determined after the sample had been immersed in the volumetric apparatus. This was accomplished by carefully separating the paraffin and soil into containers and weighing each material.

(b) *Consolidometer Ring Method.* After consolidation testing, samples removed from the consolidometers were weighed, dried in the rings, reweighed, and the dry density computed.

C.3.4 Consolidation

Consolidation samples 2.37 in. in diameter by 1 in. deep were cut from block samples with the stratification horizontal. The samples were tested at field moisture content. Some slight loss of moisture from the specimens probably took place during the test, but the effect of this loss, if any, is considered negligible.

The samples were tested on fixed-ring beam-loading consolidometers. The samples were loaded by progressively doubling the previous load over the range 575 to 36,800 psf, with an intermediate loading at 27,600 psf. The next load was applied when two successive consolidation dial readings at half-hour intervals showed less than 0.01 per cent consolidation. The loading procedure included an unload–reload cycle in accordance with the method described in the article "Importance of Natural Controlling Conditions Upon Triaxial Compression Test Conditions," by D. M. Burmister, published in Special Technical Publication No. 106 of ASTM. The duration of the consolidation tests, with the unload–reload cycle, varied from 33 to 114 hr, with an average length of 71 hr.

C.3.5 Triaxial Shear

Triaxial shear-test specimens were carved from block samples with the axis of the sample normal to the bedding planes. The specimens were approximately $2\frac{1}{2}$ in. in diameter and varied in length from 4 to $4\frac{5}{8}$ in. The ends of the specimens were trimmed as nearly square as possible and capped with either plaster of Paris or a stiff water–soil mixture.

The samples were preconsolidated at 0.6 p_n chamber pressure for approximately 1 hr, or until no further change in length of the specimen was observed. After preconsolidation the samples were tested at chamber pressures varying from 10 to 80 psi. In at least one instance, the higher chamber pressure resulted in an axial load approaching the capacity of the 1500-lb axial-load proving ring. During the testing the rate of axial strain on the proving ring was 0.05 in. per min. Except for the extreme care required in the handling of samples, no unusual difficulties were experienced in the triaxial testing program.

C.3.6 Unconfined Compression

Samples for unconfined compression tests were prepared in the same manner as for triaxial shear tests. The size of the samples varied from approximately $1\frac{1}{2}$ to $2\frac{1}{2}$ in. in diameter, with an approximate height of 2 diameters. During the testing the rate of axial strain was approximately 0.05 in. per min. In several instances unconfined compression specimens shattered at failure.

C.4 TEST RESULTS

C.4.1 Description and Classification of Material

Throughout the area there was little variation in the material samples. In the 48-in. boring the material was a clayey silt having a plasticity index ranging from 0 to 9. The soil, in general, was thinly stratified. In places, there were as many as twenty horizontal beds to 1 in. of depth with variation in density from bed to bed of the same type of material. Variation in material is more marked from one bed to the next than over a depth of several feet. Pronounced horizontal planes of weakness existed in places with only slight cohesion across the faces.

Pockets and layers of soil of high void ratio were frequent and were the cause of loss of many specimens during carving. Most of the pockets encountered were small and of the order of 1 cu in. in volume. The pockets were thought to account for some of the low densities measured by the waxed-sample method. The soil broke up rapidly in water. The cementing agent was thought to be calcium carbonate, which also existed in some beds in pieces about 8-mesh size.

The results of the liquid- and plastic-limit tests, the sieve analyses, and the field density and moisture-content tests are shown in Table C.1.

C.4.2 Consolidation Characteristics

The results of the consolidation tests are shown in Table C.2. It should be pointed out that the consolidation tests were run for the sole purpose of establishing a value of the natural prestress p_n and that the results reflect the consolidation characteristics of the material only at the field moisture content. The consolidation characteristics are thought to be more typical of the denser strata because of the difficulty in cutting test specimens from the more friable low-density materials. A typical consolidation stress–strain relation is illustrated in Fig. C.1.

C.4.3 Strength Characteristics

Summaries of the triaxial and the unconfined compression-test results are given in Tables C.3 and C.4.

The Mohr circles for peak shear strengths at various depths in the 48-in. boring have been plotted, and a suggested peak shear envelope has been developed. The suggested peak shear envelope is shown in Fig. C.2.

It should be noted that the soil-strength suggested values on Fig. C.2 are likely to be higher than actual strengths for several reasons:

1. The specimens are loaded at right angles to the planes of weakness of the material.
2. Samples could be taken only of the stronger materials in the field, and specimens could be cut only from the stronger portion of these.
3. Peak shear strengths are used in plotting the Mohr circles. The applicable shear-strength value depends on the type, duration, and direction of loading anticipated in the field, and the shear envelopes are therefore recorded as "suggested shear envelopes."
4. Tests were performed on the specimens at field moisture content. At increased moisture content the shear strength of the materials tested would be greatly reduced.

For additional soils test data see Chaps. 2 and 3.

Appendix C, as well as the information presented in Chaps. 2 and 3, has been based on the data presented in Ref. 1.

REFERENCE

1. Soil Test Data, Frenchman Flat, Nevada Test Site, Mercury, Nevada, prepared by Nevada Testing Laboratories, Ltd., Las Vegas, Nevada, and International Testing Corporation, Long Beach, California.

TABLE C.1—SUMMARY OF SOIL-CLASSIFICATION TEST*

16-in.-diameter Boring No. 7, Disturbed Samples

Depth	w	M. A. No. 8	M. A. No. 200	M. A. No. 270	M. A. No. 400	L.L.	P.L.	P.I.
2	7.5	99	73	69	68	22.8	18.3	4.5
4	8.7	100	86	81	73			
6	11.1	100	96	94	89	31.8	28.5	3.3
8	11.7	100	84	81	74			
10	9.3	100	93	91	87.5			
12	12.4	100	96	95	92			
14	11.7	100	100					
16	16.3	100	99					
18	17.7	100	99					
20	12.4	100	98					
22	16.3	100	99					
24	14.9	100	99					
26	15.6	100	98					
28	15.6	100	98					
30	13.6	100	97					
32	13.6	100	98					
34	18.3	100	99					
36	13.6	100	96					
38	14.3	100	98					
40	13.0	100	93					
42	12.4	100	93					

16-in.-diameter Boring No. 8, Disturbed Samples

Depth	w	M. A. No. 8	M. A. No. 200
2	7.5	99	83
4	7.5	100	91
6	11.1	100	99
8	13.0	100	95
10	11.7	100	99
12	8.1	100	97
14	9.3	100	99
16	6.4	100	100
18	11.7	100	100
20	11.1	100	99
22	11.1	100	99
24	11.1	100	99
26	9.3	100	100
28	17.1	100	99
30	12.4	100	98
32	13.6	100	97
34	14.3	100	98
36	14.3	100	92
38	16.3	100	94
40	14.3	100	93
42	14.3	100	95
44	14.9	100	95
46	15.6	100	93

TABLE C.1—(Continued)

48-in.-diameter Boring No. 11, Undisturbed Samples

Depth	γ	w	M. A. No. 8	M. A. No. 270	L.L.	P.L.	P.I.
2							
4							
5							
6	76	6.0					
7	69	10.0	100	99	37.0	31.8	5.2
8							
10							
12							
14							
15							
16							
17			100	96	31.0	23.4	7.6
18							
20	93	14.3	100	95	32.8	25.8	7.0
22							
24							
25	85	14.1	100	95			
26	84	13.4					
28							
	81	15.4					
30	85	14.4	100	96	32.6	25.9	6.7
	82	10.5					
32							
34							
35	77	15.8					
36							
38							
	66	15.6					
40	76	13.8	100	91	32.9	26.9	6.0

γ, dry unit, wt. %; w, moisture content, %; M.A., material passing indicated sieve, %; L.L., liquid limit; P.L., plastic limit; and P.I., plasticity index.

*The soil tested was stratified and fissured silty clay and clayey silt.

Note: Boring No. 7 is located 14 ft 6 in. east of the structure working point (Fig. 2.1); boring No. 8 is located 14 ft 6 in. west of the structure working point (Fig. 2.1); and boring No. 11 is located 14 ft 6 in. south of the structure working point (Fig. 2.1).

TABLE C.2—SUMMARY OF CONSOLIDATION-TEST RESULTS
(48-in. Boring, Undisturbed Samples)

Test No.	Depth, ft	Prestress (p_n), tsf
C-14	5 to 7	4.3
C-11	15 to 17	5.3
C-4	20	9.2
C-6	25	9.2
C-7	30	7.5
C-10	35	8.4
C-12	40	6.1

TABLE C.3—SUMMARY OF TRIAXIAL TESTS
(48-in. Boring, Project 30.4)

Test No.	Depth, ft	0.6 p_n, psi	Restraint stress (σ_3), psi	Maximum triaxial stress (σ_1-σ_3), psi	Remarks
T-5	15 to 17	61	61	197	
T-6	40 to 42	67	20	217	
T-7	35 to 36	82	82	233	Incomplete, failure
T-8	40 to 42	67	67	302	No failure
T-9	40 to 42	67	10	222	Retest of T-8
T-10	15 to 17	61	20	154	
T-11	15 to 17	61	80	303	No failure
T-12	15 to 17	61	40	217	Retest of T-11
T-13	15 to 17	61	20	170	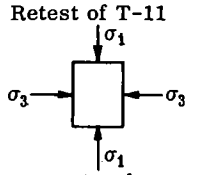
T-14	15 to 17	61	40	238	
T-15	15 to 17	61	50	276	
T-16	25 to 27	40	40	229	
T-17	Sample run as unconfined compression U-10				
T-18	40 to 42	67	10	204	p_n = natural prestress on soil
T-19	40 to 42	67	40	280	σ_3 = restraint stress σ_1-σ_3 = triaxial stress

TABLE C.4—SUMMARY OF UNCONFINED COMPRESSION TESTS
(48-in. Boring, Project 30.4)

Test No.	Depth, ft	Maximum triaxial stress (σ_1-σ_3), psi	Remarks
U-2	35 to 36	37	
U-3	25 to 27	80	
U-4	15 to 17	50	
U-5	15 to 17	45	
U-6	35 to 36	101	Retest of T-7
U-7	5 to 7	35	
U-8	25 to 27	95	
U-9	40 to 42	172	
U-10	15 to 17	38	

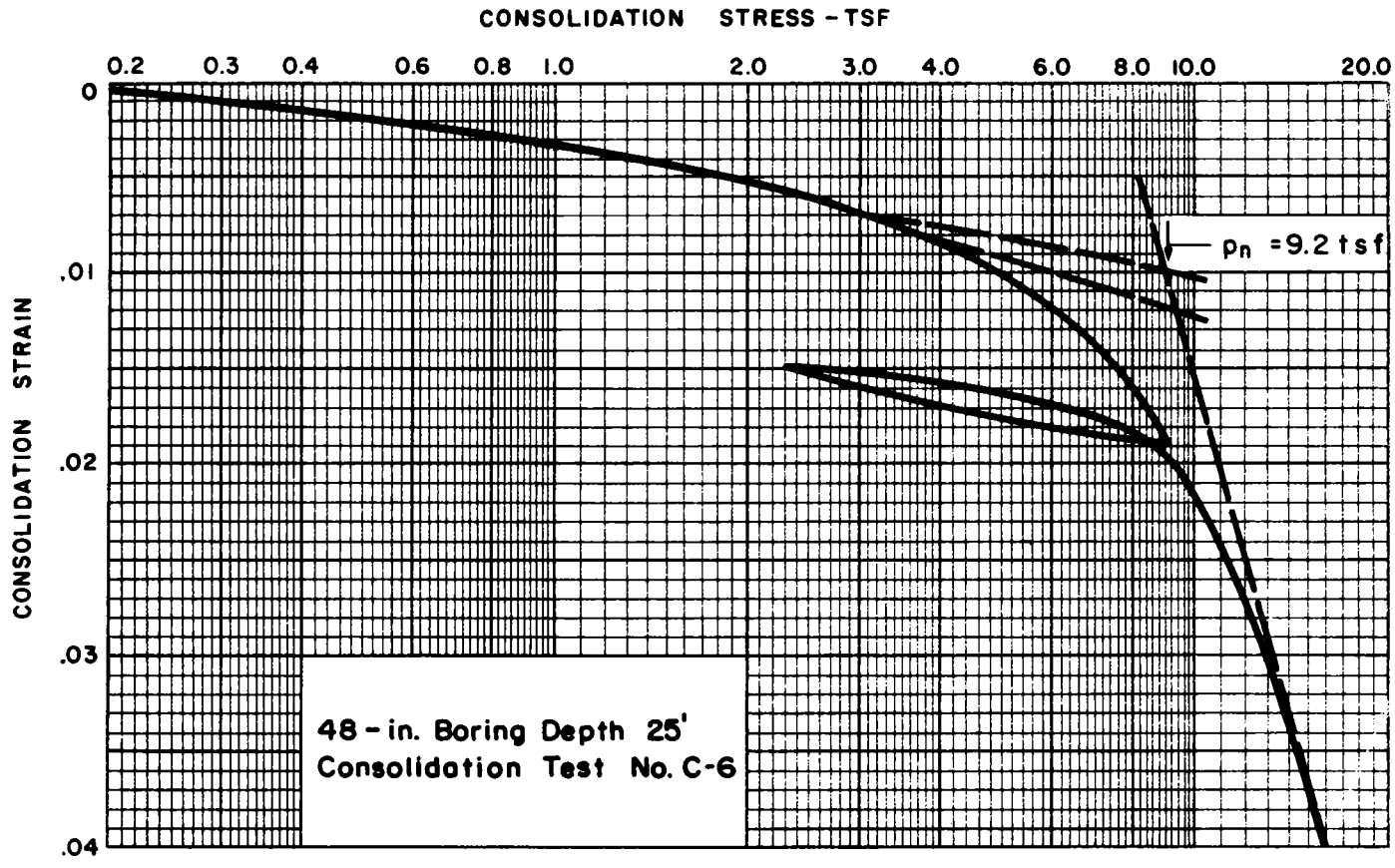

Fig. C.1—Typical consolidation test stress-strain relation.

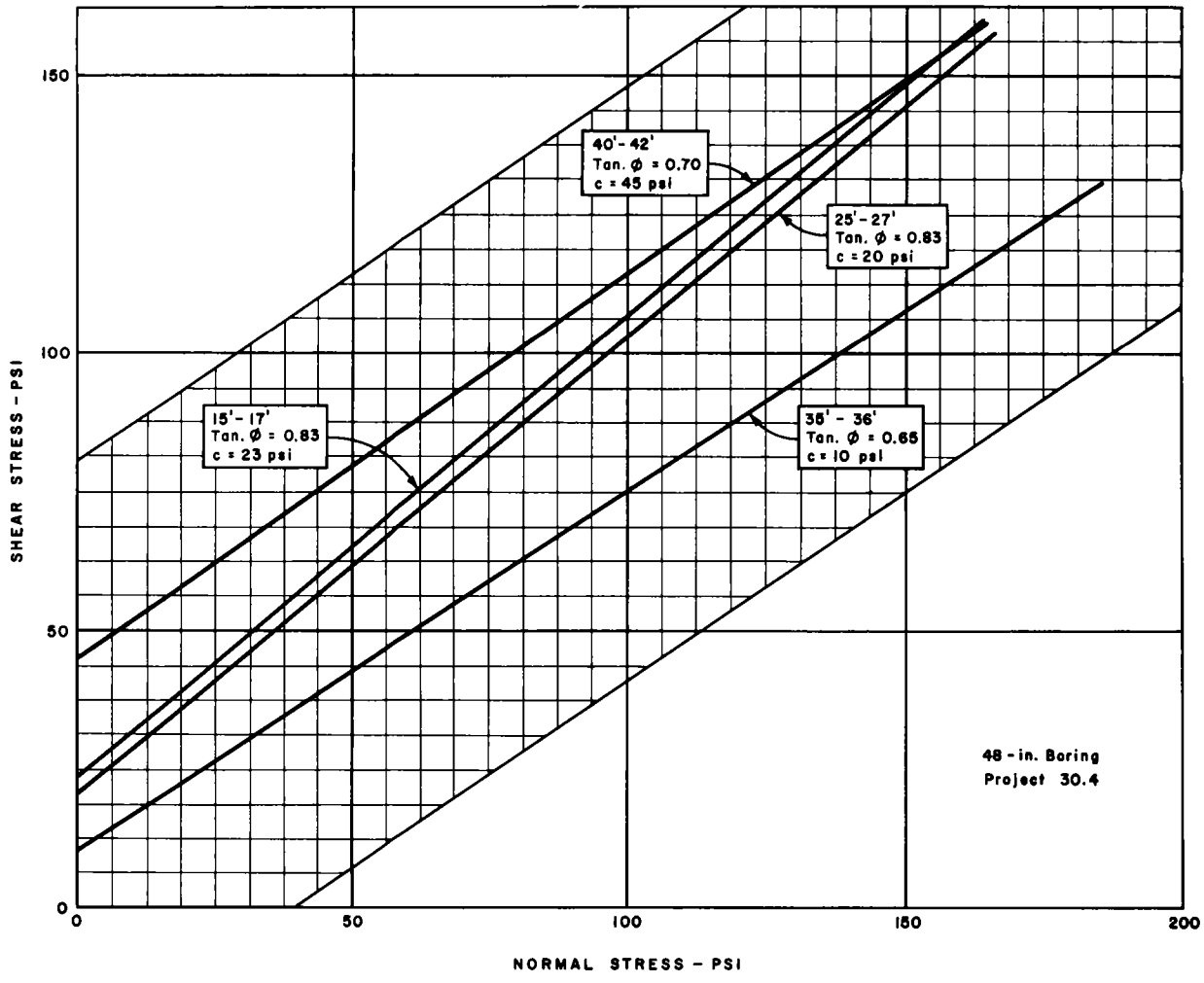

Fig. C.2—Suggested peak shear envelope.

Appendix D

POSTSHOT DYNAMIC ANALYSIS OF ROOF SLAB

D.1 GENERAL

The dual-purpose reinforced-concrete mass shelter was designed by conventional ultimate-strength theory using pressure–time relationships developed partly from theoretical data and partly from the test results of Operation Teapot. A shelter of this type was constructed at the theoretical 35-psi overpressure level and tested during shot Priscilla of Operation Plumbbob. This appendix presents the results of a postshot dynamic analysis on the roof slab of the shelter using the as-built construction and the recorded blast loading.

D.2 BLAST LOADING

For the purpose of postshot analysis, the blast loading on the roof slab of this structure was assumed to be the free-air pressure–time load recorded by the ground-baffle gauge, i.e., the earth cover was assumed not to attenuate the free-air pressure. The entire earth cover, however, was included as part of the effective mass of the slab.

D.3 STRENGTH CRITERIA

The compressive strength of the concrete was 3860 psi and was determined as the average value obtained from the 28-day test cylinders taken from the roof slab. Reinforcing steel used in the structure was intermediate grade with an average static unit stress at yield (as obtained from test specimens) of 47,976 psi. The dynamic design tensile and compressive yield stresses for steel and the dynamic ultimate compressive stress for concrete were increased over the static values to account for the rapid strain rates* caused by the blast loading.

D.4 ARCHITECTURAL AND STRUCTURAL DRAWINGS

Architecturally, the shelter was constructed as shown in Fig. 1.2. The as-built drawings shown in Figs. A.1 to A.6 show the actual reinforcement arrangement placed in the field. There is very little deviation from the original reinforcement details with the exception noted in Chap. 5 for the roof-slab reinforcement.

---

* The dynamic increase factors used in this analysis are the average values recommended in EM-1110-345-414. More accurate values can be obtained by considering the actual times of yield and utilizing Figs. 4.15 and 4.20 of the above manual.

D.5 ANALYSIS

In general, the analysis of the various members of the structure which are exposed to the blast consist in the solution of the equation of motion

$$F - R = M_e\ddot{x}$$

where F = applied blast force
R = internal resistance of the structural member
M_e = mass of an equivalent single-degree-of-freedom system
$\ddot{x}$ = acceleration of the mass

This equation of motion can be readily solved by any of several numerical integration[1] methods. The numerical method illustrated in this appendix for the analysis of the roof slab is the "acceleration impulse extrapolation method," described in Ref. 2.

Assume critical axis of rotation for R_{ult} passes through column capital

ν = Poisson's ratio, assumed zero
f'_c = 3860 psi (28-day results) } av. values of test results
f_s = 47,976 psi (use 48,000 psi) }
f'_{dc} = 3860 (1.3) = 5.02 ksi
f_{ds} = 48,000 (1.1) = 52.8 ksi
cover-top = 2 in.
bottom = 0.75 in.

$$M_{ult} = A_s f_s (d - a/2)$$

$$a = \frac{A_s f_s}{0.85\, b f'_{dc}}$$

$$A_s = pbd$$

Therefore

$$M_{ult} = pbd^2 f_{ds}\left(1 - \frac{pf_{ds}}{1.7\, f'_{dc}}\right)$$

If d is used as the average depth to the longitudinal and transverse reinforcement, one can use d = t – cover – bar diameter.

The computations for the moments at the particular sections of a typical quarter panel (see Figs. D.1 and D.2) can be conveniently presented as indicated in Table D.1.

By taking the axis of rotation as passing through the centroid of the arc, one obtains the lever arm from the axis of rotation to the centroid of the loaded area, $\bar{y}'$ or $\bar{x}'$; the total allowable moment on a quarter panel, ΣM; and the unit resistance of the member as follows:

	Area	y = x	M
14.5 (14.5)	= 210.25 sq ft	7.25 ft	1525
$-\frac{1}{4}\pi(3.5)^2$	= −9.63 sq ft	1.488 ft	−14.3
	200.62 sq ft		1510.7

$$\bar{x} = \bar{y} = \frac{1510.7}{200.62} = 7.53 \text{ ft}$$

$$\bar{x}' = \bar{y}' = 7.53 - 2.23 = 5.30 \text{ ft (axis of rotation to CG)}$$

$$\Sigma M_x = \Sigma M_y = \frac{245{,}400}{2(12)} = 10{,}230 \text{ kf}$$

$$R = \frac{10{,}230}{5.30} = 1931 \text{ k}$$

Total R per panel = 4(1931) = 7724 k

$$\text{Unit resistance} = \frac{7724}{4(200.62)} = 9.64 \text{ ksf} = 67.0 \text{ psi}$$

Relative Moment Capacities (typical interior panel):

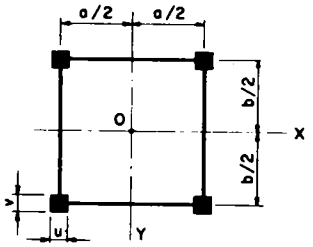

$$a = b = 29.0, \frac{a}{b} = 1.0$$

$$u = v = 7.0 \text{ ft}, \frac{u}{a} = 0.241$$

$$(M)_{x=y=0} = \frac{32,300}{180} = 179.5 \text{ kin./in.}$$

$$(M)_{x=y=a/2} = \frac{127,000}{168} = -756 \text{ kin./in.} = 4.22\ (M)_{x=y=0}$$

$$(M_x)_{x=a/2,y=0} = \frac{46,000}{180} = 256 \text{ kin./in.} = 1.425\ (M)_{x=y=0}$$

$$(M_y)_{x=a/2,y=0} = \frac{40,100}{168} = 239 \text{ kin./in.} = 1.33\ (M)_{x=y=0}$$

From Ref. 3, Table 59 ($\nu = 0.2$ and u/a = 0.241)*

$$(M)_{x=y=0} = 0.0316$$

$$(M)_{x=y=a/2} = 0.1155 = 3.66\ (M)_{x=y=0}$$

$$(M_x)_{x=a/2,y=0} = 0.0175 = 0.554\ (M)_{x=y=0}$$

$$(M_y)_{x=a/2,y=0} = 0.0476 = 1.507\ (M)_{x=y=0}$$

From the comparison above it is seen that the $(M_y)_{x=a/2,y=0}$ section is critical and will be the section of first yield. Therefore, from Table 59 of Ref. 3, one obtains the coefficient $\beta_3 = 0.0476$ for $\nu = 0.2$, and

$$(M_y)_{x=a/2,y=0} = \beta_3 q a^2$$

To obtain the uniform load corresponding to this first yield for $\nu = 0$, the equation may be written as

$$q = \frac{1.2M}{\beta_3 a^2} = \frac{239}{\frac{0.0476}{1.2}(29)^2}$$

$$q = 7.16 \text{ ksf} = 49.8 \text{ psi (for } \nu = 0)$$

It should be noted that the axis of rotation for the ultimate resistance of the quarter panel is taken as passing through the centroid of the quarter arc formed by the column capital and that the span length a in the above equation is taken from center to center of the columns. For determination of the center deflections, the span is modified to represent the effective span.

---

*The actual values of bending-moment coefficients of a flat slab at the columns generally lie between the values given in Table 59 for the conventional theory and those for the rigid connection. The actual coefficients will be slightly lower than those given in Table 59 and presented here for the u/a for this slab. For a more rigorous solution see Ref. 3, article 56.

The equation for the deflection at the center of the panel may be written as

$$w = \alpha \frac{qb^4}{D} = \alpha \frac{qb^4}{Eh^3} = [12(1 - \nu^2)]$$

where $E = 2{,}000{,}000 + 470\, f'_c = 3{,}812{,}000$ psi

$$h^3 = 12\, I_{av.} = 12 \left(\frac{I_g + I_c}{2}\right)$$

$$I_g = \frac{1}{12} h^3 = \frac{1}{12} (2.5)^3 = 1.302$$

$$I_c = Fd^3 = 0.031 \left(\frac{27.66}{12}\right)^3 = \frac{0.380}{0.841} = I_{av.}$$

b = span between points of rotation
= 29 − 2(2.23) = 24.54 ft

Consequently, for $\nu = 0$,

$$w = 0.00581 \left[\frac{49.8(24.54)^4(12)}{3{,}812{,}000(12)(0.841)}\right] = 0.0328 \text{ ft} = 0.394 \text{ in.}$$

from which one obtains

$$k = \frac{4(7.16)(200.6)}{0.0328} = 1.75 \times 10^5 \text{ k/ft}$$

By again comparing the moment capacities with the moment distribution at the various sections, it is evident that the positive reinforcement in the mid strip will yield under a slightly greater load than the positive reinforcement in the column strip and is therefore assumed to yield simultaneously. The required slab properties can be obtained as follows:

For a uniformly loaded square plate, with all edges free, supported at the four corners, the deflection at the center of the plate is

$$w_c = 0.025 \frac{q'b^4}{D} \text{ (Ref. 4)}$$

where $q' = R - q$
$= 9.64 - 7.16 = 2.48$ ksf
$= 17.2$ psi

$$h^3 = 12\, I_{av.} = 12 \left(\frac{I_g + I_c}{2}\right) = 12\,(0.841) = 10.1$$

b = 24.54 ft

Therefore

$$w_c = 0.025 \left[\frac{17.2(24.54)^4(12)}{3{,}812{,}000(12)(0.844)}\right]$$

$$= 0.0486 \text{ ft} = 0.583 \text{ in.}$$

Resistance-deflection Curve

Dead load

$$\text{Av. } t = \frac{15(29)(30) + 15(14)(30) + 4(7)(7)(44)}{(29)^2} = 33.3 \text{ in.}$$

$$\text{Av. dead load} = \left.\begin{array}{l} \frac{33.3}{12}(150) = 416 \text{ psf} \\ + 3.0(100) = 300 \text{ psf} \end{array}\right\} \text{ use } 0.72 \text{ ksf}$$

ANALYSIS

Dead load

$$R_{dl} = 0.72\ (4)(200.62) = 578\ k$$

Mass

$$\text{Total mass} = m = \frac{578}{32.2} = 17.94\ k\text{-sec}^2/ft$$

Equivalent mass

$$\text{Elastic} - (1st\ yield) = 0.34\ (17.94) = 6.10\ k\text{-sec}^2/ft$$

$$\text{Plastic} - (4th\ yield) = \frac{7}{24}\ (17.94) = 5.24\ k\text{-sec}^2/ft$$

NOTE: Use the same equivalent mass factors for the 2nd and 3rd yield conditions as is used for the 4th yield condition.

Assume the dead load, F_{dl}, and the precursor, F_{pp}, part of the pressure curve act as a static load.

Period

$$T = 2\pi\sqrt{\frac{m_e}{k_1}} = 2\pi\sqrt{\frac{6.1 \times 10^{-5}}{1.75}} = 0.037\ sec$$

$$\Delta t = \frac{T}{10} = 3.70 \times 10^{-3} \qquad \text{Use } 0.0025\ sec$$

Static load

$$F_{static} = F_{dl} + F_{pp} = 578 + 7(0.144)(4)(200.62) = 578 + 807 = 1385\ k$$

$$w_{static} = w_{dl} + w_{pp} = 0.0328\left[\frac{1385}{7.16(802.5)}\right] = 0.0079\ ft = 0.095\ in.$$

Analysis constants

$$\Delta t^2 = (0.0025)^2 = 0.625 \times 10^{-5}\ sec^2$$

$$\frac{\Delta t^2}{m_1} = \frac{0.625 \times 10^{-5}}{6.10} = 0.1025 \times 10^{-5}$$

$$\frac{\Delta t^2}{m_4} = \frac{0.625 \times 10^{-5}}{5.24} = 0.1193 \times 10^{-5}$$

$$w_{n+1} = 2w_n - w_{n-1} + a_n \Delta t^2$$

$$F = q(0.144)(802.5) - 807 = 115.5\ q - 807$$

$$a_n = \frac{F_n - R_n}{m} \qquad \text{(Ref. 1)}$$

$$a_0 = \frac{1}{m_e}\left(\frac{F_0}{2} + \frac{F_1 - F_0}{6}\right)$$

$$= \frac{1}{6.10}\left[0 + \frac{3.3(115.5) - 0}{6}\right] = 10.41$$

$$w_0 = a_0 t^2 = 10.41\ (0.625 \times 10^{-5}) = 0.651 \times 10^{-4}$$

$$w_{n+1} = 2w_n - w_{n-1} + a_n \Delta t^2$$

From Table D.2

Maximum response of slab = R_n (max) + (F_{dl} + F_{pp}) = 4476 + 1385 = 5861 k (50.5 psi)

Maximum deflection of slab = (276 + 79) $\times$ 10^{-4} = 355 $\times$ 10^{-4} ft = 0.43 in.

NOTE: The resistance of the slab vibrates about the load curve after the first reversal; therefore the maximum resistance was produced at the first reversal of the slab. If damping were included in the analysis, the maximum response of the slab would be between 5 and 10 per cent less than that obtained above.

CHECK OF SHEAR (f'_c from postshot core tests)

Allowable shear at edge of column capital (Ref. 5):

$$\text{Allowable shear} = \left[9.75 - 1.125\left(\frac{c}{d}\right)\right]\sqrt{f'_c}$$

$$= \left[9.75 - 1.125\left(\frac{66}{40.7}\right)\right]\sqrt{4900}$$

$$= 555 \text{ psi}$$

Area of quarter panel = 210.3 sq ft

$$\text{Unloaded area} = \frac{\pi(3.5 + 3.4)^2}{4} = \frac{37.3 \text{ sq ft}}{173.0 \text{ sq ft of loaded area}}$$

$$v = \frac{V}{cd} = \frac{173\ q}{(66)(40.7)} = 555 \text{ psi}$$

$$q = \frac{0.555(66)(40.7)}{173} = 8.65 \text{ ksf} = 60 \text{ psi}$$

Allowable response based on shear capacity = 60 psi

REFERENCES

1. C. S. Whitney and E. Cohen, Guide for Ultimate Strength Design of Reinforced Concrete, J. Am. Concrete Inst., 28(5): 455(November 1956).
2. Principles of Atomic Weapons Resistant Construction, Department of Civil and Sanitary Engineering, Massachusetts Institute of Technology, 1954. (Classified)
3. S. P. Timoshenko and S. Woinowsky-Krieger, Theory of Plates and Shells, Second Edition, McGraw-Hill Book Company, Inc., New York, N. Y., 1959.
4. O. Belluzzi, Scienza Della Costruzioni, Volume Terzo (Capitoli XXV-XXVI), Nicola Zanichelli Editore, Bologna, 1953.
5. Report of the Joint ASCE-ACI Committee on Shear and Diagonal Tension, Journal of the American Concrete Institute, January, February, and March, 1962.

TABLE D.1—AS-BUILT MOMENT CAPACITIES

Location	b, in.	d, in.	bd^2, cu in.	A_s, sq in.	P	pf_{ds}, ksi	$1-\left(\frac{pf_{ds}}{1.7\,f'_{dc}}\right)$	M_{ult}, kin.
kabcd	168	40.73	279,000	35.6	0.00520	0.275	0.968	74,300
		36.80	227,000	28.0	0.00453	0.239	0.972	52,700
de + jk	180	26.87	129,800	15.0	0.00310	0.164	0.981	20,900
		27.12	131,200	18.0	0.00370	0.195	0.977	25,100
ef + hj	168	28.12	132,800	28.0	0.00593	0.313	0.963	40,100
fgh	180	28.38	145,000	22.2	0.00434	0.229	0.973	32,300
								ΣM_{ult} = 245,400 kin.

TABLE D.2—DYNAMIC ANALYSIS

n	t ($\times 10^3$), sec	F_n	R_n	F_n-R_n, kip	$\Delta t^2/m$ ($\times 10^5$)	$a_n\Delta t^2$ ($\times 10^4$)	w_{n+1} ($\times 10^4$), ft	
0	0.0	0			0.1025	0.651	0.000	ΔR_1 = 4365k
1	2.5	381	11	370	0.1025	3.792	0.651	$\Delta w_1 = 249 \times 10^{-4}$
2	5.0	775	89	686	0.1025	7.032	5.094	$k_1 = 17.5 \times 10^4$
3	• 7.5	1155	290	865	0.1025	8.866	16.569	$k_2 = 4.09 \times 10^4$
4	10.0	1549	646	903	0.1025	9.256	36.910	
5	12.5	1941	1164	777	0.1025	7.964	66.507	
6	15.0	2346	1821	525	0.1025	5.381	104.068	
7	17.5	2730	2573	+157	0.1025	1.609	147.010	
8	20.0	2950	3352	−402	0.1025	−4.121	191.561	
9	22.5	3060	4060	−1000	0.1025	−10.250	232.991	
10	25.0	3140	4419	−1279	0.1193	−15.258	262.171	
11	27.5	3210	4476	−1266	0.1193	−15.103	276.093	
12	30.0	3260	4455	−1195	0.1025	−12.249	274.912	
13	32.5	3300	4219	−919	0.1025	−9.420	261.482	
14	35.0	3330	3820	−490	0.1025	−5.022	238.632	
15	37.5	3350	3333	+17	0.1025	+0.174	210.760	
16	40.0	3360	2839	521	0.1025	5.340	183.062	
17	42.5	3360	2457	903	0.1025	9.256	160.704	
18	45.0	3270	2227	1043	0.1025	10.691	147.602	
19	47.5	3110	2185	925	0.1025	9.481	145.191	
20	50.0	2920	2309	611	0.1025	6.263	152.261	
21	52.5	2750	2542	208	0.1025	2.132	165.594	
22	55.0	2590	2813	−223	0.1025	−2.286	181.059	
23	57.5	2430	3044	−614	0.1025	−6.294	194.238	
24	60.0	2270	3164	−894	0.1025	−9.164	201.123	
25	62.5	2150					198.844	
26	65.0	2030						

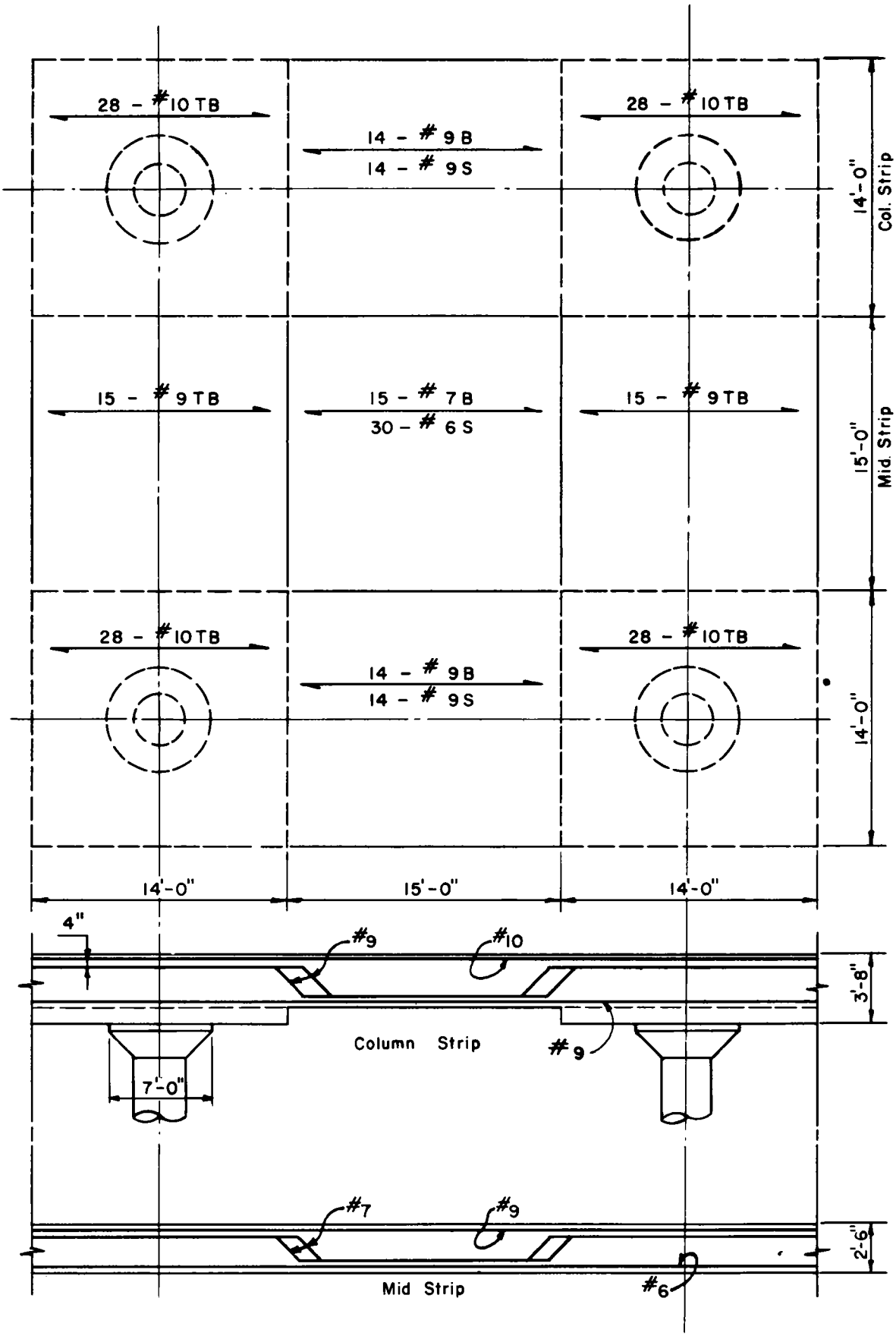

Fig. D.1—Typical roof-slab interior panel.

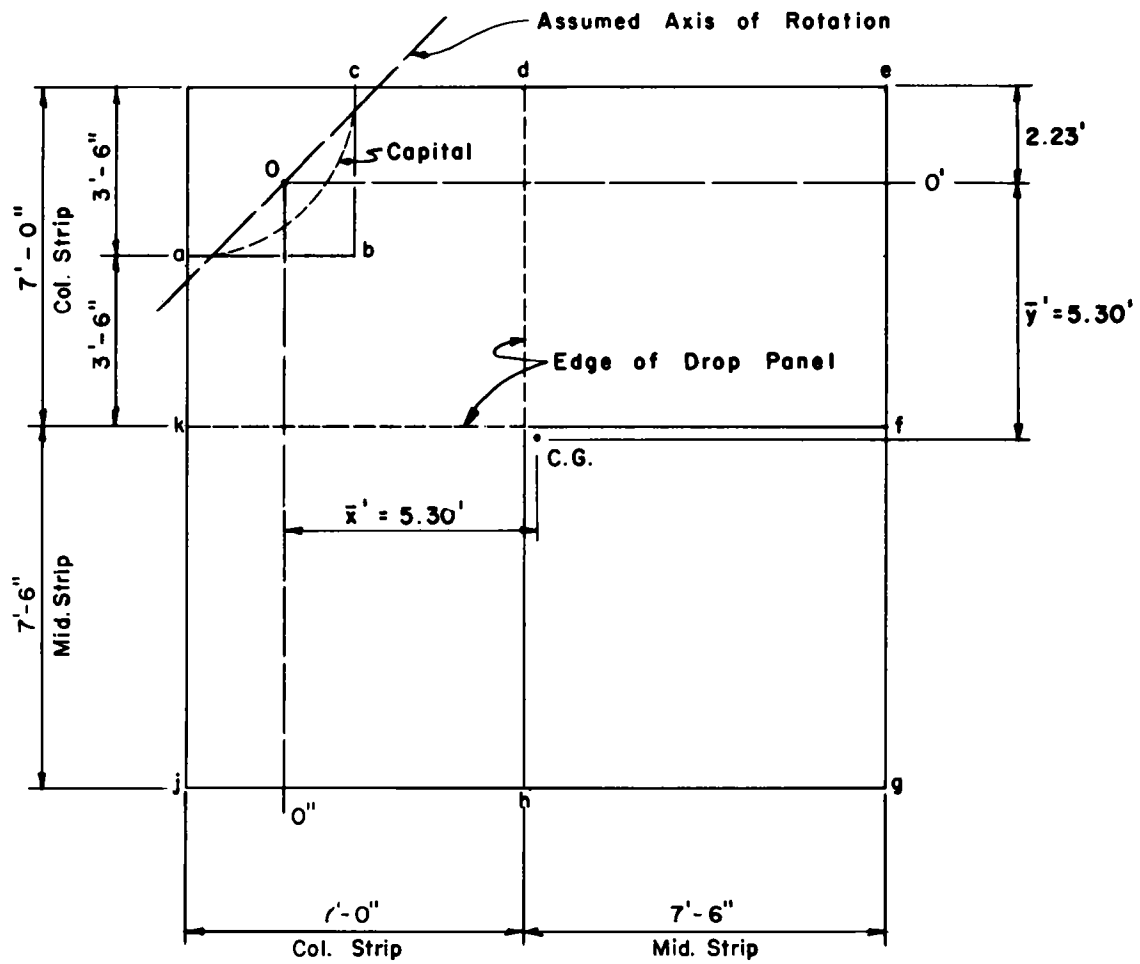

Fig. D.2—Assumed yield lines for interior quarter panel.

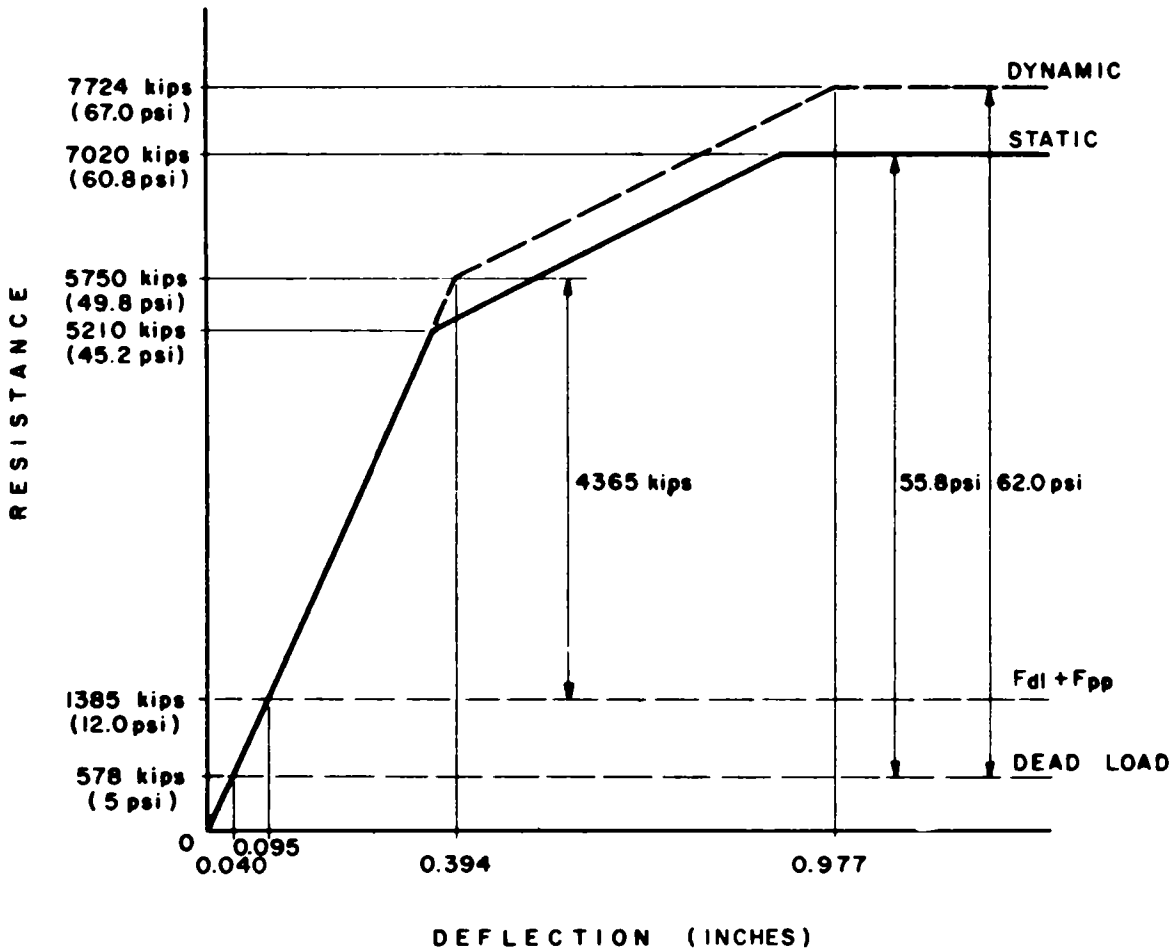

Fig. D.3—Panel resistance-deflection curve.